ABSTRACT

| | |
|---|---|
| Title of Document: | KINETIC CHARACTERIZATION AND DOMAIN ANALYSIS OF THE HELICASE RECD2 FROM *DEINOCOCCUS RADIODURANS* |
| | William Robert Shadrick, Doctor of Philosophy, 2010 |
| Directed By: | Associate Professor Douglas Julin, Ph.D. Department of Chemistry and Biochemistry |

The gram positive bacterium *D. radiodurans* is known for its extreme resistance to radiation and an extraordinary ability to reconstitute its genome after sustaining large numbers of double strand breaks (DSB's). Genome analysis does not immediately reveal a biochemical basis for this incredible DNA repair ability. In *E. coli*, DSB's are mainly repaired through the RecBCD pathway via homologous recombination. The *D. radiodurans* genome contains no known homologues of RecB or RecC, but sequence analysis has identified a homologue of RecD, termed RecD2. The function of RecD2 in *D. radiodurans* is unknown, as RecD elsewhere has only been found as a component of the RecBCD complex.

Our research has focused on biochemical characterization of RecD2. Previous work in our lab established that RecD2 is a DNA helicase with limited processivity and a preference for forked substrates. We have studied the unwinding mechanism of

the enzyme, as measured by rates of DNA unwinding and behavior on various substrates. Reactions conducted under single turnover conditions have allowed us to determine the processivity and the step size of RecD2. RecD2 pre-bound to dsDNA substrate is capable of unwinding 12 bp, but not 20 bp, when excess ssDNA is added to prevent rebinding of enzyme to substrate. Unwinding of the 12 bp substrate under single turnover conditions could be modeled using a two step mechanism, with $k_{unw} = 5.5$ s$^{-1}$ and dissociation from partially unwound substrate $k_{off} = 1.9$ s$^{-1}$. Results derived from these rate constants indicate an unwinding rate of 15-20 bp/ sec, with relatively low processivity ($P = 0.74$).

Glutaraldehyde cross-linking showed formation of multimers of RecD2 in the absence of DNA, but this was not detectable by size exclusion chromatography.

We were able to separate the N-terminal region from the helicase core of RecD2 using limited proteolysis. It was not possible to characterize the C-terminal helicase domain due to its low solubility upon overexpression in *E. coli*.

KINETIC CHARACTERIZATION AND DOMAIN ANALYSIS OF THE
HELICASE RECD2 FROM *DEINOCOCCUS RADIODURANS*


By


William Robert Shadrick


Dissertation submitted to the Faculty of the Graduate School of the
University of Maryland, College Park, in partial fulfillment
of the requirements for the degree of
Doctor of Philosophy
2010


Advisory Committee:
Associate Professor Douglas Julin, Ph.D., Chair
Professor Dorothy Beckett, Ph.D.
Associate Professor Jason Kahn, Ph.D.
Assistant Professor Barbara Gerratana, Ph.D.
Associate Professor Richard Stewart, Ph.D.

# Dedication

To my family, who have always believed in me.

# Acknowledgements

My research could not have been completed without the help of Dr. Brian Martin, at the NIH, who performed Edman degradation for my $RecB^N$ degradation. I would like to thank the ladies at the DNA sequencing facility on campus, who put up with my always wanting to turn in samples too late in the day. Dr. Zvi Kelman, one of the coolest people EVER, thanks for letting me run size exclusion on RecD2 at CARB.

I would like to thank a few people who made life bearable. First, I would like to thank Capt. Christopher Martinez, M.D. who planted the idea of Maryland in my head, and had a place for me to live for the first several years. I would like to thank Dr. Norm Hansen for offering a place to work for the summer of 2004. In Dr. Hansen's lab, Srilatha Kuntamalla was finishing up when I came, but still had time to answer questions.

Neil Campbell (now Dr. Dad), Patrick McTamney, Jennifer Adler, and all the rest of the Rokita Lab were always there to commiserate when I needed, for lunch, or even to help figure out why something wasn't working. The Kahn Lab- Aaron, Dan, Kathy and all, you're great people. Lucas especially, thanks for letting me share the cave. Whenever I couldn't find something in the Rokita lab, Gerratana lab usually had what I needed. Wei Li, Melissa Resto, Kate Connor- thanks for everything. The Beckett lab- Emily Streaker, Maria Ingaramo, Poorni Adikaram, thanks for the laughs.

Most especially, the other members of the Julin lab are how I made it this far. Dr. Julin, the boss, thanks for keeping us all in line. When I wanted to try my crazy

# Table of Contents

# List of Tables

# List of Figures

# List of Abbreviations

ATP       Adenosine triphosphate

BSA       Bovine serum albumin

CAPS      N-cyclohexyl-3-aminopropanesulfonic acid

DMSO      Dimethylsulfoxide

DNA       Deoxyribonucleic acid

dNTP      Deoxyribonucleoside triphosphate

DS        Double Stranded

DSB       Double strand break

DTT       Dithiothreitol

ESDSA     Extended Synthesis Dependent Strand Annealing

FPLC      Fast protein liquid chromatography

GST       Glutathione-S-transferase

HEPES     4-(2-hydroxyethyl)-1-piperazineethanesulfonic acid

HP        Hairpin

HR        Homologous recombination

IPTG      Isopropyl β-D-1-thiogalactopyranoside

LB        Lysogeny (Luria-Bertrani) broth

MBP       Maltose binding protein

MMC       Mitomycin C

MMS       Methylmethanesulfonate

| | |
|---|---|
| Na$_2$·EDTA | Ethylenediaminetetraacetic acid disodium salt |
| NHEJ | Non-homologous end joining |
| NTA | Nitrilotriacetic acid |
| PAGE | Polyacrylamide gel electrophoresis |
| PCR | Polymerase chain reaction |
| PEG | Polyethylene glycol |
| PEI | Polyethyleneimine |
| PIPES | piperazine-N,N′-bis(2-ethanesulfonic acid) |
| PMSF | Phenylmethylsulfonylfluoride |
| PVDF | Polyvinylidene fluoride |
| ROS | Reactive oxygen species |
| SDS | Sodium dodecyl sulfate |
| SF | Superfamily |
| ss | single stranded |
| T$_4$ PNK | T$_4$ polynucleotide kinase |
| TAE | Tris acetate EDTA |
| TBE | Tris borate EDTA |
| TEM | Transmission electron microscopy |
| TLC | Thin layer chromatography |
| Tris·HCl | Tris(hydroxymethyl)aminomethane hydrochloride |
| UV·Vis | Ultraviolet·visible spectroscopy |

# Chapter 1: Introduction

Every day, a cell has to deal with damage to its DNA from a variety of sources. These may range from ultraviolet (UV) and ionizing radiation (IR), to reactive oxygen species (ROS), and even endonucleases. Other sources of damage may even come from within the cell, as in the case of replication fork collapse and accidental incorporation of mismatched bases (1,2). Replication fork collapse can come about from blockages on the replication fork, such as chemically modified bases or tightly bound proteins. Chemical and radiation induced DNA damage often leads to strand breaks in the backbone of the DNA. Severe consequences, including cell death, can occur if DNA breaks are not immediately repaired (3).

Damage from IR is of particular interest due to the variety of lesions caused by dosage with even small amounts of radiation. IR can damage DNA by directly inducing strand breaks in the backbone of the cellular DNA. More often, however, IR causes formation of ROS by radiolysis of water molecules (4). ROS, in the form of hydroxyl radicals, then contribute to DNA damage by chemically attacking the DNA. These can lead to a variety of chemically modified bases, reviewed in (5,6). Strand breakage can occur when an abasic site forms as a result of base modification, leading to cleavage (6). When breaks occur on opposite strands within close proximity, a double strand break (DSB) occurs. Double strand breaks expose DNA to degradation within the cell, ultimately leading to death if not repaired.

Two methods of DSB repair are employed in most cells. These are non-homologous end joining (NHEJ) and homologous recombination (HR) (7). NHEJ occurs when only one copy of the chromosome is present. This pathway is most often

seen in quiescent (non-dividing) cells and is sometimes mutagenic, depending on the location of the repair site (8). NHEJ is most commonly seen as a repair mechanism in eukaryotes, although recent evidence suggests some bacteria are capable of this process (9,10). When a second chromosomal copy can be located, as during replication, the primary method of repair for DSB events is homologous recombination (7).

In *Escherichia coli* (*E. coli*), preparation of HR substrates is the responsibility of the RecBCD complex (11). The Gram-positive bacterium *Deinococcus radiodurans* is noted for its ability to survive doses of radiation capable of completely shattering its DNA into a range of subgenomic fragments (12,13). In *D. radiodurans*, no RecBCD complex has been found. An enzyme homologous to RecD has been identified, termed RecD2 (14). The function of this enzyme in DNA repair is unknown. A limited amount of biochemical characterization has been carried out on RecD2 (15).


## 1.1 *Deinococcus radiodurans*

The bacterium *D. radiodurans* has emerged as an organism of interest due to its extreme radioresistance. *D. radiodurans* is a gram-positive red pigmented bacterium that grows most efficiently in undefined rich (TGY) media at 30°C (14). *D. radiodurans* are found as spherical cells that exist in pairs or tetrads, with individual cells found present but not isolatable (16). *D. radiodurans* maintains at minimum 4 copies of its genome per cell, often more, depending on growth phase (17).

All species of the genus *Deinococcus* are extremely resistant to DNA damage. *D. radiodurans* is capable of surviving doses of ionizing radiation 250 times higher than necessary to sterilize a culture of *E. coli* (for reviews, see (16,18,19)). An ionizing radiation dose of 15 kGy (1 Gray = 100 rads = 1 J/ kg = 1 $m^2 \cdot s^{-2}$ absorbed radiation) is enough to cause 150 DSB's per genome to an exponentially growing culture of *D. radiodurans*. Even at this dose, 37 % of cells in an irradiated culture of wild type cells will survive (20). To compare, most organisms are capable of repairing only 2-3 DSB events per genome (21). Any single DSB can be fatal to a rapidly dividing cell. In *E. coli*, DSB's are primarily repaired through the RecBCD pathway via homologous recombination (*vide infra*).

As shown in figure 1.1, the genomic DNA of a culture of *D. radiodurans* is completely sheared by treatment with 7 kGy of ionizing radiation (18,22). When cells are allowed to recover with further growth after irradiation, only four and one-half hours is necessary to return the genomic DNA to full size. This can be observed in figure 1.1 by the return of larger size genomic fragments during later recovery periods. The evolutionary cause for the extreme radiation resistance phenotype observed in *D. radiodurans* is not likely to do with any natural source of radiation present on the earth, as background levels of ionizing radiation have stayed between 0.5 and 20 rads/ year (5 x $10^{-3}$ to 0.2 Gy/ year) for the last 4 billion years (14).
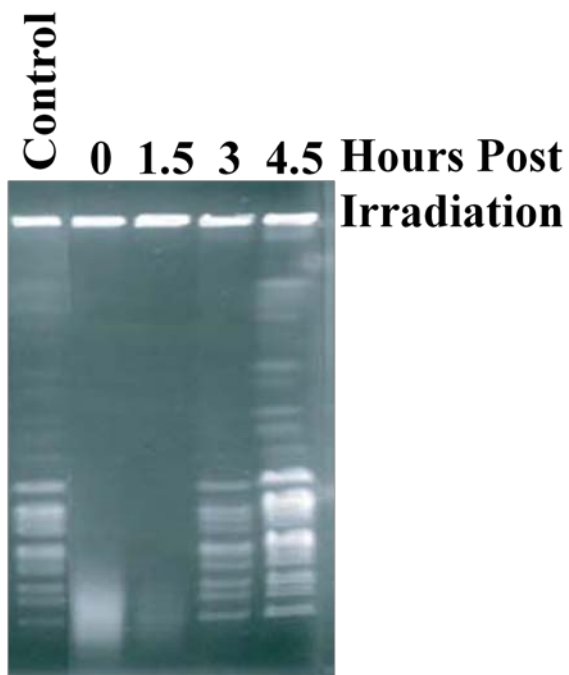
**Figure 1.1: Response of *D. radiodurans* to 7 kGy of ionizing radiation.** Lane 1: *D. radiodurans* genomic DNA, no irradiation; Lane 2: *D. radiodurans* genomic DNA immediately after irradiation; Lane 3-5: *D. radiodurans* genomic DNA 1.5, 3, and 4.5 hours recovery post-irradiation. All samples treated with *NotI* prior to loading (22).

 

Members of the family *Deinococcaceae* can be found in diverse places, reflecting their tolerance for extreme conditions (23). The tool kit of cellular components required for survival under the harsh conditions of the desert at Tataouine (24) or the inside of a can being bombarded with gamma rays (25) may indeed be similar. In the case of *D. radiodurans*, a correlation has been found between surviving desiccation and having an increased tolerance to IR (23,24,26).

1.1.2 Mechanisms of radiation resistance in *D. radiodurans*

The genome sequence of *D. radiodurans* was published in 1999 (27). A single cause for the extreme radiation resistance phenotype in *D. radiodurans* has remained elusive, however. Representatives of most DNA repair pathways are present, although often important components are missing (14,27). For example, the genome contains no known homologues of *recB* or *recC*, but sequence analysis has identified a homologue of *recD* (27).

The reasons offered for the survival of *D. radiodurans* under irradiation vary widely. Levin-Zaidman (28) offers the hypothesis that the genome of *D. radiodurans* is held in tightly packed toroids. They maintain that toroids allow for little diffusion of shattered DNA ends after cellular insult. When a cell is treated with an agent capable of causing DSB's, the repair machinery is able to locate the broken ends of the DNA quickly. This theory is based on the observation of tightly packed ring like structures when observing *D. radiodurans* with transmission electron microscopy (TEM). Fluorescent labeling showed the structures to be DNA. The smaller cross section of the toroidal organization system would expose the DNA to less of a practical dosage of radiation. Other research supports the assertion that toroidal DNA structure is a common feature of radiation resistant organisms (29).

Daly (30) proposes a different theory, based on the accumulation of $Mn^{2+}$ in the intracellular environment of *D. radiodurans*. Their model bases the resistance of *Deinococcus* on the nature of the transition metals present in the cytoplasm of the cell, specifically $Mn^{2+}$ and $Fe^{2+}$.

Although important for a number of functions, when free, $Fe^{2+}$ in the cell is also responsible for a host of problems. This is due to its role in the formation of ROS via the Fenton reaction (for reviews, see (31,32)). The ability of $Fe^{2+}$ to act as an electron donor to electronegative species such as the various forms of oxygen contributes quickly to the formation of reactive oxygen species such as hydrogen peroxide ($H_2O_2$), superoxide ($O_2^-\bullet$), and hydroxyl radicals (OH$\bullet$). The Fenton reaction makes OH$\bullet$, in a non-enzymatic fashion, from endogenous $H_2O_2$:

$$\textbf{Fe}^{2+} \ + \ \textbf{H}_2\textbf{O}_2 \ \rightarrow \ \textbf{Fe}^{3+} \ + \ \textbf{OH}\bullet \ + \ \textbf{OH}^-$$

Hydroxyl radicals (OH$\bullet$) are the most reactive of the reactive oxygen species (33).  The hydroxyl radical species produced by the Fenton reaction then causes damage to proteins and to DNA. Manganese (II) has not been characterized as being capable of Fenton like reactions, but is instead an important cofactor in the ROS scavenging enzyme superoxide dismutase (MnSOD). In addition, $Mn^{2+}$ has been shown to be capable of removing $H_2O_2$ from solutions in a non-enzymatic fashion (34).

According to work published by the Daly group (30), *D. radiodurans* can grow in $Fe^{2+}$ deficient media, but not in growth media deficient in $Mn^{2+}$. Investigation of the amounts of $Fe^{2+}$ and $Mn^{2+}$ taken up by *D. radiodurans* found that the intracellular $Mn^{2+}/Fe^{2+}$ ratio is 0.24. In contrast, the ratio of $Mn^{2+}$ to $Fe^{2+}$ for *E. coli* is 0.0072. The authors propose that a higher $Mn^{2+}/Fe^{2+}$ ratio allows *D. radiodurans* to survive much higher doses of IR due to a much lower chance that ROS will form

when higher $Mn^{2+}$ is present in the cell. The basic point of this model is that *D. radiodurans* has the ability to survive more of an IR dosage because less ROS are formed. Less ROS generated for a given dosage of radiation then leads to less damage to cellular proteins and DNA.

Zahradka, et al (22) offers the most biochemical basis for the extreme radiation resistance phenotype, proposing a model they termed extended synthesis-dependent strand annealing (ESDSA). In this system, the genome of *D. radiodurans* is first shattered into small pieces by the action of ROS or IR. As shown in figure 1.2, recovery proceeds via a two-step process. In step 1, small fragments are resected in a 5'- 3' direction by nucleases, making each small fragment into a segment of dsDNA with overhanging regions of ssDNA at each end. Where only partial overlap may be found between homologous sequences of DNA, these are used to prime synthesis of longer overhangs via a moving D-loop (brackets, step 2). Synthesis continues through this cycle, over and over (steps 3 and 4), until overhangs are generated long enough that a complementary partner strand may be found. Once this has occurred, crossover occurs, via RecA mediated homologous recombination (shown in box b).
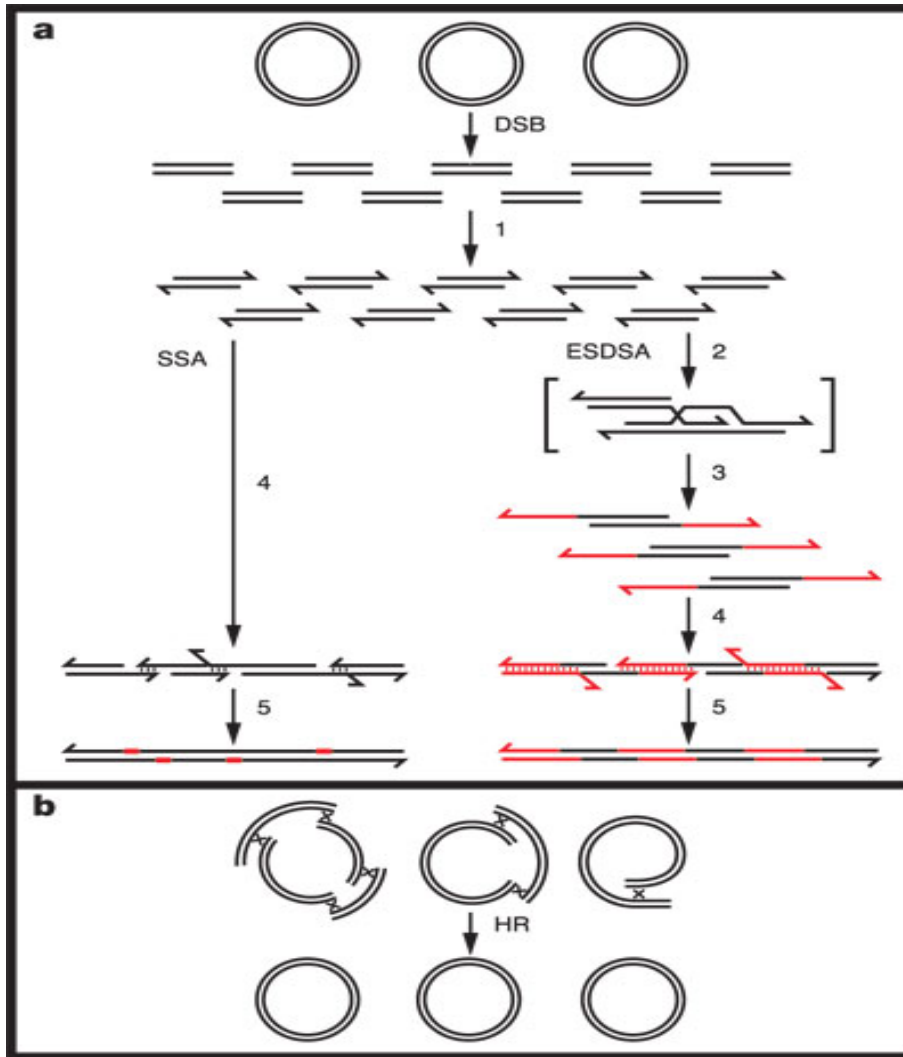
**Figure 1.2: Extended synthesis dependent strand annealing in *D. radiodurans*.**
Beginning in box **a,** IR causes fragmentation of the genome into small fragments (20-30 kb). The genome is reassembled in steps 1-5, as detailed in the text. In box **b**, larger fragments resulting from cycles 1-5 are used as substrates for homologous recombination. From Zahradka, et al (22).

## 1.2 Double Strand Break Repair in *E. coli*

The best characterized bacterial DNA repair system is in the gram negative

bacterium *E. coli*. The primary pathway for repair of DSB events in *E. coli* is

homologous recombination, where a region of undamaged double strand DNA serves

as a template for repair of damaged DNA. Homologous recombination allows cells to repair damaged sections of DNA with only minimal effect on nearby sequences (7). Preparation of a suitable substrate for homologous recombination in *E. coli* is the function of RecBCD (a complex of the protein products of the *recB*, *recC*, and *recD* genes) (11).

In *E. coli*, RecBCD is a heterotrimeric complex comprised of RecB (134 kDa), RecC (129 kDa), and RecD (67 kDa) which binds to blunt ends of double strand DNA (35-37). The RecBCD complex has several enzymatic activities, which work in concert to process DNA: the holoenzyme catalyzes ssDNA and dsDNA dependent hydrolysis of ATP, nucleolytic degradation of ssDNA or dsDNA, and unwinding of dsDNA. RecBCD is also responsible for loading RecA on to 3'-ssDNA overhangs formed as a consequence of its nuclease activity, generating RecA nucleoprotein filaments which serve as a substrate for subsequent steps in homologous recombination (for reviews, see (11,38-40)).
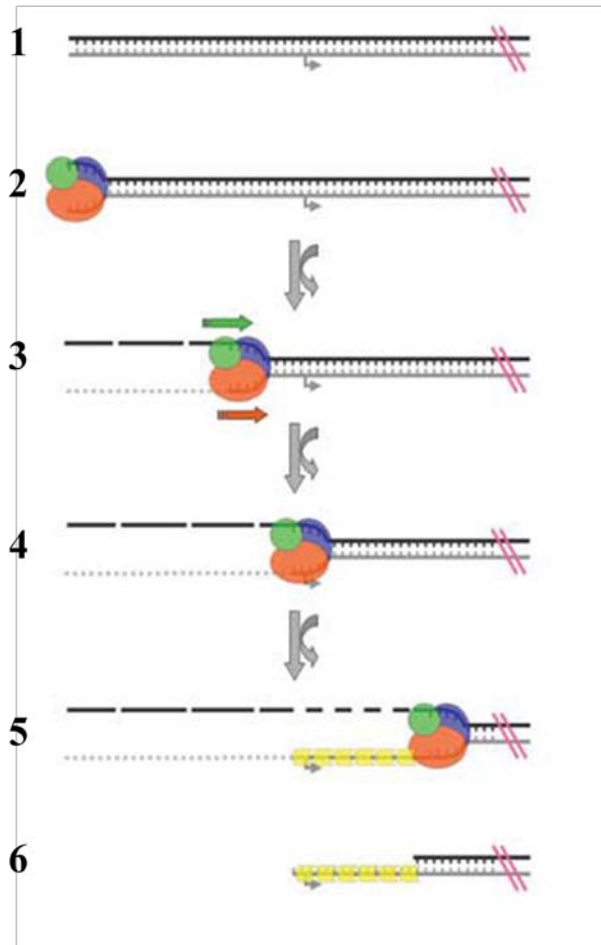
**Figure 1.3: Processing of a DNA double strand break by RecBCD.** In **1**, above, the dsDNA has a χ site, marked with→. RecBCD binds at the end of the DNA in **2**, and begins translocating along the DNA towards the χ site. In **3**, the complex is degrading both strands of DNA as it progresses. Shown in **4**, when RecBCD encounters the χ site on the 3' strand (as sensed by the complex), the complex changes activities. In **5**, the enzyme has begun loading RecA onto the 3' strand, while continuing to degrade the 5' strand. The product of the action of RecBCD is a RecA nucleoprotein filament, shown in **6** (41).

As shown in figure 1.3, RecBCD begins when it binds to a blunt piece of dsDNA. RecBCD then begins degrading both the strand reading 3'-5' (the 3'-strand) and 5'-3' (the 5'-strand) (as viewed from the direction of the break site) until it comes to a CHI (crossover hotspot instigator, χ) site on the 3' strand. Binding of the χ sequence (**5'-GCTGGTGG- 3'**; recognized from the 3' direction) at the χ

recognition site found in the RecC subunit of the complex attenuates nuclease activity on the 3' strand, and at the same time activates 5' strand degradation. The $\chi$ recognition site may be found in residues 647-663 of RecC (42).

When the $\chi$ sequence has been bound, RecBCD pauses and shifts activities. RecBCD then begins loading RecA on the 3' strand of the DNA, and continues loading RecA on the 3' strand while escalating degradation of the 5' strand. This is accomplished by the nuclease region of RecB positioning RecA for loading onto the DNA strand as it loops out of RecC (43). Single-stranded DNA bound to RecA feeds out of RecBCD in a loop. The 3'-terminus of this loop remains bound to the $\chi$ site until loading of RecA onto ssDNA is complete. The result of this activity is formation of a nucleoprotein filament of RecA bound to 3' overhang single strand DNA (1,41).

When a RecA nucleoprotein filament senses a region of homology in a region of undamaged dsDNA, it catalyzes strand invasion and exchange in an ATP dependent fashion (44). This allows undamaged DNA to serve as a template for synthesis by a DNA polymerase. Extension of the tail of the invading DNA leads to Holliday junction formation. Holliday junctions are resolved by the RuvABC complex (45).

The crystal structure of RecBCD bound to a blunt ended DNA hairpin has been solved (41). The structure (shown in figure 1.4) offers valuable insight into the functions of the various domains of this multi-component DNA processing machine. As blunt ended DNA enters the complex, the strands are separated at the "pin" domain of RecC and sent down different tunnels in the complex. RecB and RecD serve as the motors for the RecBCD complex, using 2-3 ATP's total per base traveled

along the DNA (46). The 3'-strand is sent first past the helicase domain of RecB, past

the χ scanning site in RecC, and finally on to the nuclease domain of RecB, where it

is degraded. RecB uses ATP to drive motion along the DNA, consuming on average

one ATP per nucleotide traveled (47).

The 5'-strand of DNA is sent to RecD, which acts as a second molecular

motor to help drive procession of RecBCD along the DNA. After being fed through

RecD, the 5'-strand is directed out of the enzyme and on to the nuclease domain of

RecB, where it is digested. The RecD subunit of the RecBCD complex is also

responsible for regulation of activities found on other subunits of the complex. In

Δ*recD* mutants, there is no production of χ specific fragments and RecA is loaded

constitutively on ssDNA during unwinding (48).

High salt causes specific dissociation of the RecD subunit from the rest of the

complex, indicating that the association between RecB and RecC is stronger than the

association of either with RecD (49). Separately, work with RecD found DNA

dependent ATPase activity, but detected no nuclease activity (50). Purified

separately, RecB has been found to be a DNA dependent ATPase.

Mutation of *recB* (D1080A) caused RecBCD to be inactive as a nuclease (51).

RecBCD maintained unwinding with the RecD subunit helicase activity. Production

of χ-specific fragments was completely attenuated (51). Deletion of the 30 kDa C-

terminal domain of RecB completely removed the nuclease activity of RecBCD,

leaving the helicase activity of the complex intact (51,52). Subsequent research

identified the removed domain as a nuclease (53).

Mutation of the ATPase domain in either *E. coli* RecB or RecD slows down unwinding by RecBCD. Dillingham (54) reported that wild type RecBCD unwound plasmid DNA at a maximum rate of $1460 \pm 50$ bp/s. With the ATPase deficient *recD* mutant RecBCD$^{K177Q}$, the maximum rate of unwinding was $800 \pm 20$ bp/s. When *recB* was mutated to abolish ATPase activity (RecB$^{K29Q}$CD), the maximum rate of unwinding dropped down to $480 \pm 40$ bp/s. This indicated that both helicases were important to unwinding of DNA by RecBCD. The polarity of the DNA unwinding activities of RecB and RecD has been found to be opposite to each other. RecB moves along DNA in a 3'-5' manner, while RecD moves in a 5'-3' direction (50,55).
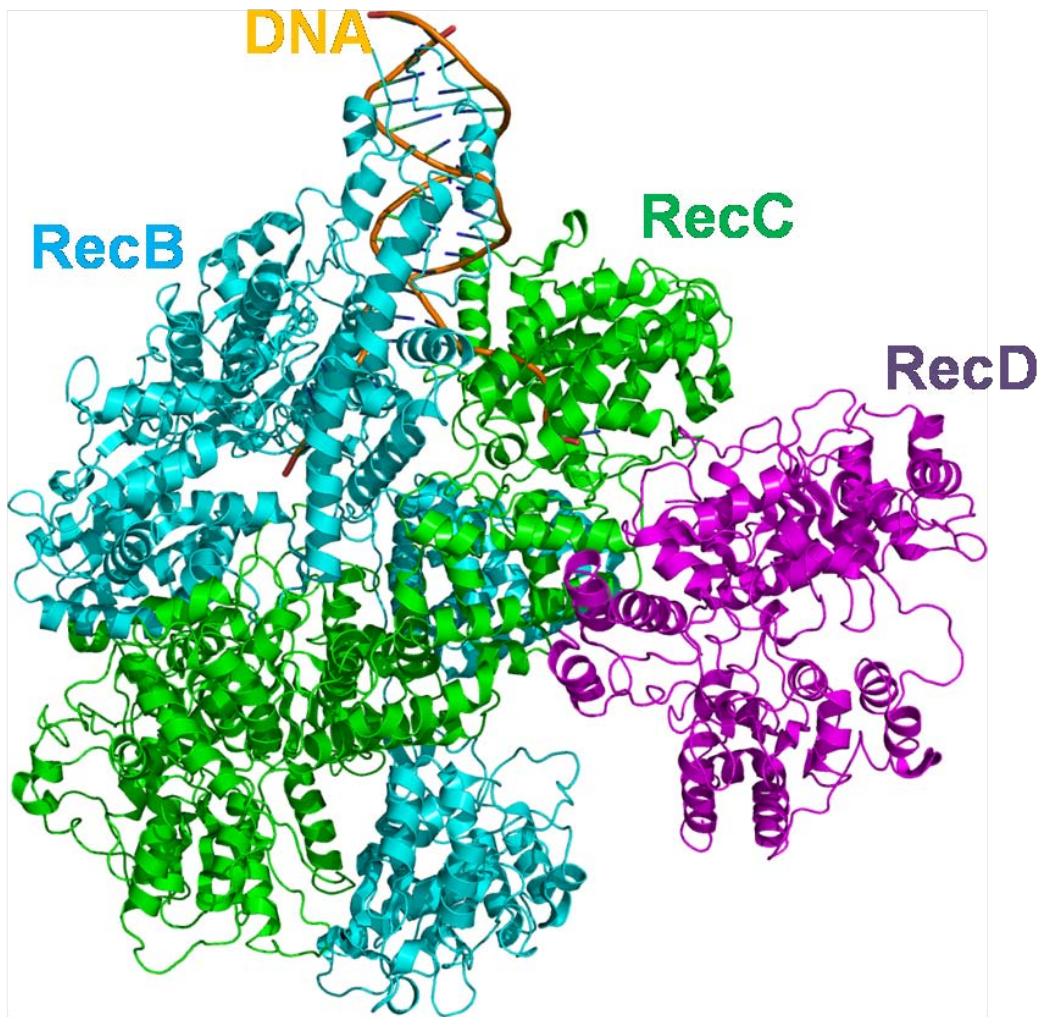
**Figure 1.4: Crystal structure of RecBCD.** Individual subunits are shown in different colors. RecB is shown in blue. RecC is green, and RecD is shown in violet. Co-crystallized hairpin DNA is shown in orange. Adapted from Singleton, et al (41).

1.2.1 Similar bacterial systems of Homologous Recombination

RecBCD mediated homologous recombination is not the only system available to bacteria for the repair of double strand breaks. When *E. coli* is rendered Δ*recBCD*, and suppressor mutations are introduced into the genes *sbcB* and *sbcC(D)* (nucleases that degrade recombination intermediates), the organism is still capable of

repairing double strand breaks. This can be achieved by using the RecFOR system, a system primarily involved in gap repair (22,56). Recent evidence suggests that the RecFOR pathway may actually be the primary pathway of DSB repair in *D. radiodurans* (57).

*Bacillus subtilis* utilizes a functional counterpart to the RecBCD complex, termed AddAB (58). Whereas the functional unit of RecBCD is trimeric, AddAB operates as a dimer. Fundamentally, the result of processing of DSB events by these different systems results in the same product: a RecA nucleoprotein filament. This filament then proceeds through the later steps of HR as mentioned above.


## 1.3 *Deinococcus radiodurans* RecD2

The *D. radiodurans* genome contains no homologues to the RecBCD complex. Sequence analysis has identified a homologue of RecD (27), termed RecD2. RecD2 from *D. radiodurans* has been used for biochemical studies, due to structural similarity with the RecD subunit of RecBCD (figure 1.5) (15). The function of RecD2 in *D. radiodurans* is unknown, as RecD homologues have been characterized only as a component of the RecBCD complex.

The disruption of *recD2* in *D. radiodurans* has been studied *in vivo* (59,60). Results of research by two different teams suggested that *recD2* mutants are sensitive to treatment by hydrogen peroxide. Both groups found sensitivity of *recD2* mutants to UV, although the degree of sensitivity was different for both studies. Zhou, et al (60) made deletion mutants of *recD2*, specific to the N- and C-terminal domains of the

protein. They found via complementation assays that the whole sequence of *recD2* was necessary for the protective effect of the enzyme *in vivo*.

Servinsky and Julin (59) performed transformation assays on **Δ***recD2* mutants of *D. radiodurans*. They found that **Δ***recD2* mutants were more easily transformable with exogenous DNA than was wild type *D. radiodurans*. In addition, the authors report that **Δ***recD2* mutants showed no increase in sensitivity to the cross-linking agent mitomycin C (MMC) or the alkylating agent methylmethanesulfonate (MMS). They suggest that RecD2 performs no critical role in alkylation repair in *D. radiodurans*. The overall findings of both papers suggest a role for RecD2 in DNA repair in *D. radiodurans*.

The sequence of *D. radiodurans recD2* suggests helicase activity based on homology of the C-terminal region to sequences of *recD* from the organism *B. subtilis* and members of the genus *Chlamydia* (14). *D. radiodurans* RecD2 has been found to unwind ssDNA in a 5'-3' direction in an ATP dependent fashion, with a preference for 5'-tailed and forked substrates of 10-12 nt overhang (15). No unwinding activity was seen on substrates with blunt ended or 3'- single strand overhangs. RecD2 has the ability to unwind substrates bearing a 5'- overhang, without the need for a fork. RecD2 was found to be less able to unwind substrates as the double stranded region increased from 20bp to 52bp (15).

The crystal structure of a C-terminal region of RecD2 has been published (61,62). The authors crystallized a truncation construct of RecD2, missing the first 150 amino acids of the overall sequence. Visible in the structure (PDB ID: 3E1S) are the residues from 191 to 715, along with the C- terminal hexahistidine tail used for

purification. This structure was compared to the previously obtained structure for *E. coli* RecBCD (41). The comparison of these two structures allowed the group to further elucidate information pertinent to the structure of RecD like proteins. Based on molecular replacement with RecD2, a greater level of refinement was possible for the helicase domains of the *E. coli* RecD, which had previously been poorly visible due to poor electron density. In addition to the crystal structure, the authors reported biochemical data that their truncation construct maintained the ability to unwind DNA.
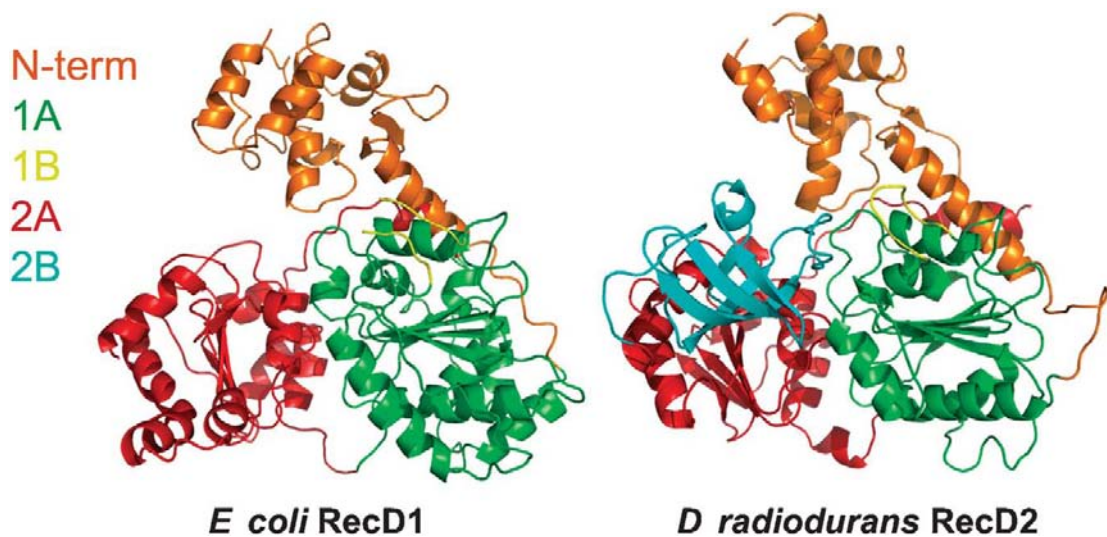


**Figure 1.5: Comparison of crystal structure of *E. coli* RecD1 with *D. radiodurans* RecD2.** Both proteins were crystallized by Saikrishnan, et al (61). Domains are colored the same in both images. The ATPase domains 1A and 2A are shown in green and red, respectively. The helicase wedge domain (1B) is yellow. The N-terminal region is colored orange, and the SH3 domain (domain 2B) is shown in blue.

Among the more important findings possible with the crystallization of RecD2 was the identification of a wedge domain responsible for the separation of individual strands as RecD2 progresses along the DNA. This region, comprising a short span of

only 10 residues from 412-419 (shown in red in figure 3.5, in section 3.3.1), was identified as important to the function of a range of helicases. When the researchers mutated this region, all unwinding activity was abolished, although ATP hydrolysis activity was still evident at wild type levels (61). The same structural feature was identified in *E. coli* RecD, but it remains unclear whether the wedge is important to activity of *E. coli* RecD (61).

One of the unusual structural features identified in the crystal structure of RecD2 is an SRC homology domain 3 (SH3) fold (shown on right in figure 1.5). A co-crystallization of RecD2 with $dT_{15}$ found interactions between the SH3 domain of RecD2 and the eight visible nucleotides (62). This domain (residues 576-640) is not commonly seen in bacterial proteins; more often, this is seen as a characteristic of eukaryotic signaling proteins. The SH3 domain serves primarily in a protein- protein signaling capacity in proteins containing it. Considerable variability has been found in the members of this family of proteins in the nature of binding to other proteins (63).

Co-crystallization of RecD2 with $dT_{15}$ was performed in the presence of either ADP or ADPNP (a non-hydrolysable ATP analog). Based on these crystals, the authors determined a reorganization of the protein was taking place upon nucleotide binding. This led to the suggestion that RecD2 translocates along DNA as a monomer, utilizing an "inchworm" model of translocation. In the structure of RecD2 with $dT_{15}$, it is interesting to note that only 8 nt are visible, in agreement with the previous finding that 10 nt are necessary for binding of RecD2 to DNA(15).

## 1.3.1 RecD2 is a superfamily I helicase

The amino acid sequence of *D. radiodurans* RecD2 indicates the C-terminal region of the enzyme belongs to the superfamily I helicases (15). *E. coli* RecBCD is a member of this family, as well as the enzymes UvrD and Dda helicase from the T4 bacteriophage (64). Members of this group are related by sequence homology and utilize ATP hydrolysis to cause unwinding of dsDNA into ssDNA. Even with this similarity, superfamily I helicases vary significantly in co-factor use, substrate preference, directionality, and processivity along DNA (65).

Within the superfamily I helicases, RecD helicases have variations of their own. RecD helicases that form a component of a RecBCD complex are shown in area A of figure 1.6. RecBCD-type RecD helicases are grouped mainly due to their association with the RecBCD complex; the most prominent example of this is RecD from *E. coli*. RecBCD-type RecD helicases also bear a resemblance to each other in the length of the N- terminal sequence prior to their first helicase motif (15,62).

Members of the RecD helicase family that are not known to associate with any other proteins are shown in figure 1.6, area B. These proteins tend to be characterized by long N-terminal sequences prior to the first helicase motif. The length of these N-terminal leader segments is variable. In the case of *D. radiodurans* RecD2, over half of the sequence is found before the beginning of the helicase region of the protein (14,15). The role of the N-terminal region in the behavior of the RecD helicases remains unreported. In the case of *D. radiodurans* RecD2, sequence analysis suggests the presence of three DNA-binding modules. This region is not well conserved among similar proteins (14).
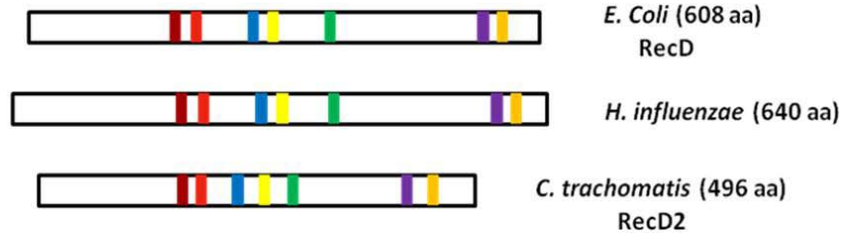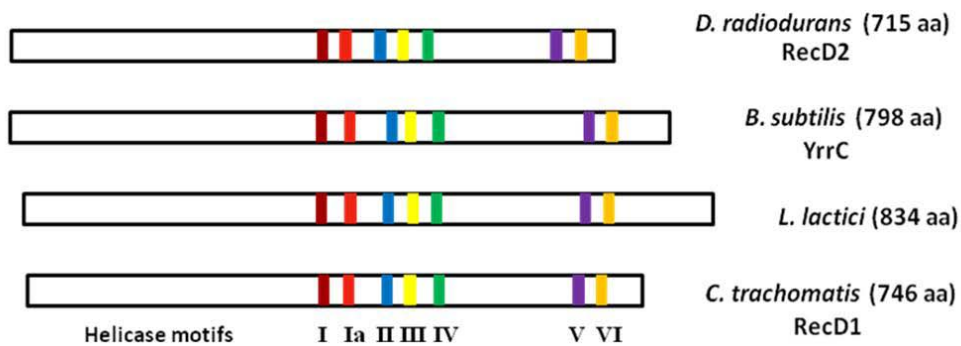
**Figure 1.6: Schematic alignment of RecD helicases.** Shown in **A**: RecD helicases that comprise part of a RecBCD complex. In **B** is shown RecD helicases that have no identified binding partner. Sequences are aligned according to the position of helicase motif **I**. Colored bars represent relative location of helicase motifs. Adapted from (15).

## 1.4 Mechanisms of DNA unwinding by helicases

Three basic mechanisms of DNA unwinding by helicases have been proposed. In the first, a monomeric helicase unit extends a region of ssDNA by an inchworm mechanism. A monomolecular helicase contains two DNA binding sites in the same protomer, alternating conformation between ATP, ADP·P, and unbound states as the helicase unzips the dsDNA (66,67). Based on the crystal structure, the authors

20

suggest RecD2 may translocate along single stranded DNA by the inchworm

mechanism detailed in figure 1.7 (61).
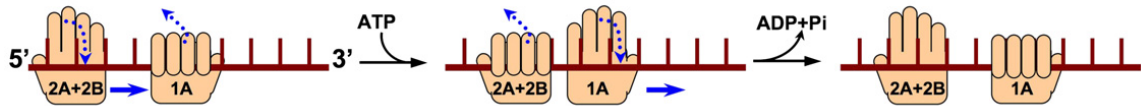


**Figure 1.7: Monomeric inchworm model of helicase translocation.** Shown above
are domains of RecD2 at the site of interaction with a strand of ssDNA. In the first
picture, binding of ATP causes domains 2A and 2B to move 5'-3' along the DNA. At
the same time, domain 1A is anchoring the DNA. Hydrolysis of ATP causes domain
1A to release, with domains 2A and 2B now anchoring the DNA. Release of ADP
causes domain 1A to move approximately 1 nucleotide along the DNA, resetting the
enzyme for the next cycle (62).

The second basic mechanism, shown in figure 1.8, involves rolling of a

dimeric helicase complex along the DNA. In this case, each binding site is located on

a separate protomer with two units acting together as a dimer (68). The mechanism of

helicase movement for dimeric helicases is thought to be the same as for the

monomeric helicases, with the complex moving along the DNA in an inchworm

fashion (68,69).
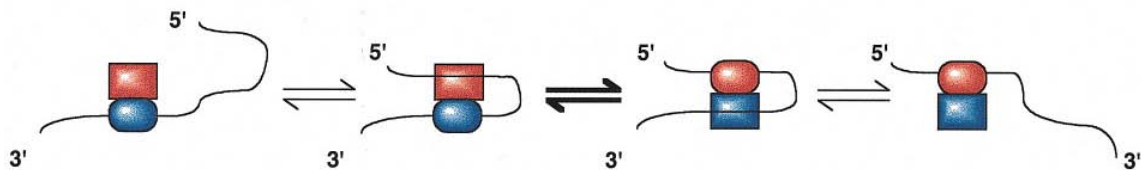


**Figure 1.8: Active rolling mechanism of helicase translocation.** This model of
movement requires two protein units (shown in red and blue) acting as a dimer. In the
above picture, each protein alternates binding of DNA with the other, causing the
complex to "roll" along the DNA in an ATP dependent fashion. The tight contacting
units are indicated by circles, with loose contacting units indicated by squares (70).

21

The hexameric helicases in superfamily 4 utilize another mechanism. In this

mechanism, each unit of the multimer acts in a sequential fashion to advance the

helicase complex along the DNA (71-73). In this model, recently reviewed (74),

ssDNA passes through the center of a doughnut shaped ring. Each monomer contacts

the DNA in succession, processing the DNA in a structure resembling a right handed

spiral staircase. These helicases consume, on average, 1 ATP per nucleotide advanced

in the DNA (75).

A proposed kinetic mechanism for DNA unwinding by a helicase is shown in

figure 1.9. A helicase (blue triangle) is bound to a DNA substrate (upper left of figure

1.9). Cycles of binding, hydrolysis, and dissociation of ATP cause the helicase to

move along the DNA, until it dissociates or until the DNA is unwound. If the helicase

dissociates from the DNA prior to completion of unwinding, the helicase must re-

bind to unwind further, or the DNA will re-anneal. The average number of bases

unwound per rate determining step of the unwinding cycle is the **kinetic step size**.

The **processivity** of a helicase is the tendency of that enzyme to remain bound to the

DNA during multiple cycles of ATP association, hydrolysis, and dissociation (45).

The processivity of a helicase is separately measured from its **unwinding rate**, which

is the speed that the enzyme moves along the DNA.

Characterization of the step size (with reference to the DNA) of DNA

helicases is an important component of the overall understanding of these proteins

(76). The kinetic step is observed based on the slowest step among the many that

occur in the process of unwinding by a helicase. Multiple steps of ATP hydrolysis

may occur in one kinetic step. Helicases with a high unwinding rate may still have a

small number of nucleotides per kinetic step. Multiple kinetic steps may be necessary

to unwind a dsDNA substrate of a given length.
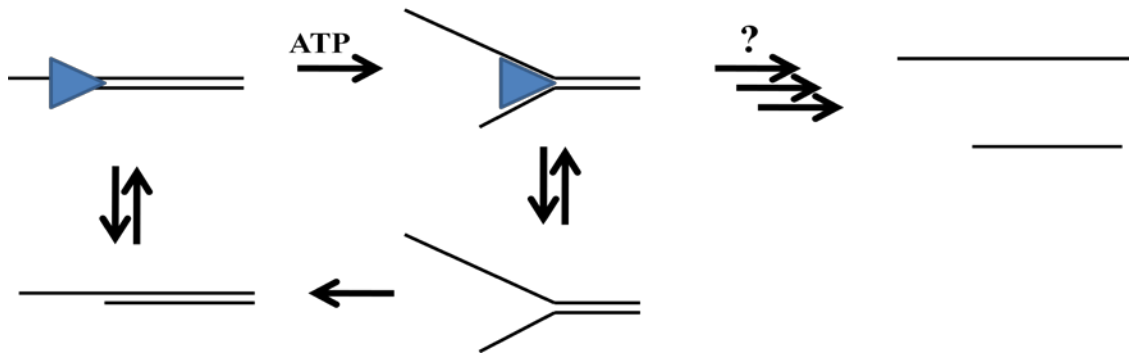


**Figure 1.9: Schematic showing a kinetic step of a helicase.** In the upper left, the
helicase (blue triangle) is bound to the DNA. Multiple ATP hydrolysis steps cause the
helicase to translocate along the DNA. If the helicase is incapable of unwinding the
whole length of the DNA in one kinetic step, it must re-bind to progress, or the DNA
will re-anneal. The number of kinetic steps a helicase must use to unwind a dsDNA
substrate (represented by a "**?**") depends on the length of the substrate.

Analysis of time courses of unwinding allows determination of the number of

kinetic steps required to unwind substrate DNA of various specific lengths.

Application of a model derived from this analysis can then be used to determine the

kinetic step size for the protein (77). Careful kinetic analysis can aid in the

determination of how many protomers are necessary to make up the active unit of a

helicase. More often, this is carried out using other methods, such as cross-linking

and size exclusion chromatography.

## 1.5 Summary of research conducted

When purified separately from RecB and RecC, RecD from *E. coli* exhibits poor solubility, making characterization of this protein challenging (49). We studied the homologous protein RecD2 from *D. radiodurans*. In *D. radiodurans*, RecD2 has no known binding partners, which facilitates more directed research into the behavior of RecD like helicases.

RecD2 from *D. radiodurans* has been purified; initial characterization has determined RecD2 is a helicase with 5'-3' specificity, and a preference for 10nt 5' overhangs (15). The role of RecD2 in DNA repair in *D. radiodurans* is yet unclear, even as the literature on this enzyme expands (15,59-62,78). Kinetic characterization of RecD2 with a range of substrates implicated as intermediates in recombination was performed to better understand this enzyme.

We sought to separate regions of RecD2 for kinetic characterization. The C-terminal domain contains all 7 of the conserved helicase motifs, according to analysis by Makarova, et al (14). Characterization of the domains of RecD2 will aid in localization of the various activities of the overall enzyme. We subjected RecD2 to limited proteolysis to investigate the minimum portion of the protein required for helicase activity. After identification of a region of RecD2 refractory to proteolysis, we generated truncation constructs based on this area of the protein. We were able to purify the N-terminal region in soluble form. We were not able to purify the C-terminal region in soluble form.

As part of the continued characterization of the RecBCD enzyme carried out by previous members of the Julin group, we sought to characterize the effect of

mutation in the metal binding residues of the active site of the nuclease domain of RecB from *E. coli*. Mutants in the $Mg^{2+}$ binding site of the nuclease domain of RecB generated by Shamali Roychoudhury were investigated. Mutants were characterized by Fenton degradation and the ability to digest ssDNA.

# Chapter 2: Kinetic characterization of RecD2

## 2.1 Introduction

The characterization of RecBCD from *E. coli* has been an ongoing effort, carried out even to the stage of crystallization of the complex (41,62). Individual activities have been biochemically separated from the overall complex by limited proteolysis (53) or by selective reconstitution (49). These efforts and others have allowed a quite detailed knowledge of the various functions of RecBCD. Knowledge of the behavior of RecBCD has been limited, however, by the limited solubility of *E. coli* RecD in the absence of the other members of the RecBCD complex. Efforts to bridge this gap have included reconstitution of RecBCD with RecD refolded from inclusion bodies (49,50). When expressed individually, the RecD of *E. coli* behaves as a helicase that couples translocation along DNA with hydrolysis of ATP (50).

Our efforts have been focused on the kinetic characterization of the RecD homolog RecD2 from *D. radiodurans*, which possesses no known partners homologous to RecB or RecC from *E. coli*. It is hoped that the ability of this protein to be expressed in a soluble form in the absence of any binding partners will allow more detailed characterization of the biochemical and enzymatic properties of RecD family proteins.

Previous work with RecD2 from *D. radiodurans* has found the enzyme is a helicase with a preference for 5' overhang or fork substrates, with a minimum overhang requirement of 10 nucleotides. Experiments were conducted to establish ATP hydrolysis and dsDNA unwinding rates for RecD2. Based on the slopes of the

early linear part of the unwinding time courses, RecD2 was found to unwind dsDNA at a rate of 2 ($\pm$ 0.5) bp/ RecD2/ sec for a 5' overhang substrate, and 16 ($\pm$ 2) bp/ RecD2/ sec for a forked substrate. The authors reported ATP hydrolysis linked to unwinding occurred at a rate of 9 ($\pm$ 0.3) ATP hydrolyzed/ sec/ RecD2 (15).

Our kinetic characterization of RecD2 was carried out using a series of reactions that were set up to address the unwinding behavior under single turnover conditions. Single turnover kinetics allowed us to measure unwinding rates and step size for RecD2 (77). The performance of these reactions was carried out with a variety of dsDNA substrates. Further reactions were carried out using a rapid quench flow device, to allow for the mixing and quenching of reactants on the millisecond time scale.

When performing single turnover experiments, an ssDNA "trap" is added to a mixture of enzyme pre-bound to substrate DNA. This prevents re-binding of the enzyme to the substrate during the course of unwinding, if the enzyme dissociates. In figure 2.1, a single turnover kinetic system is shown. The ssDNA trap is shown in green; red X's are placed on the steps that cannot proceed in the presence of trap.
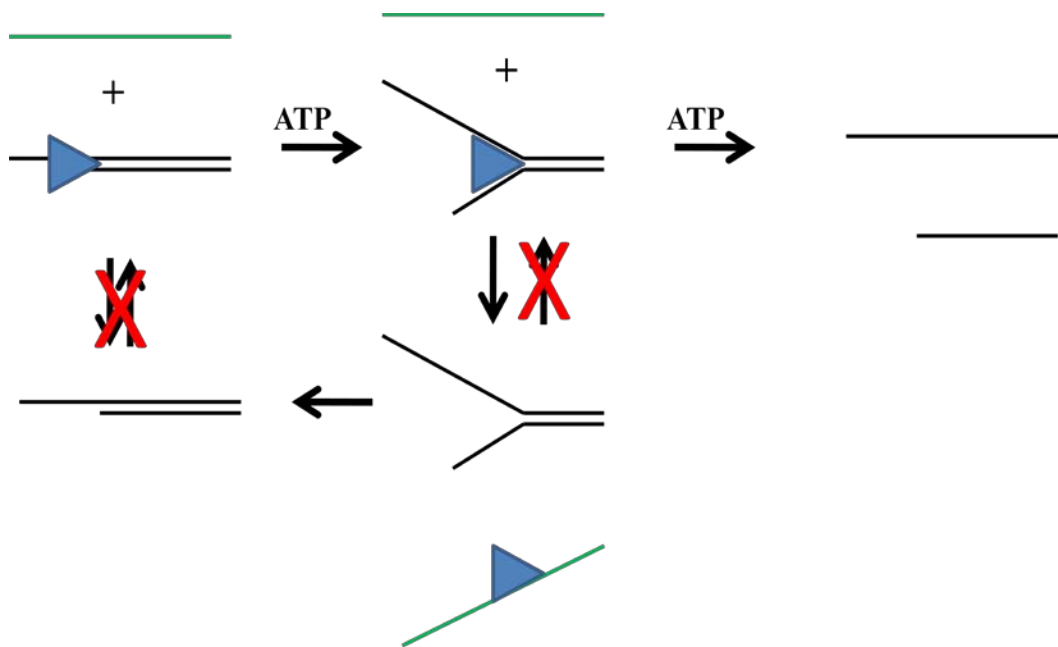
**Figure 2.1: Unwinding of DNA by a helicase under single turnover conditions.** In the presence of an ssDNA competitor (green line), the enzyme (blue triangle) cannot re-bind if it dissociates prior to complete unwinding of substrate DNA. Reactions are monitored for production of ssDNA, shown at right.

We used cross-linking and SEC to expand our understanding of the active complex involved in unwinding of DNA by RecD2. Cross-linking with glutaraldehyde was performed according to established protocols (79,80). Cross-linking was performed under a variety of conditions to capture any protein-protein interactions that could occur in an active unwinding complex.

## 2.2 Materials and Methods

### 2.2.1 Expression and Purification of *D. radiodurans* RecD2 in *E. coli*

*Deinococcus radiodurans* RecD2 was expressed with a C-terminal hexahistidine fusion tag in vector pET21a (Novagen), as constructed by Jianlei Wang (15). The plasmid for this construct (termed pDrRecD-21) was transformed into chemically competent BL21-DE3 and plated on LB agar with 100 µg/ml ampicillin. Plates were then grown overnight at 37 °C. The next day, a single colony was removed from the plate and grown at 37 °C with vigorous shaking overnight in 50 ml LB media with 100 µg/ml ampicillin. After another day, this culture was inoculated into 1 L of ZYP-5052 medium (1% bacto-tryptone, 0.5% yeast extract, 1 mM $MgSO_4$, 25 mM $(NH_4)_2SO_4$, 50 mM $KH_2PO_4$, 50 mM $Na_2HPO_4$, 2.8 mM dextrose, 5.8 mM lactose and 0.5% glycerol, pH unadjusted) plus 100 µg/ml ampicillin (1:20 dilution) in a 4 L Erlenmeyer flask and placed at 20 °C with shaking overnight.

On day two, cells were harvested by centrifugation at 5,000 x g in a Beckman model J2-21 centrifuge and the cell pellet placed at -80 °C overnight. On day three, the cell pellet was re-suspended in $Ni^{2+}$ ·column buffer (20 mM potassium phosphate, pH 7.5, 0.5 M NaCl, 1 mM DTT) containing 20 mM imidazole and sonicated. Sonication was performed on a Branson Sonifier model 450 with microtip and the settings: duty cycle 50, intensity 5, duration 10 minutes on ice. PMSF (5 mM final) was added to the buffer immediately prior to sonication to inhibit serine protease activity. After sonication, the lysate was centrifuged at 10,000 x g for 2 hours at 4 °C and the supernatant filtered through a 0.45 µm filter.

Filtered lysate was then loaded onto a 5 ml $Ni^{2+}$-NTA column (Pro-Bond Resin, Invitrogen Corp.) and washed with 5 column volumes of wash buffer (60 mM potassium phosphate, pH 7.5, 0.5 M NaCl, 20 mM imidazole, and 1 mM DTT). Protein was eluted from the column by a 50 ml gradient of 60-500 mM imidazole in $Ni^{2+}$ column buffer. Samples (24 µl) of each fraction were taken, mixed with 6 µl 6x SDS loading buffer (350 mM Tris·HCl pH 6.8, 10% SDS, 30% glycerol, 6 mM DTT, 0.01% bromphenol blue), and placed at 95 °C for 1 minute. These samples were then loaded onto 10% SDS-PAGE gels (29:1 acrylamide: bis-acrylamide) and run at 150 V constant for 1 hour. Gels were then stained with Coomassie brilliant blue gel stain (9.75% glacial acetic acid, 45% methanol, 45% $dH_2O$, and 0.25% Coomassie brilliant blue R-250) for 30 minutes and destained with fast destain (7% glacial acetic acid, 40% methanol, and 53% $dH_2O$) until developed. Fractions containing the highest level of eluted protein were pooled and placed in a dialysis bag (Spectra-Por, MWCO 12-14,000 Da, Spectrum Medical). The dialysis bag was then placed in 2 L of buffer A (20 mM potassium phosphate, pH 7.5, 5 mM DTT, 1 mM $Na_2$·EDTA, 10% glycerol) containing 250 mM NaCl and allowed to dialyze overnight at 4 °C.

The next day, dialyzed eluant was loaded on to a 5 ml ssDNA·cellulose column (Sigma) and washed with 5 column volumes of Buffer A + 500 mM NaCl. Step gradient elution followed, with 30 ml steps of 1 M and 1.5 M NaCl in Buffer A. Fractions were analyzed by 10% SDS-PAGE. Fractions containing the largest amount of protein were combined into a dialysis bag. This dialysis bag was placed into 2 L of enzyme storage buffer (20 mM potassium phosphate, pH 7.5, 250 mM NaCl, 5 mM DTT, 1 mM $Na_2$·EDTA, and 50% glycerol) and dialyzed overnight at 4 °C. The

following day, the concentration of the purified RecD2 was determined by absorbance at 280 nm with a calculated extinction coefficient of 52,060 $M^{-1}cm^{-1}$ (ProtParam, ExPasy.org). Aliquots (100 µl) were numbered and placed in a -80 °C freezer for later use. The best yield from this method was 2.8 mg purified RecD2 from 10 g wet cells.

## 2.2.2 Size Exclusion Chromatography

Size exclusion chromatography was conducted on RecD2 to determine the oligomeric state of the protein. For this study, either 500 µl of Bio-Rad gel filtration standards or 500 µg of RecD2 in 500 µl storage buffer was loaded onto a Superdex 200 10/300 GL column attached to an Akta FPLC (GE Life Sciences) located at UMBI-CARB in the lab of Zvi Kelman, Ph.D. The column had been previously equilibrated with a buffer containing 50 mM potassium phosphate, pH 7.5 and 150 mM NaCl, at room temperature.

Molecular weight standards were run over the column for the purpose of generating a molecular weight standard curve for the column. Peak retention times were plotted against the $\log_{10}$ of the molecular mass for each of the protein standards. This was then used to correlate the molecular weight of any eluted protein in the range with the elution volume of that protein by matching the y-intercept of the peak elution volume on the standard curve. Back calculating from the y-intercept value gave the apparent molecular mass of the eluted protein.

With this standard curve, FPLC runs with RecD2 could be analyzed for peak retention times and fit to the standard curve. From this, the molecular weight of peak

fractions was estimated. Three runs were completed and analyzed by this method using Excel. Samples were also analyzed by 10% SDS-PAGE (29:1 acrylamide: bis-acrylamide) and stained with Coomassie stain, to confirm the UV trace data.

## 2.2.3 Cross-Linking of RecD2 using glutaraldehyde

Initial cross-linking experiments were conducted as a time course according to established methods (79,81,82). RecD2 (1 µM final) was added to a cross-linking solution containing 25 mM HEPES pH 7.5, 10% glycerol, 1 mM EDTA, 1 mM β-ME, and 50 mM NaCl. All cross-linking experiments were conducted at room temperature. Addition of glutaraldehyde started the reaction. Samples were removed at various times up to 20 minutes. Each aliquot was quenched with addition of Tris·HCl to a final concentration of 100 mM, along with 6x SDS loading buffer, and stored on ice until the time course was complete. Samples were loaded on to 7.5% SDS-PAGE (37.5:1 acrylamide: bis-acrylamide) and run at 150 V for 1 hour. Gels were either developed by the silver staining protocol or by the western blot protocol with the RecD2 antibody (see section 3.2.4 for method).

To determine the minimum amount of glutaraldehyde necessary to cross-link, a series of reactions was performed with 1 µM final RecD2 in cross-linking buffer, supplied with either 14 µM, 140 µM, 1.4 mM, or 14 mM (final) glutaraldehyde. Reactions were allowed to proceed at room temperature for twenty minutes before being quenched as above. Samples were loaded on to 7.5% SDS-PAGE (37.5:1 acrylamide: bis-acrylamide) and run at 150 V for 1 hour. Gels were developed by the silver staining protocol.

## 2.2.4 DNA Binding and Unwinding Assays

Synthetic DNA oligonucleotides (shown in Table 2.1) were purchased from IDT Corp. and purified via passage over a P6 size exclusion spin column (Bio-Rad). Concentrations of purified oligonucleotides were determined on a Cary 500 UV-Vis spectrophotometer by calculation based on absorbance at 260 nm and extinction coefficients provided by the manufacturer for each oligonucleotide.  Stock solutions of oligonucleotides were made with 10 mM Tris·HCl pH 8.0 and stored at -20 °C until use.

| Name | Length (nt) | Sequence 5'-3' |
|------|-------------|----------------|
| **Table 2.1.  Oligonucleotides used** | | |
| **HMC 1** | 32 | GCCGTAGTATGCACATCGACATCCATCACAT |
| **HMC 2** | 20 | GTCGATGTGCATACTACGGC |
| **HMC 3** | 20 | GCCGTAGTATGCACATCGAC |
| **HMC 3a** | 12 | GCCGTAGTATGC |
| **HMC 4** | 32 | TACAGCTACCTAGTCGATGTGCATACTACGGC |
| **HMC 4ext** | 44 | TACAGCTACCTAGTCGATGTGCATACTACGGCGCATACTACGGC |
| **HP1** | 55 | TACAGCTACCTAGTCGATGTGCATACTACGGCTTTGCCGTAGTATGCACATCGAC |

## 2.2.5 5'- labeling of DNA with polynucleotide kinase using γ-$^{32}$P-ATP

Substrate DNA was end labeled with $T_4$ polynucleotide kinase (PNK) (Fermentas, Inc.) using γ-$^{32}$P-ATP. Each 30 µl labeling reaction contained 50 mM

Tris·HCl, pH 7.6, 10 mM $MgCl_2$, 5 mM DTT, 200 µM spermidine, 200 µM EDTA, 107 nM γ-$^{32}$P-ATP (Perkin Elmer, 6000 µCi/ mmol), and 333 nM DNA. Before addition of PNK, 1 µl of the reaction mixture was removed for scintillation counting and 0.5 µl was spotted on to a TLC plate (JT Baker, Inc), that had been pre-treated by soaking in 2 M NaCl for 2 hours, rinsing in $dH_2O$, and allowing the plate to air dry.

The reaction was started by addition of 15 units of PNK and placed into a 37 °C water bath. After 1 hour had elapsed, 333 nM (final conc.) of ATP (non-radioactive) was added, and the reaction was allowed to proceed for 30 minutes more. At the conclusion of this time, 0.5 µl of reaction was spotted on to the TLC plate. Excess unreacted ATP, free phosphate, and enzyme were removed from the now 5'-$^{32}$P-labeled DNA via treatment with the Qiagen nucleotide cleanup kit (Qiagen, Inc.). Labeled HMC 3a was purified by passage over a P6 column. After cleanup was complete, 1 µl was taken for scintillation counting, and 0.5 µl was spotted on to the TLC plate. The TLC plate was PEI-cellulose for the solid phase and 1 M $NaH_2PO_4$ pH 3.5 for the mobile phase. After developing, the TLC plate was dried via heat lamp and placed into a cassette for imaging on a STORM phosphorimager. Quantitation was carried out with ImageQuant and data workup was in Excel. Scintillation samples were diluted 1 µl into 199 µl of $ddH_2O$ and mixed into 3 ml of biodegradable scintillation cocktail (Bio-Safe II, Research Products International) before being counted on a Beckman Coulter scintillation counter.

2.2.6 Annealing of dsDNA substrates for binding and unwinding assays

Annealing of dsDNA substrates (shown in Table 2.2) for binding and unwinding reactions was carried out using a mix of labeled ssDNA and a complementary sequence of unlabeled ssDNA. Each annealing mixture contained 20 mM Tris·HCl pH 7.5, 50 mM NaCl, and 1 mM $MgCl_2$, along with 20 nM of each piece of ssDNA. Some annealing mixtures contained an additional 8 mM $MgCl_2$ to aid annealing. Annealing was carried out by heating the mixture to 96 °C in a water bath for three minutes, then allowing the mix to cool to room temperature before use.

| Table 2.2. DNA structures used | | | |
|---|---|---|---|
| **Name** | Composed of | Bases Paired | Overhang |
| **12nt:20bp** | HMC 3 + HMC 4 | 20 | 12nt (5') |
| **24nt:20bp** | HMC 3 + HMC 4ext | 20 | 24nt (5') |
| **12ntY20bp** | HMC 1 + HMC 4 | 20 | 12nt fork |
| **20nt:12bp** | HMC 3a + HMC 4 | 12 | 20nt (5') |
| **HP1** | HP1 | 20 | 12nt (5') |

2.2.7 Binding of RecD2 to substrate DNA

Binding studies were performed in order to characterize the affinity of RecD2 for various DNA substrates. For these experiments, varying concentrations of RecD2 were mixed in a micro-centrifuge tube with a fixed concentration of DNA. Substrate DNA (1 nM, 10 nM, or 100 nM) was added to a micro-centrifuge tube containing the final concentrations of the following reagents: 10 mM $MgCl_2$, 50 mM Tris·HCl, pH 7.4, 1 mM DTT, 0.1 mg/ml BSA, and 5% glycerol. RecD2 was added in varying amounts according to the conditions, and mixtures were allowed to sit at room temperature. After 20 minutes, glycerol was added to a final concentration of 5%, and

samples were loaded on to a 10% TBE-PAGE (29:1 acrylamide: bis-acrylamide)

native gel. Gels were run at 50 mA (constant) for 1 hour with 1x TBE running buffer,

and then placed on a piece of Whatman DE81 diethylaminoethyl cellulose paper

which had been placed on a piece of Whatman gel drying filter paper. This was

placed in a Bio-Rad model 583 gel dryer and covered with plastic wrap before drying

for 1 h 30 min. Dried gels were exposed overnight in phosphorimager cassettes (GE

life sciences) and imaged on a STORM phosphorimager (GE life sciences).

Quantitation of gels was conducted with the program ImageQuant (GE life sciences).

The percent DNA bound was determined by quantitation of the relative amounts of

bound and unbound $^{32}$P-DNA present in each lane. Subsequent data workup and

curve fitting were conducted with either Excel (Microsoft) or Origin (Origin Labs).

Quantitation for the binding reactions was performed with the program

ImageQuant and the data fit to the equation, below, using the software package

SigmaPlot (Systat Software). In this equation, **F** is the fraction bound, corresponding

to the **y** values on the curve. **$F_{max}$** is the maximum fraction bound in the curve, and **$E_t$**

is the concentration of RecD2, in nM, at any point in the curve (corresponding to the

**x** values). The total concentration of DNA present is **$D_t$**. The least squares fit returned

a value for **$K_d$**.

$$F = F_{max} * \{(K_d + E_t + D_t) - [(K_d + E_t + D_t)^2 - 4E_tD_t\}^{1/2}\}/ 2D_t$$

2.2.8 Binding of RecD2 to dsDNA in the presence of ssDNA

Binding reactions were performed with increasing amounts of ssDNA to

investigate the effect of protein trap on binding by RecD2. For these reactions, a fixed

amount of RecD2 was allowed to bind a fixed amount of dsDNA substrate in the presence of an increasing amount of ssDNA. Reaction mixtures contained 50 mM Tris·HCl, pH 7.4, 2.5 mM DTT, 0.1 mg/ml BSA, 10 mM $MgCl_2$, and 5% glycerol. In addition, they contained 1 nM labeled ssDNA substrate and 20 nM RecD2. Reactions were set up to incorporate an increasing amount of unlabeled ssDNA (the same sequence as the labeled binding substrate) across a range. Binding reactions were allowed to proceed 20 minutes at room temperature, before addition of a one-fifth volume of 30% glycerol. Samples were then immediately loaded on to 15% TBE-PAGE and run for 1 hour at 150 V constant with 1x TBE running buffer. Gels were then dried and imaged as above. Quantitation of gels was conducted with the program ImageQuant (GE life sciences). The amount of DNA bound at each point was determined by quantitation of the amount of bound $^{32}$P-dsDNA and unbound $^{32}$P-ssDNA present in each lane. The amount of $^{32}$P-ssDNA present in the **0** protein trap lane was subtracted from the total amount bound for each lane. Subsequent data workup and curve fitting was conducted with either Excel (Microsoft) or Origin (Origin Labs).

2.2.9 Unwinding in the presence of protein trap: The A/B/C Reactions

Unwinding of dsDNA substrates by RecD2 was conducted via a series of intertwined reactions called the A/B/C reactions. Unwinding reactions were carried out in the presence or absence of 2 µM ssDNA protein trap (DrDSH3Down15- a 40mer). All reactions were carried out at room temperature, with 20 minutes pre-incubation. Before starting the reaction, 10 µl was taken for running on a binding gel;

37

to this sample, 2 µl of 30% glycerol was added (5% final) and the mix loaded on 15% TBE-PAGE (29:1 acrylamide: bis-acrylamide). Another 10 µl was taken to serve as a 0 time point; to this sample was added 3.5 µl of 4x helicase quench (40% glycerol, 2.4% SDS, 100 mM EDTA, 20 nM cold ssDNA, and 0.1% bromphenol blue) and the resulting mix was allowed to sit until the other time points had been taken. Time points were measured from addition of ATP (to a final concentration of 1 mM) and 10 µl samples were taken. All of these samples were quenched with 3.5 µl of 4x helicase quench. After completion of the time course, quenched samples were loaded on 15% TBE-PAGE and allowed to run 1 hr at 150 V constant with 1x TBE running buffer. Gels were dried, exposed, and imaged as above. Quantitation of gels was conducted with the program ImageQuant (GE Life Sciences). The amount of DNA unwound at each time point was determined by quantitation of the amount of $^{32}$P-dsDNA and $^{32}$P-ssDNA present in each lane. The amount of $^{32}$P-ssDNA present in the **0** time point lane was subtracted from the total amount unwound for each lane. Subsequent data workup and curve fitting was conducted with either Excel (Microsoft) or Origin (Origin Labs).

## 2.2.10 The "A" Reaction

Unwinding in the "A" reaction served as a positive control of unwinding, and also served in kinetic analysis of unwinding. Reaction mixtures contained (final concentrations in 100 µl) 50 mM Tris·HCl, pH 7.4, 2.5 mM DTT, 0.1 mg/ml BSA, 10 mM MgCl$_2$, and 5% glycerol. Most reactions contained 1 nM dsDNA substrate and 20 nM RecD2.

## 2.2.11 The "B" Reaction

Unwinding in the "B" reaction tested addition of 2 µM ssDNA protein trap in the reaction. In the "B" reaction, 2 µM ssDNA protein trap (random oligonucleotide 40mer) was added at the same time as the dsDNA (prior to pre-incubation), to directly compete with dsDNA substrate for binding to RecD2.

## 2.2.12 The "C" Reaction

Unwinding in the "C" reaction tested addition of 2 µM ssDNA protein trap in the reaction, but at a different point. In the "C" reaction, ssDNA protein trap (2 µM random oligonucleotide 40mer) was added at the same time as the ATP (after pre-incubation, at the start of the reaction), to allow dsDNA substrate no competition for binding to RecD2 during the pre-incubation. This would ensure only one RecD2 was bound to each dsDNA molecule.

## 2.2.13 Kinetic analysis of RecD2 with the KinTek Rapid Quench Flow device

Certain substrates, such as 12ntY20bp and 20nt:12bp, were unwound too fast by RecD2 at room temperature to conduct accurate experiments by hand. Unwinding was mostly complete in the first 15 seconds (see section 2.3). To examine kinetics of unwinding by RecD2 for these substrates, it was necessary to employ the use of a KinTek model RQF-3 Rapid Quench Flow device.

The KinTek Rapid Quench Flow device requires samples to be set up on the principle of 1:1 mixing during the reaction. Two lines, labeled "A" and "B", contain the reagents prior to mixing. The ingredients for each system are detailed below.

In line A was a solution mixed with the following reagents: 40 nM or 200 nM RecD2, 2 nM substrate dsDNA, 50 mM Tris·HCl pH 7.4, 2 mM DTT, 0.1 mg/ml BSA, 10 mM $MgCl_2$, and 5% glycerol. In reactions where ssDNA trap was added at the same time as substrate dsDNA, 40mer ssDNA trap was added to a concentration of 4 μM.

In line B was mixed the following reagents: 2 mM ATP, 50 mM Tris·HCl pH 7.4, 2 mM DTT, 0.1 mg/ml BSA, 10 mM $MgCl_2$, and 5% glycerol. In reactions where ssDNA trap was added at the same time as ATP, 40mer ssDNA trap was added to a concentration of 4 μM.

## 2.2.14 Reaction Setup

Each line solution was allowed to pre-incubate at room temperature prior to being placed in the RQF-3. For samples containing 20nt:12bp substrate, this pre-incubation was 5 minutes. For each reaction, line A was filled with 15 µl of line A solution. Line B was filled with 15 µl of line B solution. Reaction times were set on the RQF-3, and the appropriate reaction loop was set. Upon pressing the start button, the RQF-3 pressed a solution containing 50 mM Tris·HCl pH 7.4, 2 mM DTT, 0.1 mg/ml BSA, 10 mM $MgCl_2$, and 5% glycerol through lines A and B. These solutions were pushed through the reaction loop, and on to an exit line. In the exit line was added a quench solution containing 400 mM EDTA (pH unadjusted), and 0.7 % SDS.

An excess of this solution quenched the reaction. A combination of the length of the reaction loop (from the feed lines to the connection with the quench solution) and the push speed of the piston on the RQF-3 determined the time of the reaction. After mixing with the quench solution, the whole mix was then pushed out the bottom of the RQF-3, to a waiting receiving tube.

In the receiving tube was a solution containing enough ssDNA to present a final concentration of 5 nM in the overall mixture. Unlabeled ssDNA served as a re-annealing trap in the quenched solution. This ssDNA was an unlabeled oligonucleotide that had a sequence corresponding to the labeled sequence in the reaction mixture.

After each reaction was completed, samples were placed on ice until the complete series was finished. Samples of each quenched reaction mixture were taken (10 µl) and mixed with 3.5 µl of 4x unwinding quench. This was then loaded on to a 15 % non-denaturing TBE-PAGE in 1x TBE buffer and run 1 hour at 150 V constant. Samples containing 20nt:12bp were run at 4 °C. Gels were dried and placed in a phosphorimager cassette overnight. The next day, cassettes were imaged on a STORM phosphorimager (GE Life Sciences) and analyzed using ImageQuant (GE Life Sciences).

## 2.3 Results

### 2.3.1 Size Exclusion Chromatography

Size exclusion chromatography (SEC) is a commonly used technique when the oligomeric state of a protein is being investigated (83). SEC allows the investigation of interactions under a relatively simple set of conditions. The reliable sensitivity of this method and the availability of equipment make this a popular technique among researchers and the pharmaceutical industry alike (84).

For our purposes, RecD2 was injected in a buffer containing 50 mM potassium phosphate, pH 7.5, and 150 mM NaCl. The pH of the buffer was the same as utilized for the unwinding and binding determinations and is the same as used for purification of the protein (*vide infra*). The concentration of salt was chosen to minimize the formation of aggregate species which had been observed during purification of the enzyme. Three separate injections with different RecD2 concentrations were conducted to assess the behavior of RecD2 under SEC conditions (Fig. 2.2). The concentrations of RecD2 for the injections were 250 nM, 11 µM, and 107 µM. Major peaks from each injection were picked and correlated to a molecular weight standard curve.
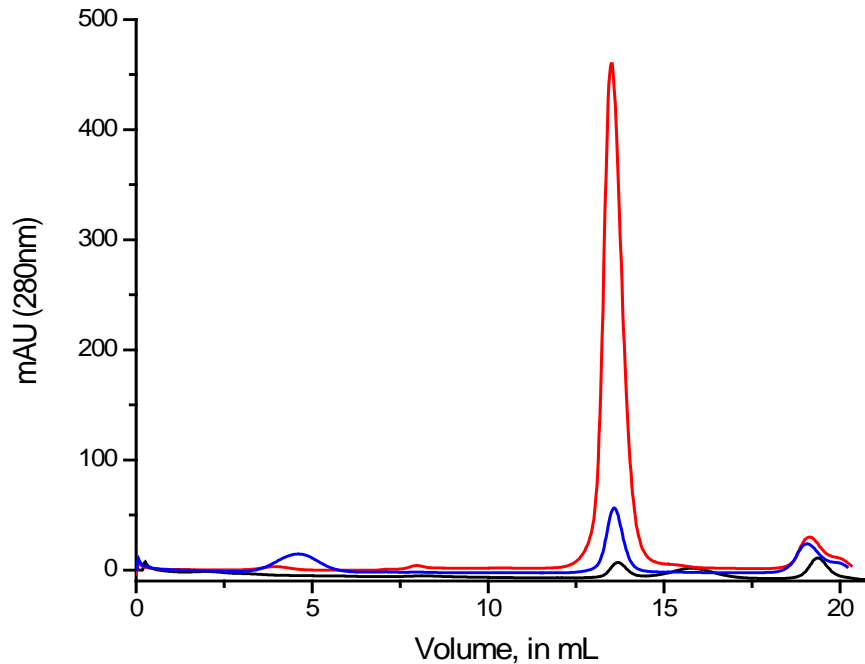
**Figure 2.2: Elution of RecD2 from Superdex 200 size exclusion column.** RecD2 was injected on a Superdex 200 10/300 GL column in a buffer containing 50 mM potassium phosphate pH 7.5 and 150 mM NaCl. Each color shows a separate injection of RecD2. The peak at ~5 minutes retention time is the void volume of the column. The peak at ~19 minutes retention time is the total volume of the column. Concentrations of each injection are: Black- 250 nM, Blue- 11 µM, Red- 107 µM.


Bio-Rad gel filtration standards were injected under the same buffer

conditions as the RecD2 injections to comprise a molecular weight standard curve

(Fig. 2.3). These standards consisted of the following proteins: thyroglobulin (660

kDa), bovine γ-globulin (158 kDa), chicken ovalbumin (44 kDa), equine myoglobin

(17 kDa), and vitamin B12 (1.3 kDa).
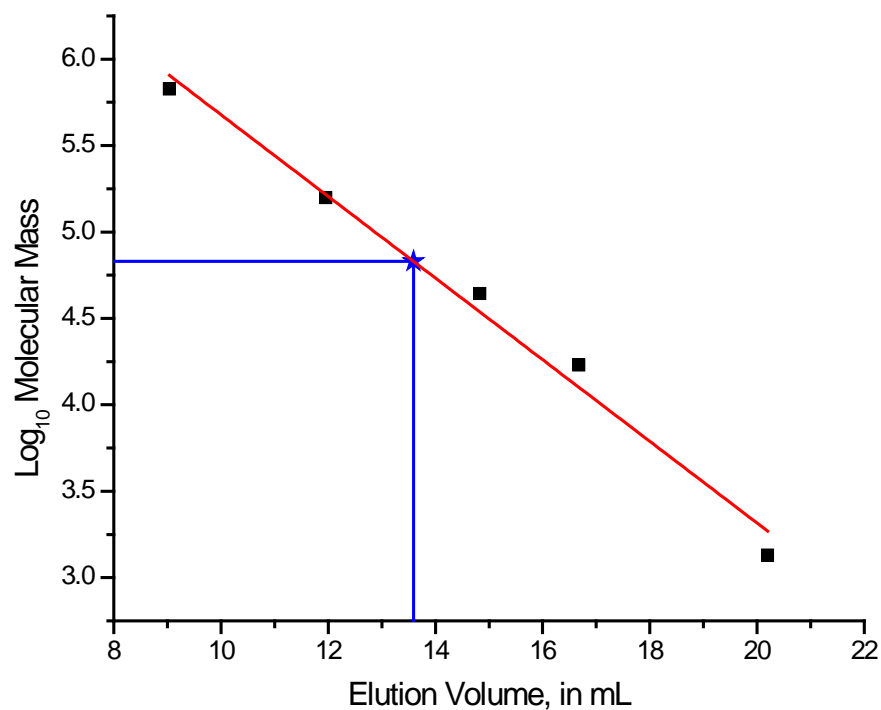
**Figure 2.3: Molecular weight standard curve showing elution of RecD2 from size exclusion column.** Red line- linear regression of standards plotted as $\log_{10}$ of molecular weight against elution volume of each standard, in ml. Blue star shows elution volume of RecD2.

In all injections, only one protein species was observed eluting from the column (Fig. 2.2). The average volume of this elution was $13.6 \pm 0.1$ ml, yielding a calculated molecular weight of $68 \pm 3$ kDa. This compared favorably with an expected molecular weight of 78 kDa for a monomer of RecD2, assuming a small amount of interaction of the protein with the column bed material.

2.3.2 Glutaraldehyde cross-linking of RecD2

Glutaraldehyde cross-linking was performed on RecD2. In these experiments, RecD2 was treated either in the presence or absence of ssDNA. Most experiments were followed by use of the silver stain protocol. Due to the availability of the RecD2 antibody (85), reaction progress could also be followed through use of the western blot technique.

Initial experiments were conducted to ascertain the amount of glutaraldehyde necessary to observe higher order species. A series of reactions was performed with 1 µM (final) RecD2 in cross-linking buffer, treated with various concentrations of glutaraldehyde (Fig. 2.4).
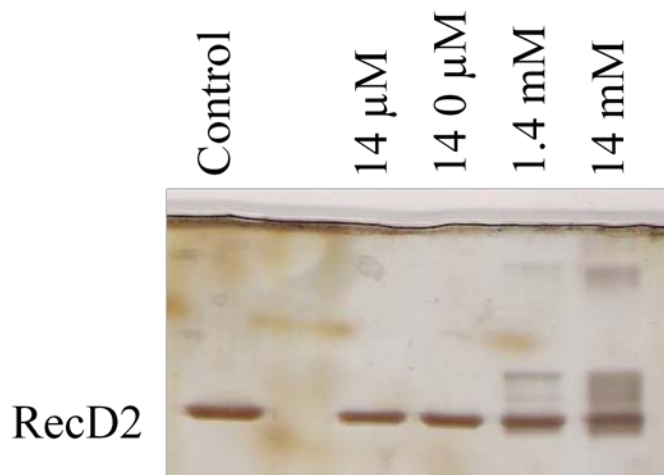


**Figure 2.4: Cross-linking of RecD2 with glutaraldehyde.** Solutions of RecD2 (1 µM) were treated with the indicated concentrations of glutaraldehyde for 20 min at room temperature and quenched with 100 mM Tris· HCl pH 8.0. Quenched samples were loaded on 7.5 % SDS-PAGE and stained by the silver staining protocol.

Following these results, a time course was conducted with 14 mM glutaraldehyde, in the above conditions, to determine the ideal time for the most efficient cross-linking (Fig. 2.5). This concentration of glutaraldehyde is comparable

to levels used by others (79,81). Reactions were conducted at room temperature and

quenched as above.
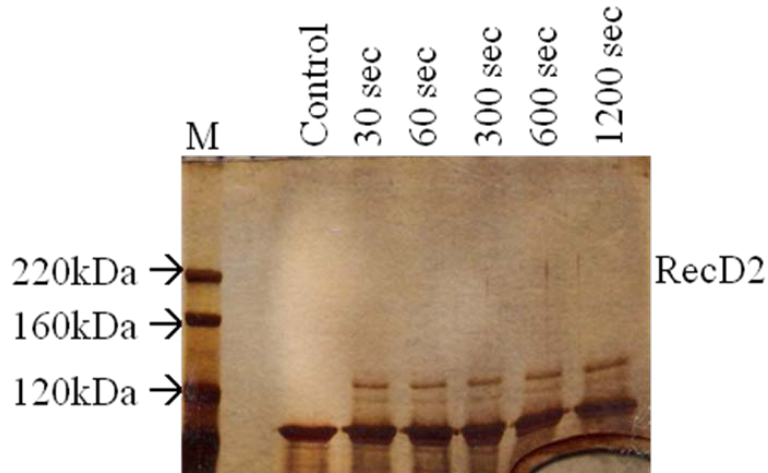


**Figure 2.5: Time Course of cross-linking of RecD2 with glutaraldehyde.**
Solutions of RecD2 (1 µM) were treated with 1.4 mM of glutaraldehyde at room
temperature. Samples were quenched at each time point with 100 mM Tris• HCl pH
8.0 and 6x SDS loading buffer before being loaded on 7.5% SDS- PAGE. Gels were
developed by the silver staining protocol.

Observation of a soluble cross-linked species migrating in the area above the

mass of the monomer (~78 kDa, Figures 2.5 and 2.6) was questioned by us due to the

apparent molecular mass of the migrating species. At approximately 110 kDa, and

present immediately upon addition of glutaraldehyde, this did not correspond to the

mass of any higher order forms of RecD2. The lack of any DNA in the cross-linking

mixtures suggested the possibility that the observed higher order species was not

indicative of the actual behavior of RecD2 on DNA. Cross-linking of RecD2 was

carried out in the presence of ssDNA to address this issue.
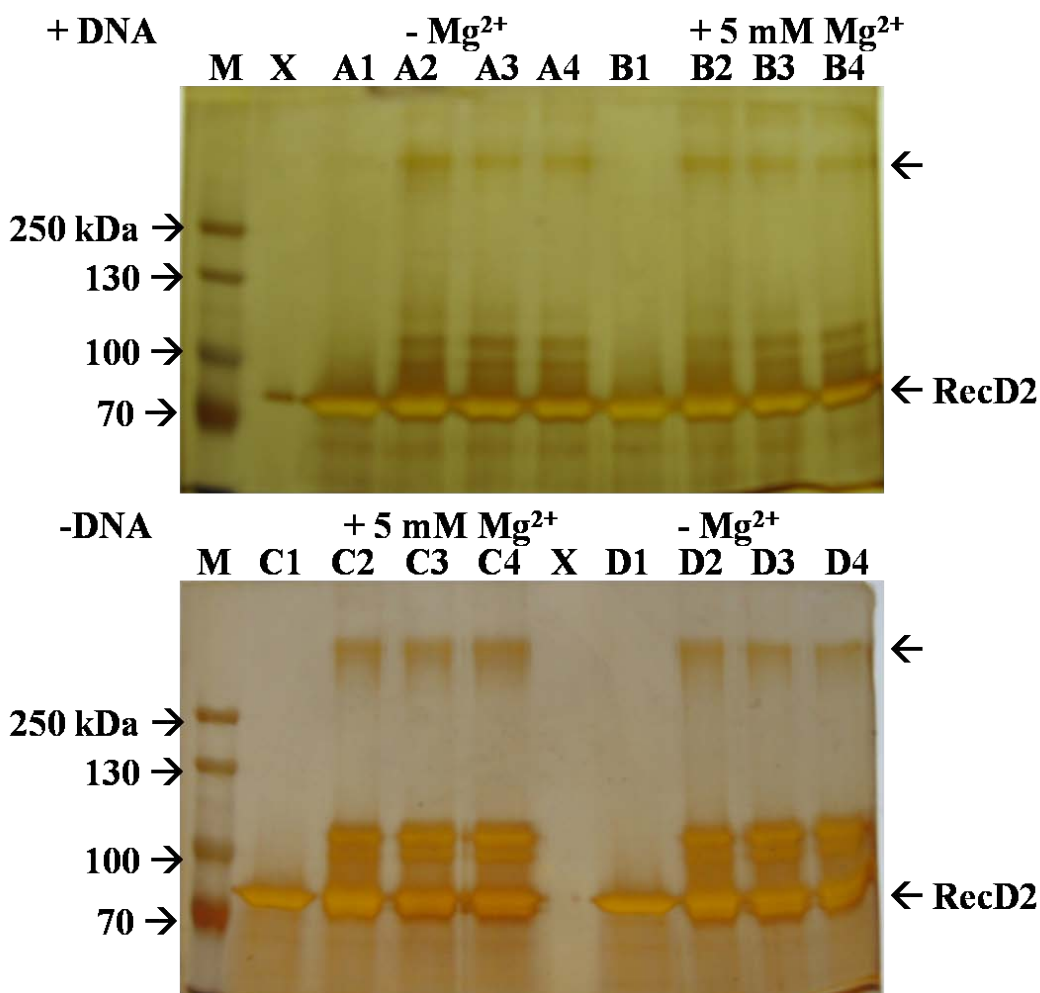
**Figure 2.6: Cross-linking of 1 µM RecD2 with glutaraldehyde in the presence or absence of 1 µM ssDNA.** Solutions were premixed, and then treated with 1.4 mM of glutaraldehyde at room temperature. Lanes 1: Control RecD2. Lanes 2: treated with 0.6 Units benzonase nuclease. Lanes 3: treated with 0.6 Units benzonase nuclease and 25 mM NaBH$_4$. Lanes 4: treated with 25 mM NaBH$_4$. Unlabeled arrows show higher order species observed outside of mass range. Samples were quenched after 20 minutes with 100 mM Tris• HCl pH 8.0 and 6x SDS loading buffer before being loaded on 7.5% SDS- PAGE. Gels were developed by the silver staining protocol.

When the cross-linking reaction was conducted in the presence of 1 µM RecD2 and 1 µM ssDNA, another high molecular mass soluble species was observed (Fig. 2.6). The mass of this higher order species (shown with an unlabeled arrow) was more in line with the possibility of multimer formation than the lower band, shown

47

just above un-crosslinked RecD2 in figure 2.6. The mass of the upper species was, however, outside the resolving range of our system. Possible causes of this result included glutaraldehyde mediated aggregation of RecD2, so we decided to investigate further.

We repeated the cross-linking of RecD2, this time subjecting the gels to western blot analysis with the RecD2 antibody (Figures 2.7 and 2.8). Reactions were conducted in either the presence or absence of ssDNA.
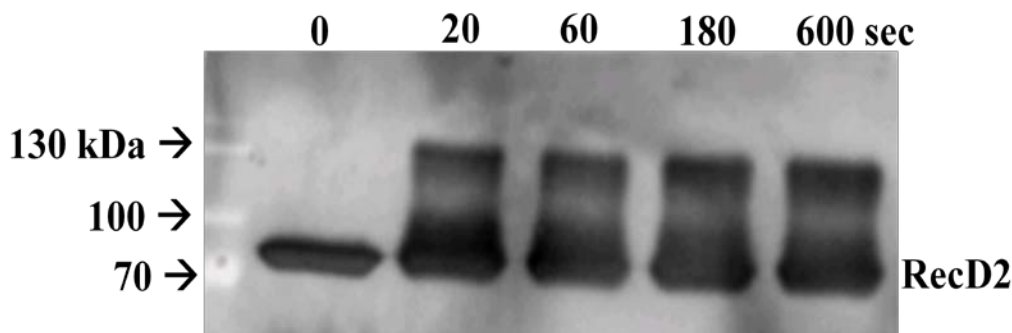


**Figure 2.7: Western blot showing crosslinking of RecD2.** RecD2 (1 µM) was incubated at room temperature in the presence of 1.4 mM glutaraldehyde. Samples were quenched at each time point with 100 mM Tris• HCl pH 8.0 and 6x SDS loading buffer before being loaded on 12% SDS- PAGE. Gels were developed by the western blot protocol with the RecD2 antibody. The reaction conducted in the absence of ssDNA was inadvertently loaded on to a 12% SDS-PAGE.

The higher order species observed with silver staining were again observed with the western blot under each set of conditions. Given the small proportion of cross-linking present at even the longest time point, and the seeming independence of the cross-linking with regard to time, it was decided that this was not evidence for any specific interactions between monomers of RecD2 in the presence of DNA.
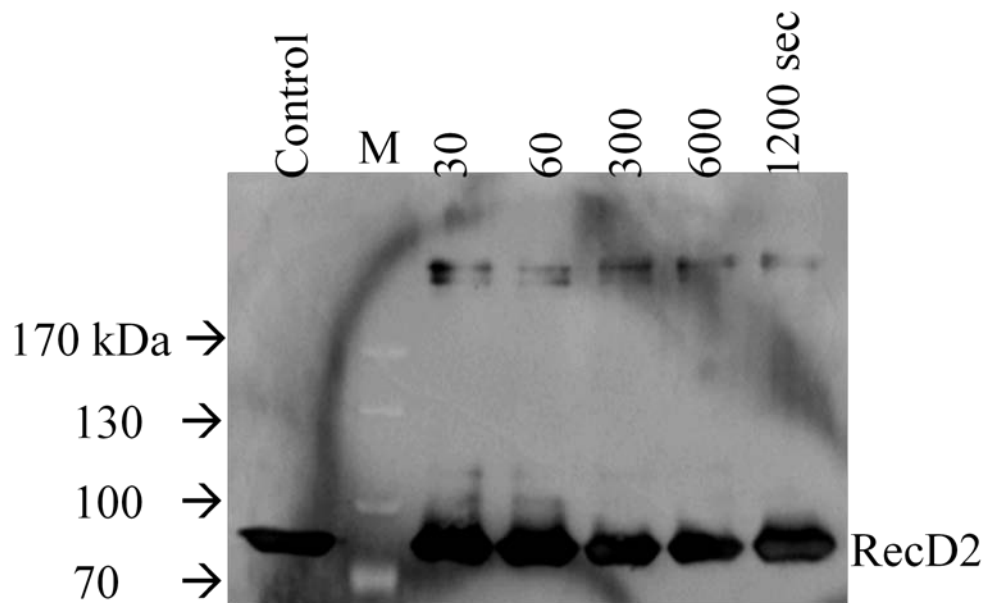
**Figure 2.8: Western blot showing crosslinking of RecD2 in the presence of ssDNA.** RecD2 (1 µM) was incubated at room temperature in the presence of 1 µM ssDNA and 14 mM glutaraldehyde. Samples were quenched at each time point with 100 mM Tris• HCl pH 8.0 and 6x SDS loading buffer before being loaded on 7.5% SDS- PAGE. Gels were developed by the western blot protocol with the RecD2 antibody.

Glutaraldehyde cross-linking is capable of detecting even transient or weak interactions between proteins (81). As a consequence, it is sometimes difficult to interpret cross-linking results as specific interactions between proteins. This is particularly true when concentrations of either protein or glutaraldehyde are not ideal (82).

## 2.3.3 Binding of RecD2 to DNA

The first priority in the establishment of conditions for kinetic characterization of RecD2 was determination of the binding affinity of RecD2 for substrate DNA

(shown in figure 2.9). A model hairpin based substrate was employed for this purpose, to mimic a DNA unwinding substrate. HP1 has a 12nt overhang with a 20bp double stranded region, formed into a hairpin by three connecting thymidine bases (Table 2.2).
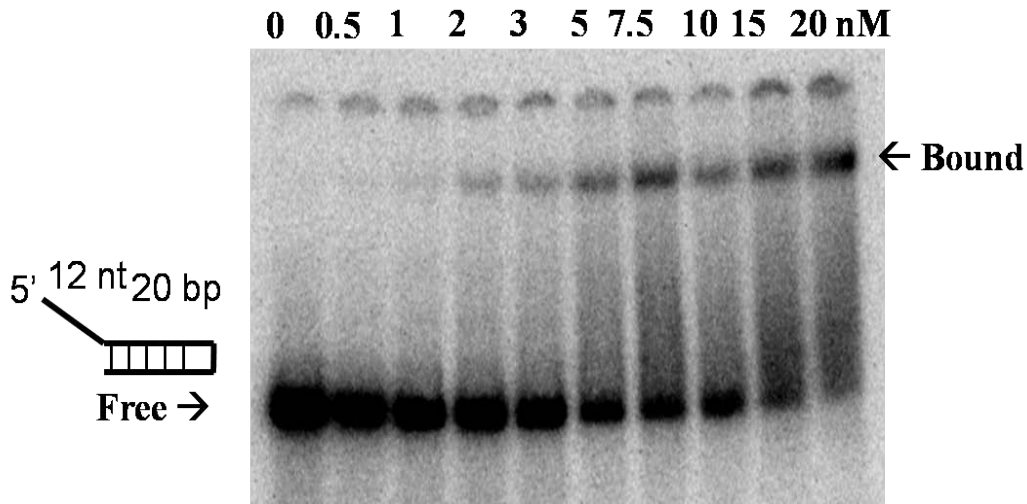


**Figure 2.9: Binding of 5'- 12nt overhang dsDNA to RecD2.** A solution containing 1 nM dsDNA was incubated with increasing concentrations of RecD2 for 80 minutes on ice. Reactions were stopped by addition of glycerol (7% final) and immediately loaded onto a 10% TBE-PAGE. Gels were run for 30 minutes at 250 V (constant) and temperature controlled at 4 °C.

Quantitation for the binding reactions was performed with the program ImageQuant and the data fit to the equation shown below using the software package SigmaPlot (Systat Software).

$$F = F_{max} * \{(K_d + E_t + D_t) - [(K_d + E_t + D_t)^2 - 4E_tD_t\}^{1/2}\}/ 2D_t$$

Shown in figure 2.10 is the binding curve resulting from averaging three independent experiments. In this equation, **F** is the fraction bound, corresponding to the **y** values on the curve. **$F_{max}$** is the maximum fraction bound in the curve, and **[$E_t$]**

is the concentration of RecD2, in nM, at any point in the curve (corresponding to the **x** values). The value for $D_t$ was 1 nM. Three independent experiments were performed. The $K_d$ for the binding of RecD2 to HP1 DNA was determined by fitting to the above formula, resulting in an average $K_d$ of 2.3 ($\pm$ 1.6) nM.
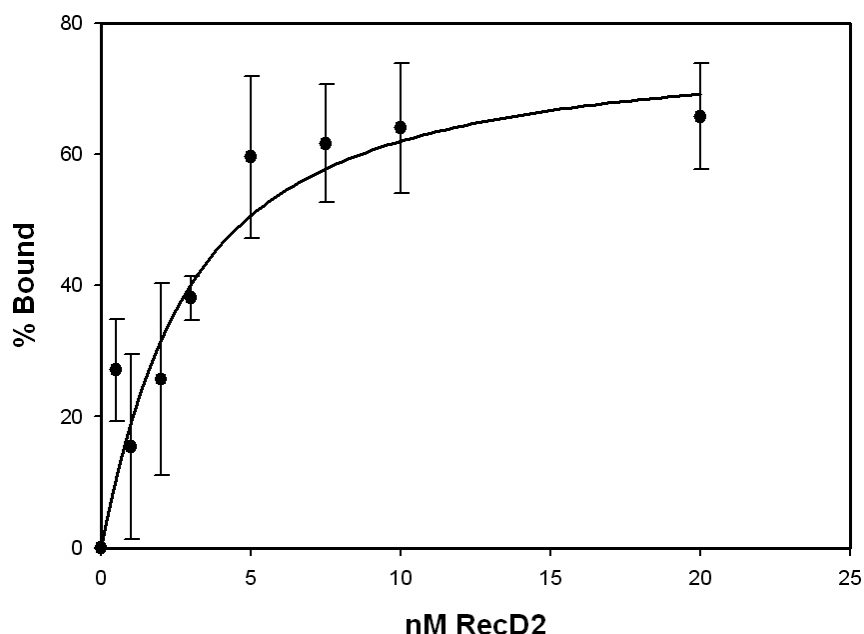


**Figure 2.10: Plot of binding of RecD2 to HP1 DNA.** Shown above is the average binding results from three independent experiments. Shown also is the least squares best fit line obtained by applying the above mentioned binding formula to the experimental data.

2.3.4 Unwinding under single turnover conditions

To examine the rate and mechanism of DNA unwinding by RecD2, it was decided to set up a single turnover reaction system. This system would allow the examination of individual steps in the unwinding of dsDNA by RecD2, through use of substrates with differing structure. In order to achieve this, the initial goal was to

make sure only one molecule of RecD2 was bound to each dsDNA molecule when the reaction started.


## 2.3.5 Effect of increasing ssDNA trap on DNA unwinding by RecD2

To obtain single turnover conditions, a quantity of enzyme should be pre-bound to the dsDNA substrate. The reaction is then allowed to proceed with an excess quantity of ssDNA to trap RecD2 not bound to dsDNA. This requires sufficient ssDNA that the enzyme is only ever going to be bound to a dsDNA molecule once - that is, at the start of the reaction. After that, there must be sufficient ssDNA present to ensure any unbound enzyme never re-binds to dsDNA.

To find the amount of ssDNA needed to function in this capacity, a series of reactions was conducted with increasing amounts of ssDNA protein trap present in the unwinding mixture (Fig. 2.11). Analysis of the reaction showed unwinding in the presence of unlabeled ssDNA to be significantly reduced compared to reactions where no trap was included. This shows that presence of the ssDNA protein trap is reducing the unwinding rate of RecD2. Greatest inhibition was observed with 2 µM trap. This level was used for subsequent experiments.
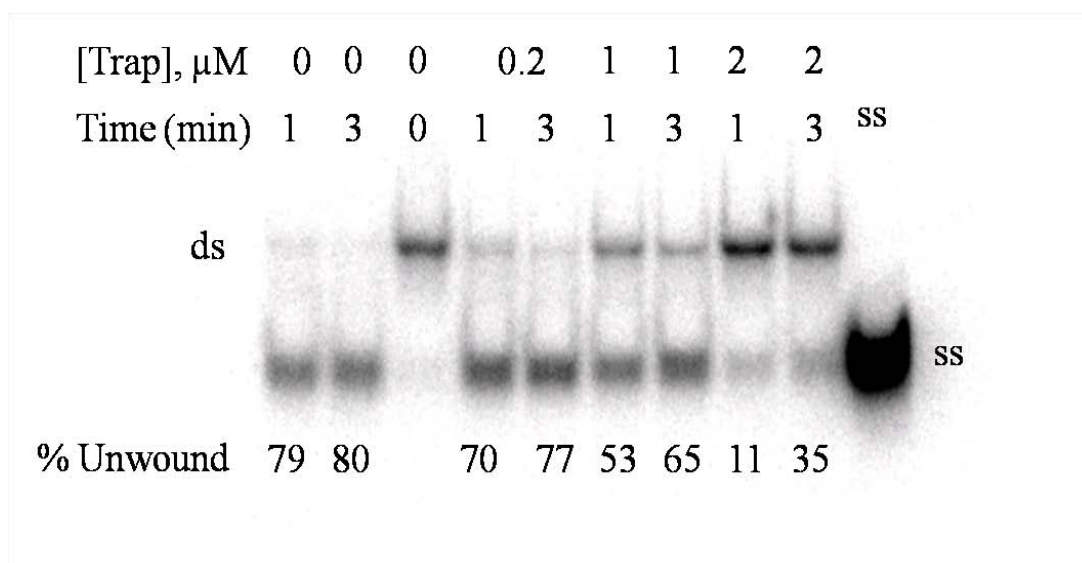
**Figure 2.11: Effect of increasing ssDNA competitor on unwinding of 1nM 12nt:20bp dsDNA substrate by 20nM RecD2 at room temperature.** DNA and ATP were mixed in reaction buffer, and reaction was started by addition of RecD2. Reactions were allowed to proceed for either 1 or 3 minutes before quenching.

2.3.6 The A/B/C Reactions

Three reactions were set up in parallel with slight differences. Together, these were termed the A/B/C reactions. The standard setup of the A/B/C reactions included three unwinding reactions, labeled A, B, and C, along with one binding reaction as a control. This system examined the effect of competitor on unwinding for each dsDNA substrate. Each of these substrates will be discussed in further detail below.

In each "A" reaction, no ssDNA trap was added. This served as a positive control for the overall A/B/C reaction system.  In "B" reactions, ssDNA competitor was added at the same time as substrate dsDNA, to allow RecD2 a chance to bind either to substrate or competitor in the absence of ATP. "B" reactions served as a negative control, to show inhibition of unwinding activity by the ssDNA trap. Excess

ssDNA protein trap present during the pre-incubation period in the "B" reactions should keep RecD2 from ever binding to dsDNA substrate. In case an insufficient concentration of ssDNA trap is used, the "B" reaction should show unwinding.

The "C" reaction is started by addition of ATP and ssDNA competitor at the same time. This allowed RecD2 a twenty minute pre-incubation period with the substrate dsDNA before ssDNA trap was added. If RecD2 is able to unwind the entire length of a particular substrate dsDNA without dissociating from the substrate, the "C" reaction should show nearly the same amount of unwinding as the "A" reaction for the same substrate.

If RecD2 is not capable of unwinding the whole length of the substrate dsDNA without dissociation from the substrate dsDNA, only the "A" reaction should show unwinding. This assumed single turnover conditions, which meant once the enzyme was bound to the substrate DNA, RecD2 should not have any interaction with the ssDNA trap until it has completed unwinding of the pre-bound substrate. If the processivity of the enzyme is such that multiple turnover events are required to complete unwinding of the substrate, then the enzyme will have the opportunity to interact with the ssDNA trap, due to dissociation from the substrate partway through the course of unwinding.

One binding reaction was set up as a control to confirm binding of RecD2 to substrate during pre-incubation. This was achieved by running a sample of each reaction under non-denaturing conditions on 15% TBE-PAGE, prior to starting each reaction with ATP. An example can be seen below in Fig. 2.12, where the substrate 12nt:20bp has been mixed with RecD2 for a set of A/B/C reactions. In the "A" and

"C" reactions, there is RecD2 and dsDNA substrate present in the solution, so there is a shift in the 15% TBE-PAGE gel. Under the conditions of this system, this often appeared as a smear, representing a mix of species, most probably due to different possible binding conformations on the substrate. This is most probably due to non-ideal conditions in the binding gel. In the "B" reaction, 2 µM ssDNA protein trap has been added to the system. As RecD2 has an excess of unlabeled trap to bind to in the solution, the labeled dsDNA is not bound, so there is no shift in the gel.

## 2.3.7 12nt 5'- overhang (12nt:20bp)

Previous work by Jianlei Wang had shown that RecD2 was capable of unwinding a dsDNA substrate containing a 12nt 5'- overhang with a 20bp annealing region (12nt:20bp) (15). Our research expanded on this, now using this substrate as a basis of comparison against other substrates.
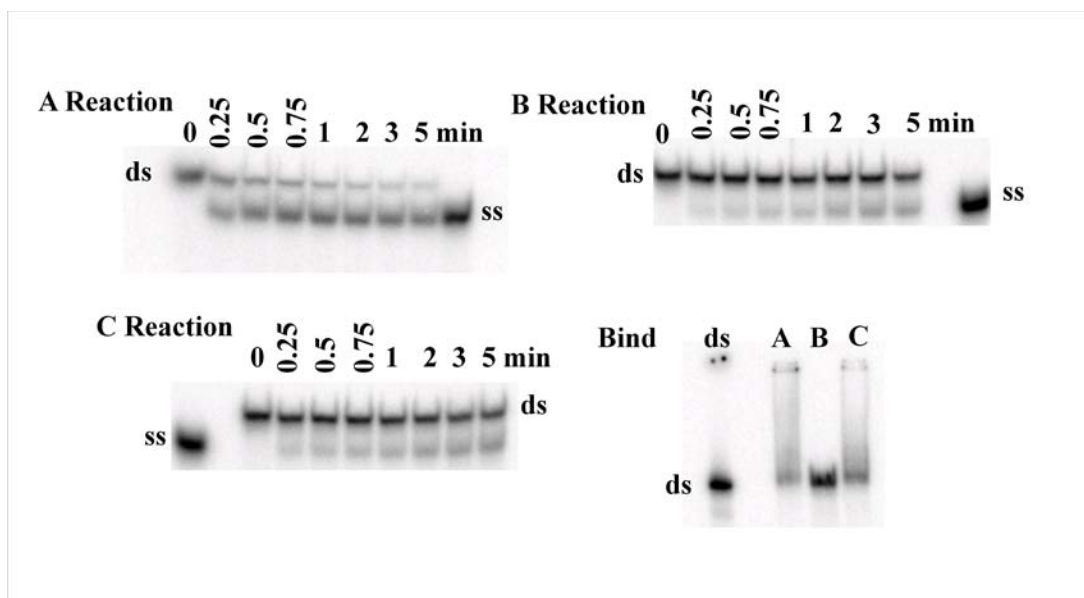
**Figure 2.12: A/B/C reactions with the 12nt:20bp substrate.** Shown above is unwinding of 1 nM 12nt:20bp by 20 nM RecD2 in the presence or absence of 2µM ssDNA trap at room temperature. Reactions were conducted as detailed in **Materials and Methods** and loaded on 15% TBE·PAGE. "A" reaction- unwinding in the absence of trap. "B" reaction- unwinding in the presence of 2 µM ssDNA trap, trap added prior to incubation of RecD2 and substrate DNA. "C" reaction- unwinding in the presence of 2 µM ssDNA trap, trap added at the same time as ATP. "Bind" reaction- samples prior to the start of each reaction, to verify binding of RecD2 to substrate dsDNA.

Quantitation of the A/B/C reactions was conducted, and the results of four independent experiments are graphed in Fig. 2.13. In the absence of ssDNA competitor, RecD2 is capable of unwinding this substrate at a reproducible rate. The addition of competitor brings the unwinding down to a negligible level, regardless of whether the competitor was added at the same time as the substrate dsDNA, or at the same time as the ATP. This suggests that RecD2 is insufficiently processive to unwind the entire length of a 20bp double strand region of duplex DNA.
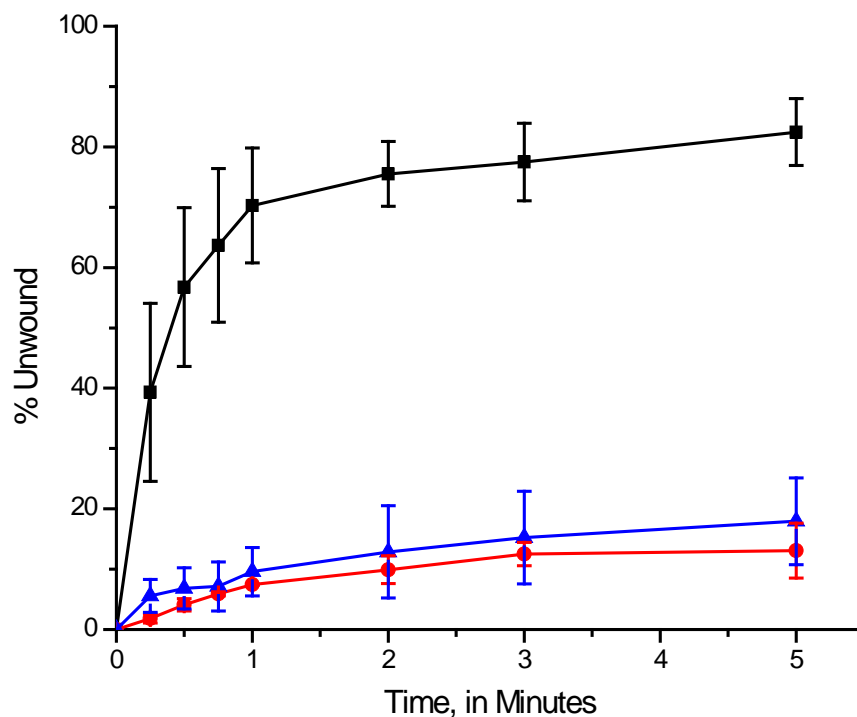
**Figure 2.13: Plot of unwinding of 1 nM 12nt:20bp dsDNA substrate by 20 nM RecD2 in the presence or absence of 2 µM ssDNA trap.** Addition of 1 mM ATP started each reaction. Lines shown above are the average of four independent experiments conducted at room temperature. Bars at each data point are the standard deviation for each data point. Black squares- unwinding of dsDNA in the absence of trap (A reaction). Red circles- unwinding in the presence of 2 µM ssDNA competitor, added prior to pre-incubation (B reaction). Blue triangles- unwinding in the presence of 2 µM ssDNA competitor, added with ATP (C reaction).

It should be noted that the maximum percentage of dsDNA substrate unwound in the A/B/C reactions never reaches 100 %. When quantitation is performed, the background percentage of unwinding present in the unwound area at the zero time point is subtracted from all samples. This accounts for a reduction in the observed extent of reaction.

2.3.8 Determination of concentration of ATP needed for dsDNA unwinding

In order to have confidence in the results of the dsDNA unwinding in the "B" and "C" reactions, it was necessary to confirm adequate quantities of ATP were present in the reaction mixture. This was to ensure any small extent of unwinding observed in these reactions was not simply from insufficient ATP. RecD2 was pre-incubated with the dsDNA for twenty minutes at room temperature. Reactions were started by addition of ATP. These reactions were carried out in the presence or absence of 2 µM ssDNA protein trap added at the same time as ATP, with $Mg^{2+}$ adjusted to always maintain at least 1 mM free $Mg^{2+}$. The greatest difference in unwinding in the absence versus presence of ssDNA trap was found at 1 mM ATP (Fig. 2.14), so this level was used for subsequent reactions.
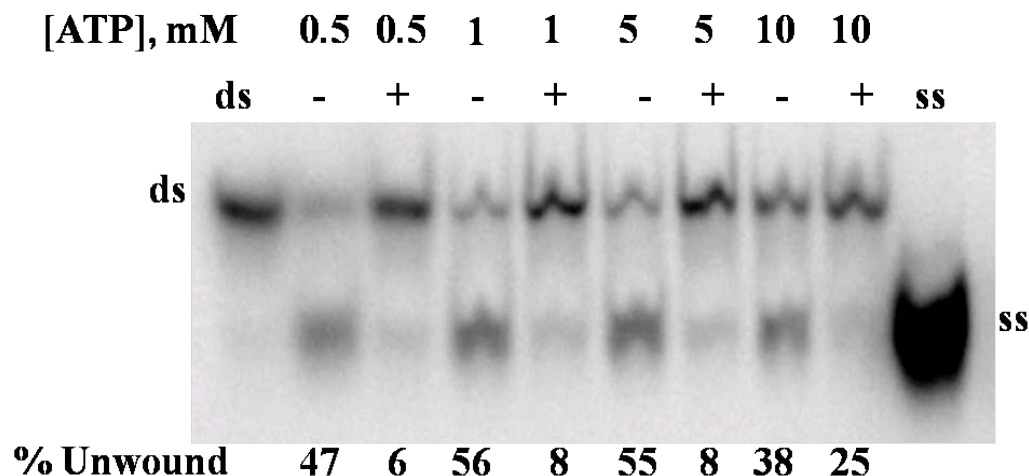
**Figure 2.14: Determination of [ATP] necessary for efficient unwinding of a dsDNA substrate by RecD2.** Unwinding reactions were conducted with 20 nM RecD2 and 1 nM 12nt:20bp substrate in the absence (-) or presence (+) of ssDNA trap, at varying concentrations of ATP at room temperature. Reactions were stopped by addition of quench loading buffer at 5 minutes and loaded onto a 15% TBE-PAGE. Values shown below each lane result from quantitation of the lower band (ssDNA) as a percentage of the total counts for that lane. Background correction was by subtraction of the counts present in the ss region of the dsDNA control lane.

2.3.9 Effect of pH on Unwinding Behavior of RecD2

Previous work by Jianlei Wang had suggested that RecD2 was more processive at pH 6.5 than at pH 7.4 (15). This observation was tested against the backdrop of the unwinding of 1nM 12nt:20bp dsDNA in the presence of 2 μM ssDNA trap. Results show unwinding in 25 mM PIPES buffer at pH 6.5 was decreased relative to unwinding in 50 mM Tris at pH 7.4 in the absence of trap (Fig. 2.15). The total extent of unwinding showed no dependence on when the protein trap was added, as the "B" and "C" reactions showed the same behavior at pH 7.4 and pH 6.5.
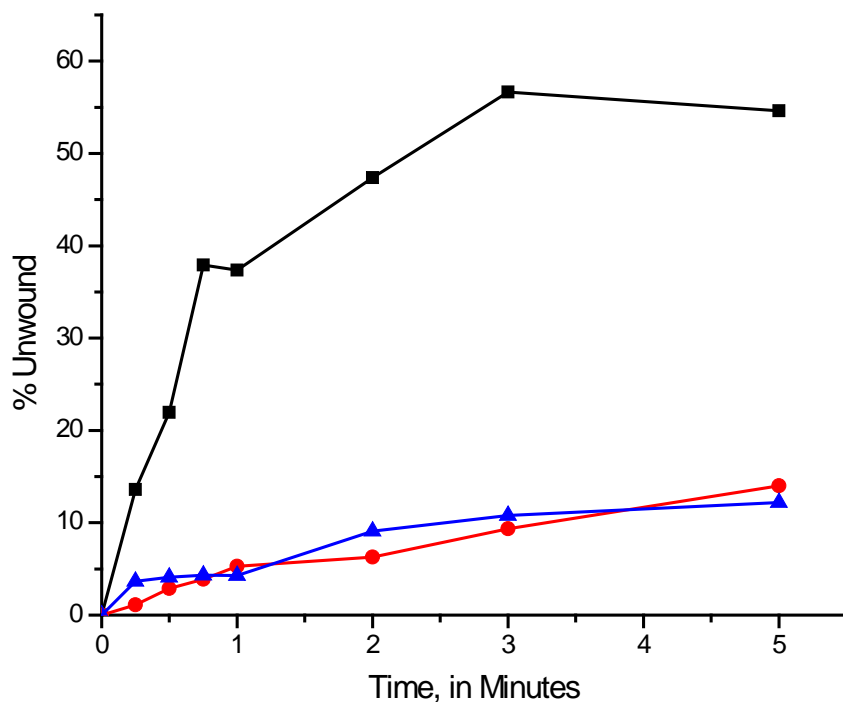
**Figure 2.15: Plot of unwinding of 1 nM 12nt:20bp by 20nM RecD2 at pH 6.5 in the presence or absence of 2 μM ssDNA trap.** Addition of 1 mM ATP started each reaction. Reactions were conducted in a buffer containing 25 mM PIPES pH 6.5, 10 mM $MgCl_2$, and 5 % glycerol. Lines shown above are from one experiment conducted at room temperature. Black squares- unwinding of dsDNA in the absence of trap. Red circles- unwinding in the presence of 2 μM ssDNA competitor, added prior to pre-incubation. Blue triangles- unwinding in the presence of 2 μM ssDNA competitor, added with ATP.

2.3.10 Effect of Pre-incubation on unwinding

Our reaction methodology for the A/B/C reactions required a pre-incubation for twenty minutes at room temperature. It was necessary to be able to exclude degradation of the protein during this pre-incubation. Degradation of any of the components in the reaction buffer during a pre-incubation could potentially cause a decrease in the overall amount of unwinding observed in our system. In order to

ensure the pre-incubation did not introduce systematic error into our observations, we examined the effect of pre-incubation on unwinding by RecD2 in the absence of ssDNA trap.
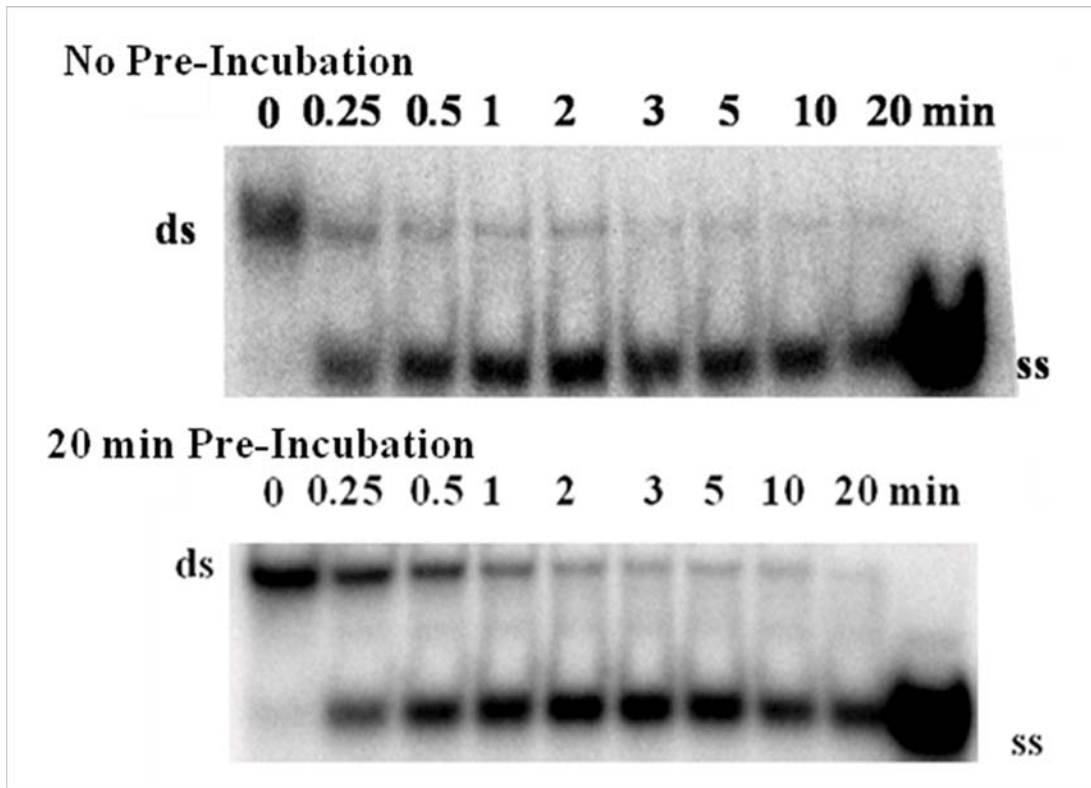


**Figure 2.16: Effect of 20 minutes pre-incubation on unwinding of 1 nM 12nt:20bp dsDNA by 20 nM RecD2.** RecD2 and dsDNA substrate were mixed in reaction buffer and allowed to incubate at room temperature for 20 minutes. Reactions were started by addition of ATP. Reactions were carried out at room temperature.

Unwinding of the 12nt:20bp substrate was performed to examine the effect of pre-incubation on unwinding by RecD2 (shown in Fig. 2.16). Unwinding was performed with reagents allowed no pre-incubation, or 20 minutes pre-incubation, prior to reaction start by addition of ATP. Both reactions were performed in the absence of ssDNA trap. Results (Fig. 2.17) show no significant difference in

61

unwinding between allowing 20 minutes pre-incubation and not allowing pre-incubation.
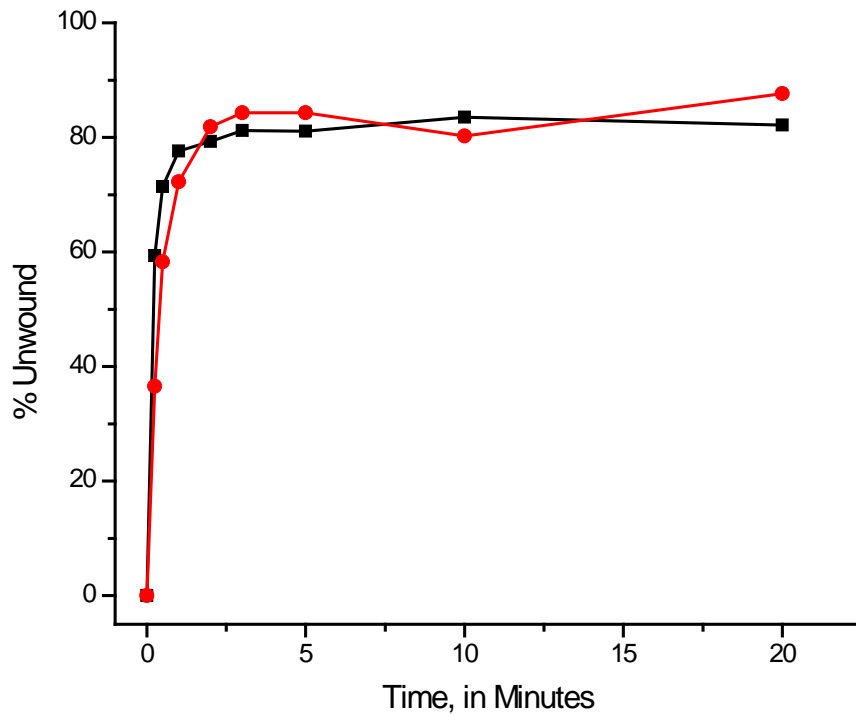


**Figure 2.17: Plot showing effect of pre-incubation on unwinding of 1 nM 12nt:20bp dsDNA substrate by 20 nM RecD2.** Red Circles- Reagents mixed 20 minutes prior to reaction start. Black Squares- No pre-incubation prior to reaction start. Reactions were started by addition of 1 mM ATP. Time courses are the result of one experiment each, conducted independently.

2.3.11 12nt fork (12ntY20bp)

Previous research by Jianlei Wang showed that unwinding of forked 12ntY20bp substrate by RecD2 was much more rapid than for the 12nt:20bp dsDNA substrate (15). Under the A/B/C conditions, this structure also showed an increase in

the rate of unwinding relative to the 12nt 5'- overhang substrate 12nt:20bp in the absence of trap (Fig. 2.18).
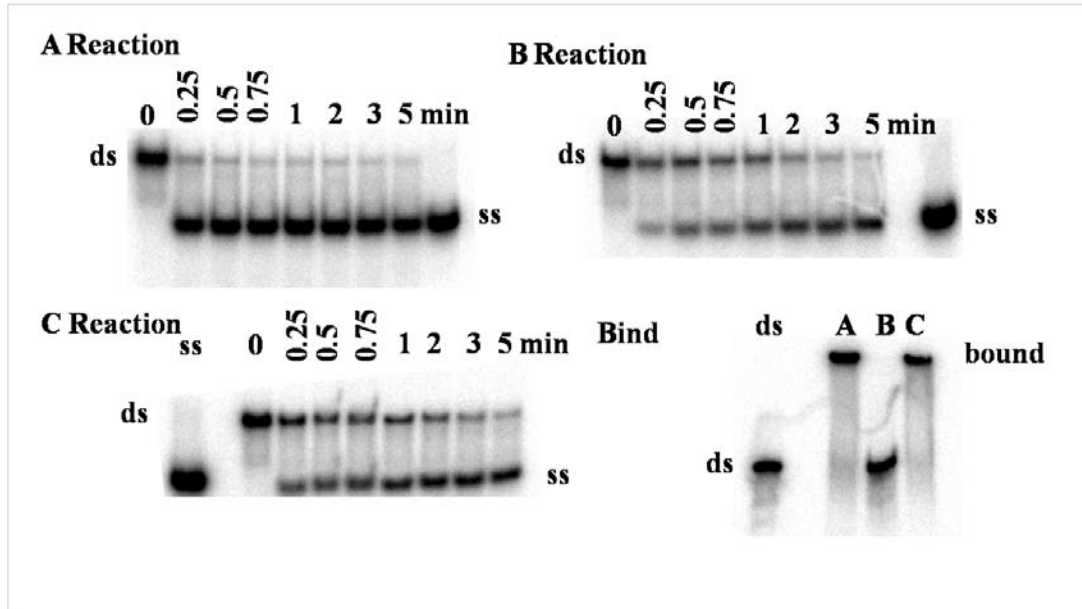


**Figure 2.18: Unwinding of 1 nM 12ntY20bp by 20 nM RecD2 in the presence or absence of 2 µM ssDNA trap.** Reactions were conducted at room temperature as detailed in **Materials and Methods** and loaded on 15% TBE·PAGE. "A" reaction-unwinding in the absence of trap. "B" reaction- unwinding in the presence of 2 µM ssDNA trap, trap added prior to incubation of RecD2 and substrate DNA. "C" reaction- unwinding in the presence of 2 µM ssDNA trap, trap added at the same time as ATP. "Bind" reaction- samples prior to the start of each reaction, to verify binding of RecD2 to substrate dsDNA.

Only a small reduction in unwinding rate was observed when competitor was included, regardless of when it was added to the reaction. As reactions progressed, however, the continued unwinding in the "B" and "C" reactions relative to the "A" reaction (which had by then leveled off) caused the total unwinding in all the reactions to approach parity (Fig. 2.19). The poor ability of ssDNA competitor to slow activity in both the "B" and "C" reactions suggested the concentration of ssDNA

63

trap present in the "B" and "C" reactions may be insufficient to inhibit unwinding activity of RecD2 with this substrate. This is possibly due to the relative binding of RecD2 to the fork substrate being too high relative to the ssDNA trap to observe inhibition at the concentrations of ssDNA used.
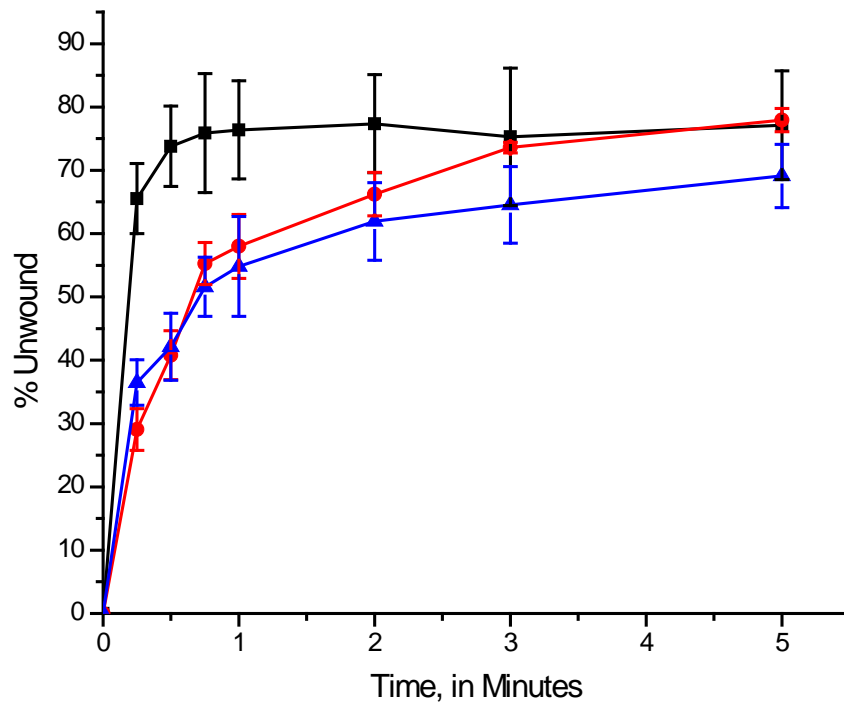


**Figure 2.19: Plot of unwinding of 1 nM 12ntY20bp dsDNA substrate by 20 nM RecD2 in the presence or absence of 2 μM ssDNA trap.** Addition of 1 mM ATP started each reaction. Lines shown above are the average of three independent experiments conducted at room temperature. Bars at each data point are the standard deviation present at each data point. Black squares- unwinding of dsDNA in the absence of trap. Red circles- unwinding in the presence of 2 μM ssDNA competitor, added prior to pre-incubation. Blue triangles- unwinding in the presence of 2 μM ssDNA competitor, added with ATP.

Further investigation confirmed that the amount of ssDNA trap used in the previous experiments was insufficient. An increase in the amount of trap to levels sufficient to completely inhibit unwinding of dsDNA by RecD2 was conducted. Results from these experiments found no apparent difference in processivity of RecD2 on the 12ntY20bp fork substrate, relative to the 12nt:20bp and 24nt:20bp substrates (Fig. 2.20).
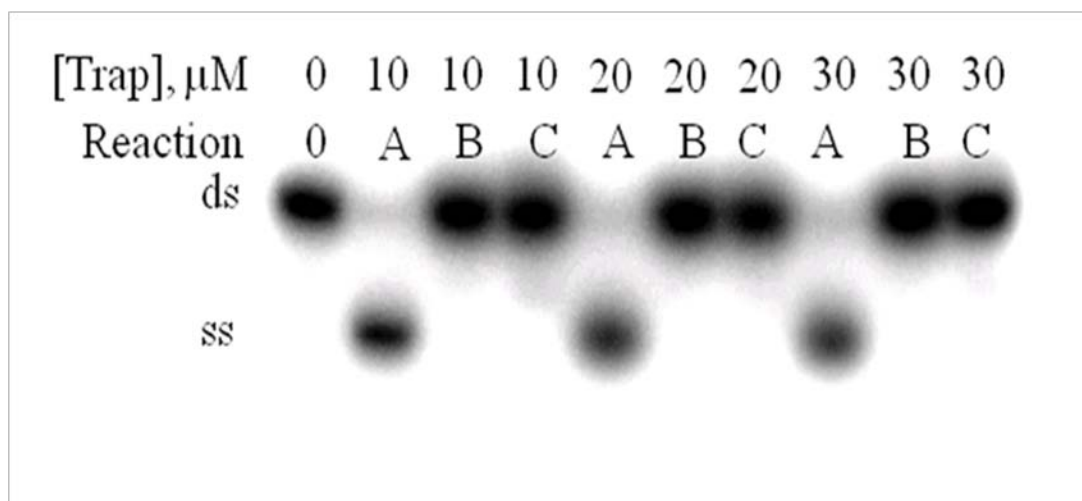


**Figure 2.20: Unwinding of 12ntY20bp by 20 nM RecD2 in the presence of increasing concentrations of ssDNA trap.** Unwinding of 1 nM substrate was conducted with the indicated concentration of ssDNA trap added. Reactions were allowed to pre-incubate 20 min before addition of 1 mM ATP started the reaction. Reactions were quenched after 5 minutes. Reaction A: no trap present. Reaction B: trap added with substrate prior to pre-incubation. Reaction C: trap added with ATP.

2.3.12 24nt 5'- overhang (24nt:20bp)

A dsDNA molecule containing a 24nt 5'- overhang with a 20bp annealed region (24nt:20bp) was investigated to determine whether an increase in the number of nucleotides on the overhang would lead to an increase in the rate or extent of

unwinding (Fig. 2.21). Some SF1 helicases demonstrate an increase in unwinding

rate, or an ability to clear blockages, due to loading of additional molecules of the

helicase on the overhang (86,87).
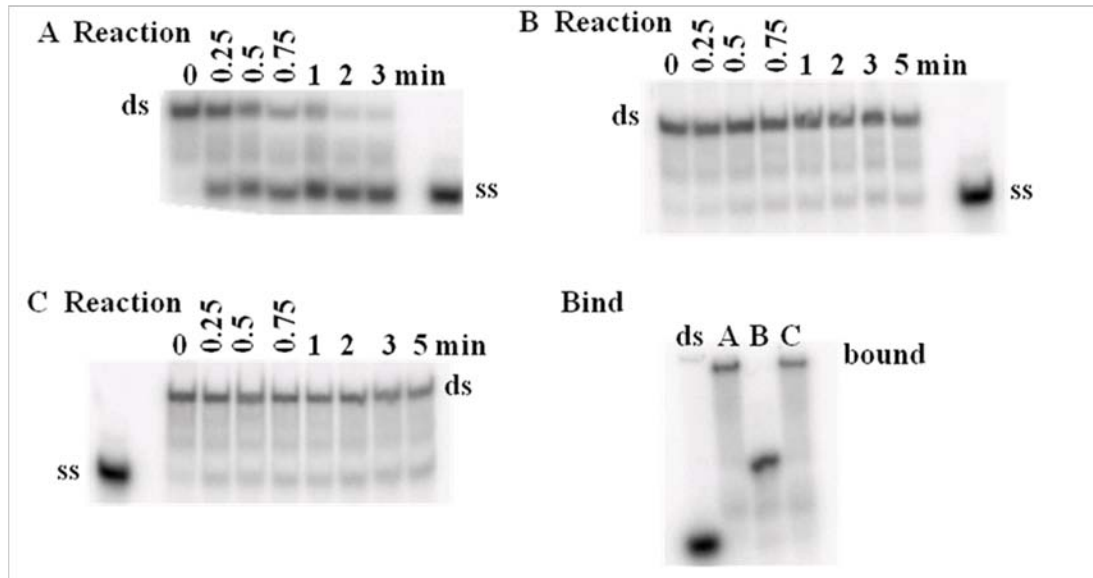


**Figure 2.21: Unwinding of 1 nM 24nt:20bp by 20 nM RecD2 in the presence or absence of 2 µM ssDNA trap.** Reactions were conducted at room temperature as detailed in **Materials and Methods** and loaded on 15 % TBE·PAGE. "A" reaction- unwinding in the absence of trap. "B" reaction- unwinding in the presence of 2 µM ssDNA trap, trap added prior to incubation of RecD2 and substrate DNA. "C" reaction- unwinding in the presence of 2 µM ssDNA trap, trap added at the same time as ATP. "Bind" reaction- samples prior to the start of each reaction, to verify binding of RecD2 to substrate dsDNA.

Despite the extended overhang, no fundamental difference in rate of

unwinding, nor susceptibility to competitor, was observed with this substrate relative

to the 12nt 5'- overhang (12nt:20bp). This result, shown in Fig. 2.22, suggests that the

minimum overhang requirement of 10-12 nucleotides first found by Jianlei Wang was

correct. When the overhang on the substrate is changed from 6nt to 12nt there is a

positive relationship between overhang length and binding/ unwinding behavior

shown by RecD2 (15). This correlation does not extend to ssDNA overhangs longer than 12nt, as a change to a 24nt overhang does not modify the unwinding behavior of RecD2.

Binding gels for these reactions showed apparent unwinding of the control dsDNA (Fig. 2.21). It should be noted that all binding reactions for the various substrates were run under the same conditions, and that these conditions were designed for the 12nt:20bp substrate. We believe the reason for this observation may be spontaneous denaturation of the double strand marker in the gel. Controls for the unwinding gels did not share this issue, so the binding gels were discounted and the unwinding gels accepted.
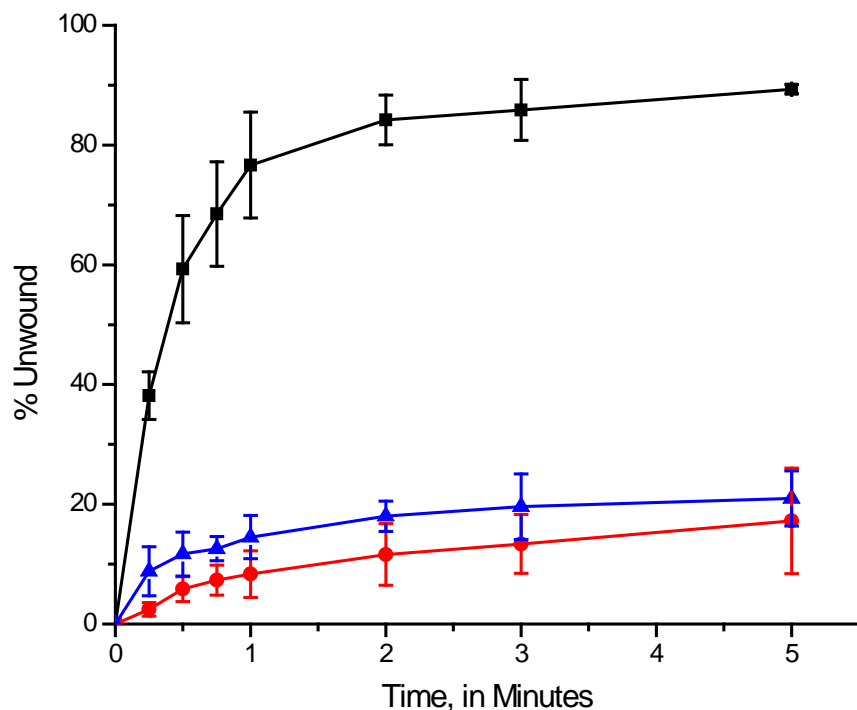
**Figure 2.22: Plot of unwinding of 1 nM 24nt:20bp dsDNA substrate by 20 nM RecD2 in the presence or absence of 2 µM ssDNA trap.** Addition of 1 mM ATP started each reaction. Lines shown above are the average of three independent experiments conducted at room temperature. Bars at each data point are the standard deviation present at each data point. Black squares- unwinding of dsDNA in the absence of trap. Red circles- unwinding in the presence of 2 µM ssDNA competitor, added prior to pre-incubation. Blue triangles- unwinding in the presence of 2 µM ssDNA competitor, added with ATP.

2.3.13 20nt 5'- overhang with 12bp annealing region (20nt:12bp)

This structure was utilized to investigate our hypothesis that RecD2 was poorly processive. The annealing region on this structure is only 12 base pairs in length, as opposed to the 20 base pairs present in the other structures. This presented challenges to the A/B/C reaction system, as it was found that a 20 minute pre-

incubation at room temperature caused almost complete unwinding of the substrate in the absence of enzyme.

Further investigation of the reaction conditions necessary for the generation of consistent results was carried out. Results found a pre-incubation period of 5 minutes at room temperature was all that was required, but that much higher concentrations of RecD2 (100 nM) would have to be applied. To prevent unwinding of the substrate in the absence of enzyme, it was also found that 20nt:12bp reaction gels would have to be run at 4 °C, in the cold room, with recirculation to keep the gels cold while running.
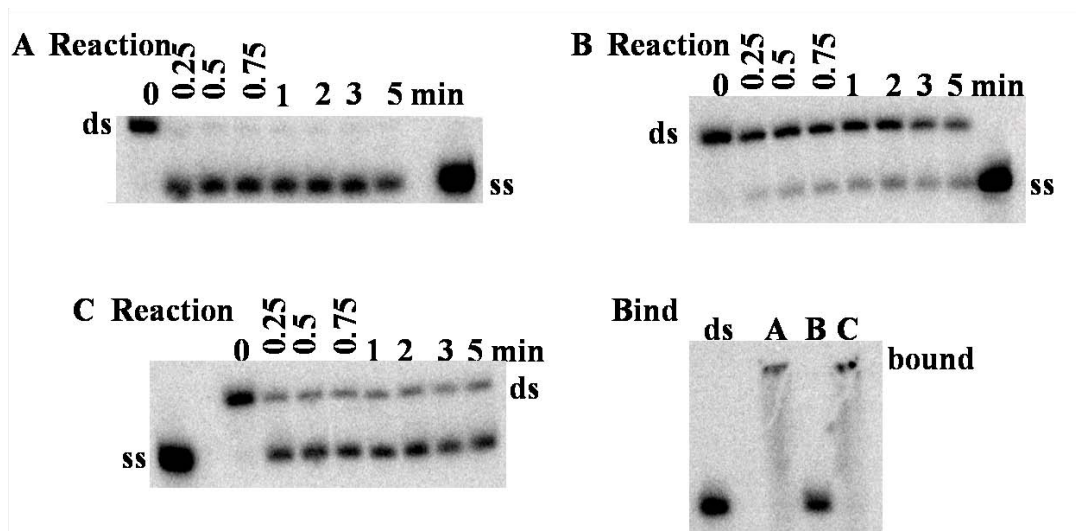


**Figure 2.23: Unwinding of 1 nM 20nt:12bp by 20 nM RecD2 in the presence or absence of 2 µM ssDNA trap.** Reactions were conducted at room temperature as detailed in **Materials and Methods** and loaded on 15% TBE·PAGE. "A" reaction-unwinding in the absence of trap. "B" reaction- unwinding in the presence of 2 µM ssDNA trap, trap added prior to incubation of RecD2 and substrate DNA. "C" reaction- unwinding in the presence of 2 µM ssDNA trap, trap added at the same time as ATP. "Bind" reaction- samples prior to the start of each reaction, to verify binding of RecD2 to substrate dsDNA.

Results of this series of experiments show significant levels of product formation in the single turnover "C" reaction, which had not been observed with the other substrates (Figures 2.23 and 2.24). This suggests RecD2 is capable of unwinding the entire length of the 20nt:12bp substrate, but is not capable of unwinding the entire length of any of the studied 20 bp substrates (12nt:20bp, 24nt:20bp, or 12ntY20bp).
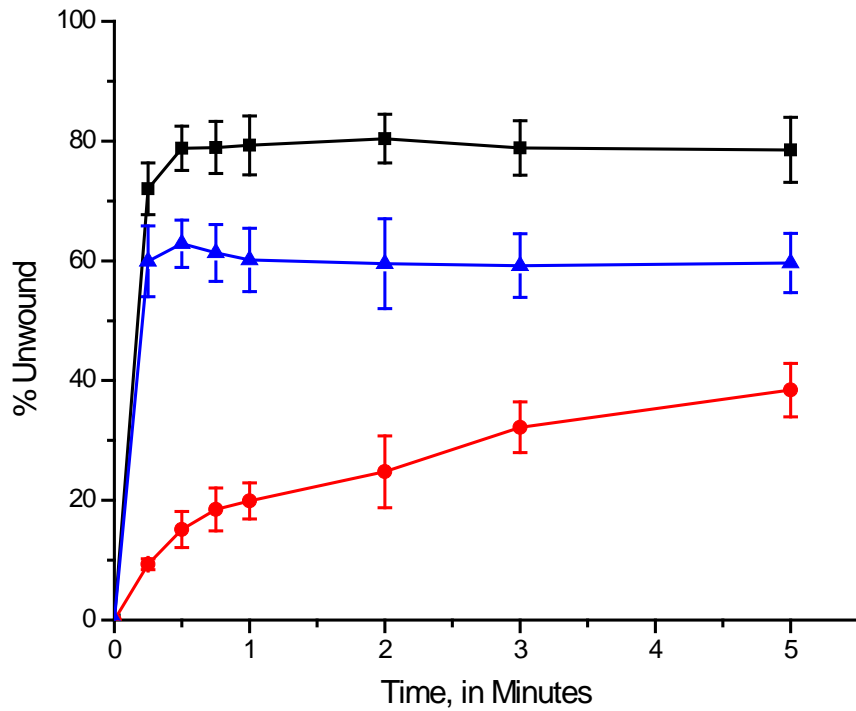


**Figure 2.24: Plot of unwinding of 1 nM 20nt:12bp dsDNA substrate by 100 nM RecD2 in the presence or absence of 2 μM ssDNA trap.** Addition of 1 mM ATP started each reaction. Lines shown above are the average of four independent experiments conducted at room temperature. Bars at each data point are the standard deviation present at each data point. Black squares- unwinding of dsDNA in the absence of trap. Red circles- unwinding in the presence of 2 μM ssDNA competitor, added prior to pre-incubation. Blue triangles- unwinding in the presence of 2 μM ssDNA competitor, added with ATP.

2.3.14 Effect of increasing [RecD2] on unwinding of dsDNA

Most unwinding reactions set up for these studies used 20 nM RecD2 and 1 nM substrate. This concentration had been set on due to early binding experiments that showed complete binding of a model substrate under these conditions. Our binding experiments were, however, not conducted with the actual dsDNA substrate used in the unwinding reactions (*vide supra*). In order to model a reaction mechanism for unwinding of dsDNA by RecD2, it was necessary to be certain that we had 100 percent of the substrate bound at the start of the reaction.

Therefore, we decided to conduct a series of unwinding experiments to determine the maximum rate of unwinding for our set concentration of each substrate. These reactions were performed in the absence or presence of ssDNA trap. In the interests of efficiency, when reactions were performed in the presence of trap, the trap was added at the same time as the ATP (as in the "C" reaction).  The "B" reaction was omitted. For all reactions trap was added, trap was included at a concentration of 2 μM.

We measured unwinding of 1 nM dsDNA substrate by varying concentrations of RecD2. Our hypothesis held that processivity of the enzyme was insufficient to complete unwinding of a 20bp substrate in a single step without dissociation. If this hypothesis was correct, an increase in the concentration of enzyme should increase the chance that an active enzyme will continue with the partially unwound substrate, after the initially bound enzyme has dissociated. When the concentration of the enzyme in the system becomes sufficiently large, there would be a plateau in the rate of reaction.

Unwinding of 1 nM 24nt:20bp was conducted in the presence of 1 nM, 20 nM, and 100 nM RecD2. As the concentration of RecD2 approached 100 nM with 1 nM dsDNA substrate, the reaction demonstrated saturation of the substrate (Fig. 2.25).
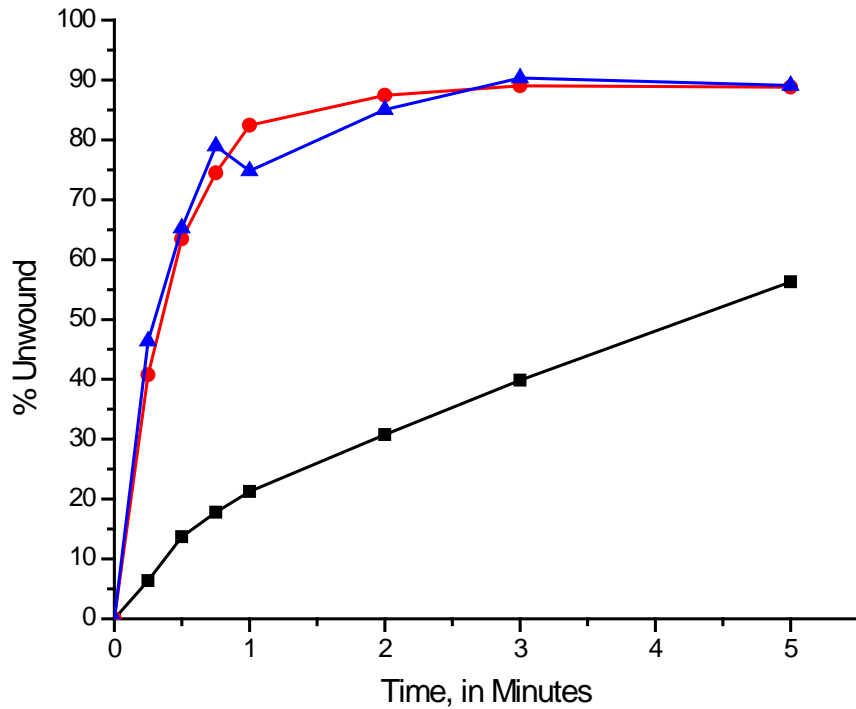


**Figure 2.25: Plot of unwinding of 1 nM 24nt:20bp by increasing concentrations of RecD2.** Lines represent results of one set of experiments conducted together, as detailed in Materials and Methods. Black squares- 1 nM RecD2. Red circles- 20 nM RecD2. Blue Triangles- 100 nM RecD2.

Unwinding of 1 nM 20nt:12bp was conducted in the presence of 1 nM, 10 nM, and 100 nM RecD2. Results shown in Fig. 2.26 show concentration dependence for reactions conducted with 1 or 10 nM RecD2. Saturation of the reaction system has occurred by 100 nM.
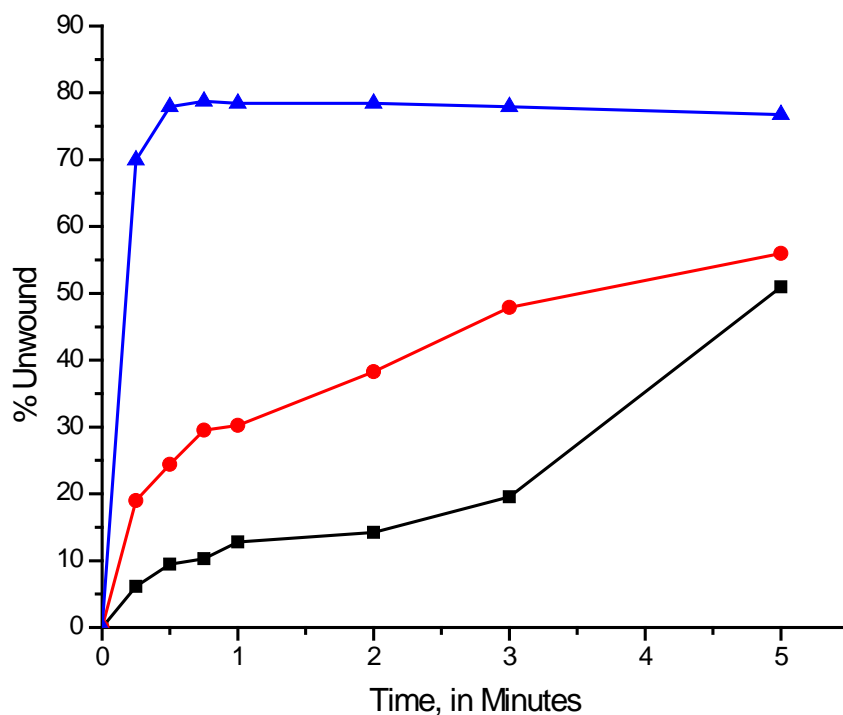
**Figure 2.26: Plot of unwinding of 1 nM 20nt:12bp by increasing concentrations of RecD2.** Lines represent results of one set of experiments each, conducted on separate days, as detailed in Materials and Methods. Black squares- 1 nM RecD2. Red circles- 10 nM RecD2. Blue Triangles- 100 nM RecD2.

2.3.15 Comparison of early unwinding period with various substrates

RecD2 behaved differently on most dsDNA substrates used in the course of this study. One of the key differences in different substrates was found in the early part of the time course. It became readily apparent early on that certain substrates were unwound too fast to be studied by hand.
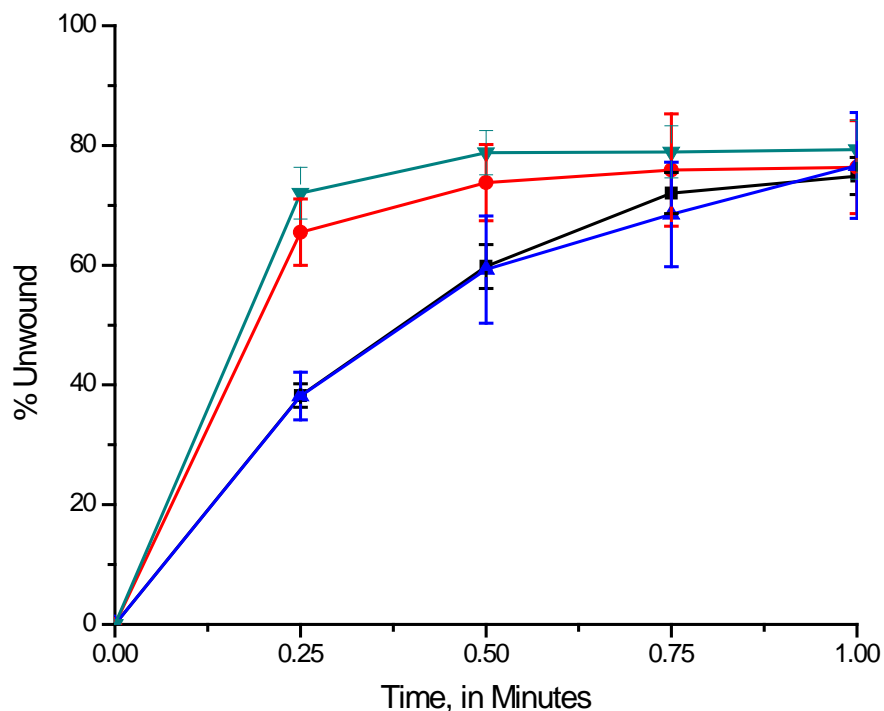
**Figure 2.27: Comparison plot of unwinding in the absence of ssDNA trap with dsDNA substrates 12nt:20bp, 12ntY20bp, 24nt:20bp, and 20nt:12bp.** Black squares- 12nt:20bp; Red circles- 12ntY20bp; Blue triangles- 24nt:20bp; Turquoise inverted triangles- 20nt:12bp. Comparisons reflect unwinding of 1 nM dsDNA substrate by 20 nM RecD2, except unwinding of 1 nM 20nt:12bp was by 100 nM RecD2.

We used information from the early part of the time course (shown in Fig. 2.27) to decide which substrates would be further investigated using the KinTek rapid quench flow device. The substrates chosen for further study were the 12ntY20bp and 20nt:12bp substrates. In the figure above, both substrates are shown to be over 60% unwound within the first 15 seconds. In the case of unwinding by RecD2 of the 20nt:12bp dsDNA substrate, it should be remembered that use of 100 nM RecD2 in the A/B/C reaction system was necessary to obtain consistent results with the 5 minute pre-incubation period.

74

## 2.3.16 DNA unwinding by RecD2 with the RQF-3 Rapid Quench Flow Device

Unwinding of dsDNA by RecD2 proceeded too fast with the 12ntY20bp and 20nt:12bp substrates to be studied by hand sampling techniques. For this reason, a RQF-3 rapid quench flow apparatus (KinTek) was employed. The RQF-3 allows rapid mixing and quenching of reagents, on the millisecond time scale. Reaction times are controllable by the rate of flow through the reaction loop, and the length of the chosen reaction loop.

Multiple turnover reactions were not conducted for the 20nt:12bp substrate in the rapid quench device. When moving to the rapid quench apparatus, unwinding was conducted under single turnover conditions. RecD2 was allowed to unwind 20nt:12bp substrate in the presence of ssDNA trap added at the same time as ATP.
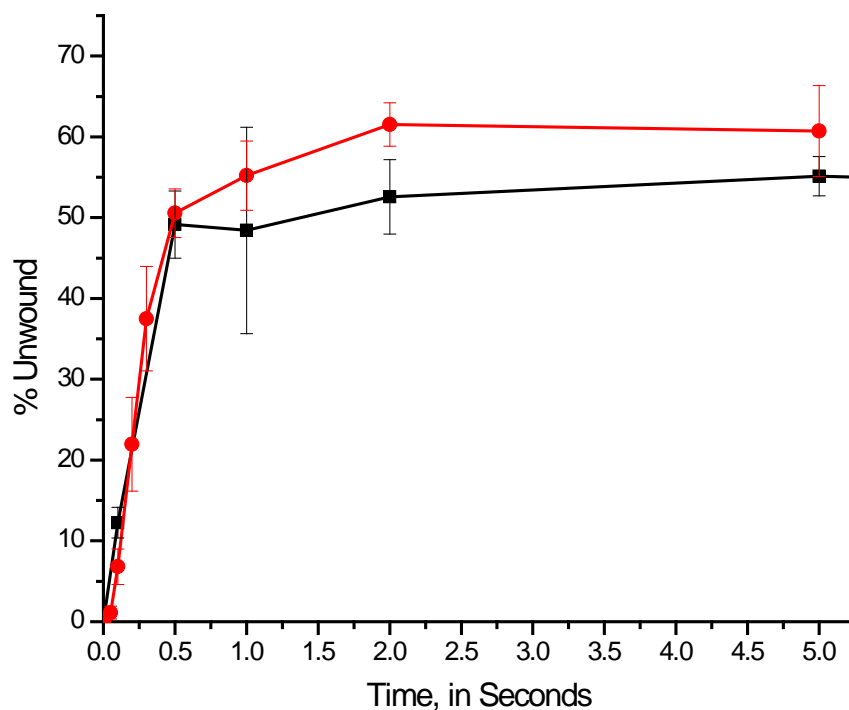
**Figure 2.28: Plot of unwinding of 1nM 20nt:12bp dsDNA substrate by 20 nM or 100 nM RecD2 in the presence of 2μM ssDNA trap.** Reactions were conducted with the rapid quench flow apparatus as detailed in **Materials and Methods**. Lines shown above are the average of three independent experiments conducted at room temperature. Bars at each data point are the standard deviation present at each data point. Black squares- unwinding of dsDNA by 20 nM RecD2. Red circles- unwinding of dsDNA by 100 nM RecD2.

Two different concentrations of RecD2 were studied under these conditions (Fig. 2.28). When 20 nM RecD2 unwound 1 nM 20nt:12bp dsDNA substrate in the presence of 2 μM ssDNA trap, the reaction plateau was observed at about the same time as when 100 nM RecD2 was used. When 100 nM RecD2 was used, the total percentage of dsDNA substrate unwound at the end of the reaction was greater, but only by about ten percent.

While the statistical deviation in the collected data shows the difference between the two curves to be significant, the difference is small, and only for a brief period in the reaction progress. At five seconds, the difference in fraction unwound for the 20 nM reaction and the 100 nM reaction is insignificant. This suggests that the unwinding of the 20nt:12bp dsDNA substrate is no longer concentration dependent under these conditions. The high level of unwinding seen under these conditions, in the presence of an excess of trap, suggests that RecD2 is capable of unwinding the entire length of a 12bp substrate without a significant amount of interference from ssDNA trap.

Unwinding of 20nt:12bp by 100 nM RecD2 was modeled using KinTekSim (KinTek, Corp.). Use of the shorter substrate and single turnover conditions allowed modeling with a relatively simple reaction scheme. For the unwinding of a 12 base pair dsDNA substrate by RecD2, a two step kinetic mechanism was sufficient to generate a model curve most closely approximating the unwinding data. We expect that longer substrates would require more kinetic steps. Each kinetic step shown represents the slowest mechanistic step involved in the unwinding of the 12bp substrate. This slow mechanistic step appears every 3-4 bases during unwinding, after multiple cycles of ATP association, hydrolysis, and dissociation. This may represent a pause of the enzyme as it progresses along the DNA.

When modeling the unwinding, we found that the most important feature of the unwinding scheme (Fig. 2.29) was the partition of the enzyme at the second step between the dissociation from the partially unwound substrate, and the completion of

unwinding. A small change in the ratio of these numbers had a large effect on the

simulated curve generated.

$$E + DS \xleftarrow{\textbf{0.01 s}^{-1}} E{\cdot}DS \xrightarrow{\textbf{5.5 s}^{-1}} E{\cdot}DS_{(A)} \xrightarrow{\textbf{5.5 s}^{-1}} E + SS$$

$$\downarrow \textbf{1.95 s}^{-1}$$

$$E + DS$$
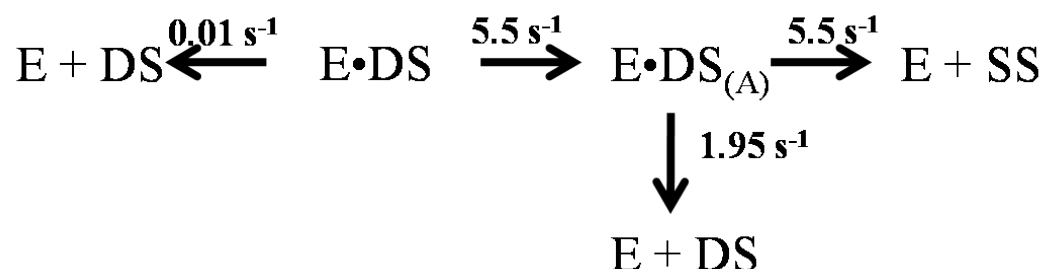
**Figure 2.29: Schematic of unwinding of a 12bp substrate by RecD2.** Kinetic steps
shown represent the slowest mechanistic steps in unwinding of a 12bp substrate by
RecD2. More steps would be expected with a longer substrate- to represent this in this
picture, the partially unwound substrate is denoted (A).

According to our simulations, the rate of dissociation of the substrate from

the enzyme prior to the first unwinding step was minor, at $0.01$ s$^{-1}$. The first and

second unwinding steps occurred at a rate of $k_{unw} = 5.5$ s$^{-1}$. When the enzyme had

progressed through the first unwinding step, enzyme dissociation from partially

unwound substrate occurred at a rate of $k_{off} = 1.95$ s$^{-1}$. As shown in figure 2.30,

unwinding by RecD2 correlates well with the model, with most elements of the

unwinding curve reproduced in the model curve.
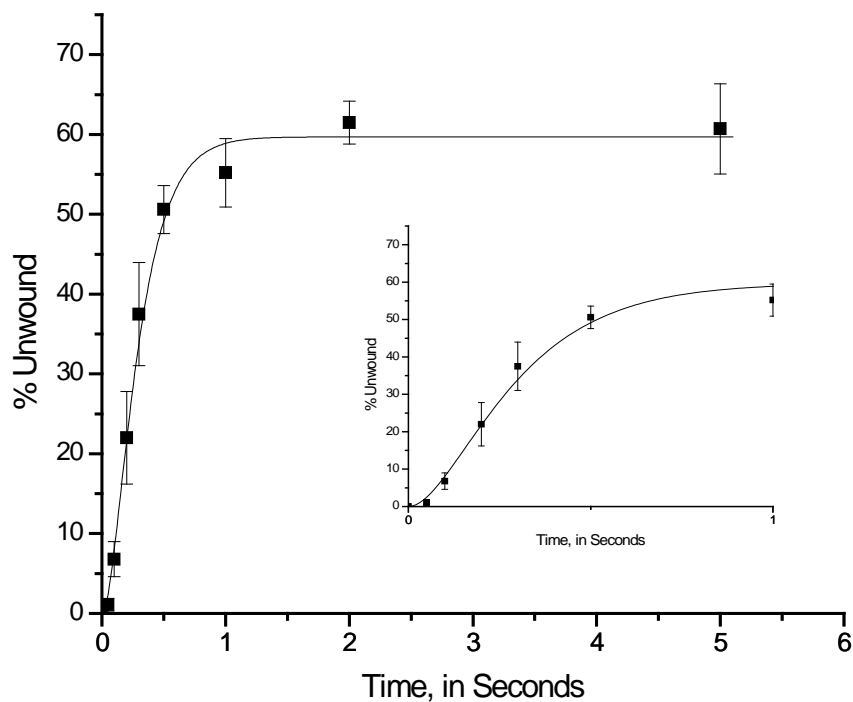
**Figure 2.30: Plot of unwinding of 1 nM 20nt:12bp dsDNA by 100 nM RecD2.**
Black squares show unwinding, with bars representing standard deviation at each data
point. Unwinding was compared to a model curve generated with a two step kinetic
mechanism by KinTekSim (black line).

An unwinding rate of 5.5 $s^{-1}$ with a substrate of 12bp being unwound in two

steps corresponds to 15-20 bp/ sec, assuming the last 4-6 bp will unwind non-

enzymatically, once the rest of the substrate has been unwound (76). This delivers a

calculated step size of 3-4 bp/ step. Processivity of RecD2 was calculated using the

formula $P = k_{unw}/ (k_{unw}+ k_{off})$, where $P$ represents the processivity of the enzyme.

Using the above values, the processivity of RecD2 is $P = 0.74$.

A series of reactions was carried out with the 12ntY20bp substrate in the rapid

quench device to generate data for simulation by KinTekSim. In addition, data

previously obtained by hand was also examined. We were able to successfully simulate the data for unwinding of the 12ntY20bp substrate by either 1 nM RecD2 or 100 nM RecD2. This was achieved by use of a kinetic mechanism that allowed for four kinetic steps to unwind the 20 bases. Relative to the two step kinetic mechanism that models the unwinding of 12 bases, there is more apparent complexity to the mechanism for unwinding of twenty bases. This is mere illusion, however, as the extra two steps proceed at the same rate as the first two steps. The dissociation steps that may occur along the way have the same rates as the first dissociation step. The four step mechanism has another seeming complexity added, as well. The data modeled with the four step mechanism was generated under multiple turnover conditions, so steps for the association of RecD2 to substrate DNA were necessary. When modeling this data, we found that a four step multiple turnover mechanism was insufficient to match our observations. Successful modeling of our observations was only possible when we included the possibility of RecD2 associating with itself in the absence of substrate DNA. In the crosslinking experiments (section 2.3.2), we found higher order species present when RecD2 was crosslinked with glutaraldehyde in the absence of DNA. With self association now included in the kinetic mechanism (shown in figure 2.31), we were successfully able to model the unwinding of the 12ntY20bp substrate by RecD2.
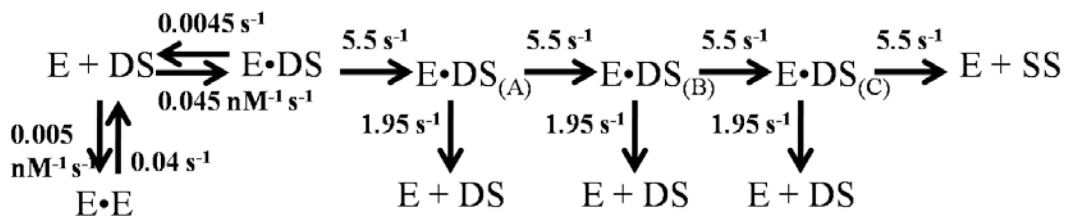
**Figure 2.31: Model of unwinding of 12ntY20bp by RecD2.** Values for unwinding and association/ dissociation were generated by KinTekSim. A, B, and C represent increasingly unwound substrate DNA present at each step.

Unwinding of the 12ntY20bp substrate by RecD2 proceeded at the same rate as when RecD2 was unwinding the 20nt:12bp substrate, at 5.5 s$^{-1}$. We found modification of unwinding rates significantly affected the shape of the modeled curve. The association of the enzyme with the substrate was best modeled with a forward rate of 0.045 nM$^{-1}$ s$^{-1}$ and a reverse rate of 0.0045 s$^{-1}$. We found the values for association of enzyme to substrate varied with the substrate, not with the concentration of the enzyme in the reaction. Shown in figure 2.32 is the model curve compared to the data for unwinding of the 12ntY20bp substrate by 1 nM RecD2. Figure 2.33 shows the model curve generated for unwinding of the same substrate by 100 nM RecD2 compared against the observed data.
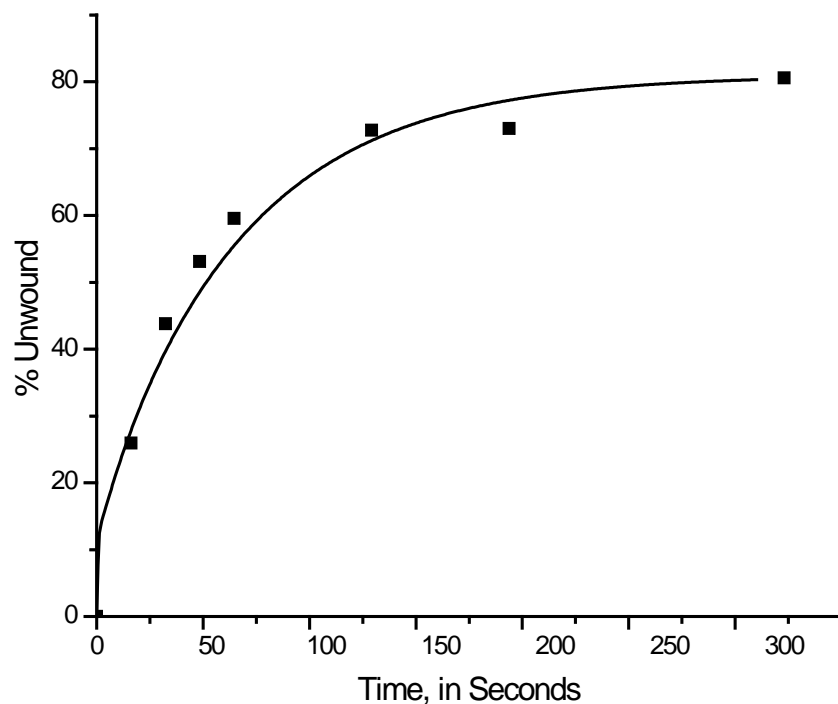
**Figure 2.32: Plot of unwinding of 1 nM 12ntY20bp dsDNA substrate by 1 nM RecD2 in the absence of ssDNA trap.** Reactions were conducted by hand as detailed in **Materials and Methods**. Data points shown above are one representative set from three independent experiments conducted at room temperature. Black squares- unwinding of dsDNA in the absence of trap. Black line- Closest simulation generated with KinTekSim and four step mechanism (detailed above), using rate constant values given in figure 2.31.
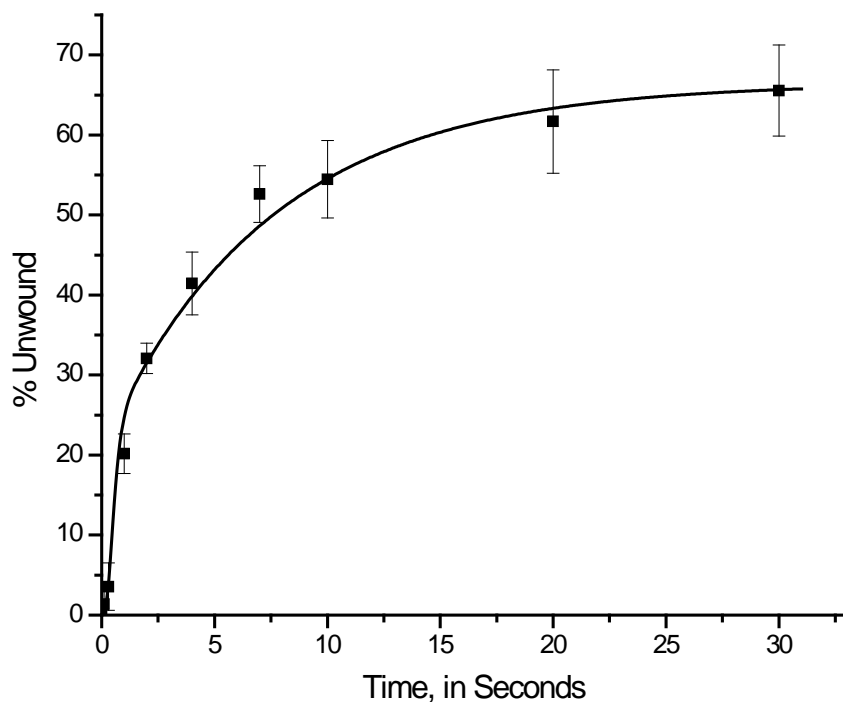
**Figure 2.33: Comparison of unwinding of 1 nM 12ntY20bp by 100 nM RecD2 to simulation generated by KinTekSim.** Data points (black squares with error bars) are the average of three independent experiments. The black line shown is the result of the best simulation generated by KinTekSim with the four step kinetic mechanism and rate constant values given in figure 2.34.

Modeling of the unwinding of various substrates by RecD2 was extended to previously obtained data for unwinding of the 5' overhang 12nt:20bp substrate. These data had been collected by hand, and as such, represented unwinding occurring on a longer time scale than was observed through use of the rapid quench device, shown above. The kinetic mechanism (Fig 2.34) determined for the 12ntY20bp substrate was found to correlate well with the 12nt:20bp unwinding data, except that the rate

constant for association of RecD2 to substrate had to be lower for the 12nt:20bp

substrate (figure 2.34), compared to the 12ntY20bp substrate (figure 2.31).

$$E + DS \underset{0.007 \text{ nM}^{-1}\text{s}^{-1}}{\overset{0.0045 \text{ s}^{-1}}{\rightleftarrows}} E \cdot DS \xrightarrow{5.5 \text{ s}^{-1}} E \cdot DS_{(A)} \xrightarrow{5.5 \text{ s}^{-1}} E \cdot DS_{(B)} \xrightarrow{5.5 \text{ s}^{-1}} E \cdot DS_{(C)} \xrightarrow{5.5 \text{ s}^{-1}} E + SS$$

$$0.005 \text{ nM}^{-1}\text{s}^{-1} \uparrow\downarrow 0.04 \text{ s}^{-1}$$

$$E \cdot E \qquad\qquad 1.95 \text{ s}^{-1}\downarrow \qquad 1.95 \text{ s}^{-1}\downarrow \qquad 1.95 \text{ s}^{-1}\downarrow$$

$$E + DS \qquad E + DS \qquad E + DS$$
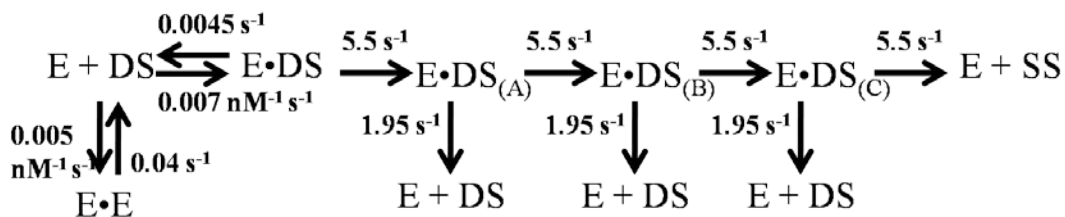
**Figure 2.34: Kinetic model of unwinding of 12nt:20bp substrate by RecD2.**
Values for each kinetic step are the same as for other substrates modeled; the only
difference between this kinetic mechanism and the kinetic mechanism for unwinding
of the 12ntY20bp substrate is a change in the association of enzyme and substrate,
reflecting a difference in the structure of the two substrates.

Shown in figure 2.35 is the unwinding data for the 12nt:20bp substrate with

various concentrations of RecD2. The data were simulated using the four step

mechanism shown in figure 2.34. Model curves generated correlated well with the

data, when three or more reactions had been conducted for a given concentration of

enzyme. Correlation of the model curves with the data was closest for unwinding of 1

nM 12nt:20bp DNA substrate by 20 nM and 100 nM RecD2. Only two reactions each

were performed at lower concentrations, so the model curves did not relate well to the

data.
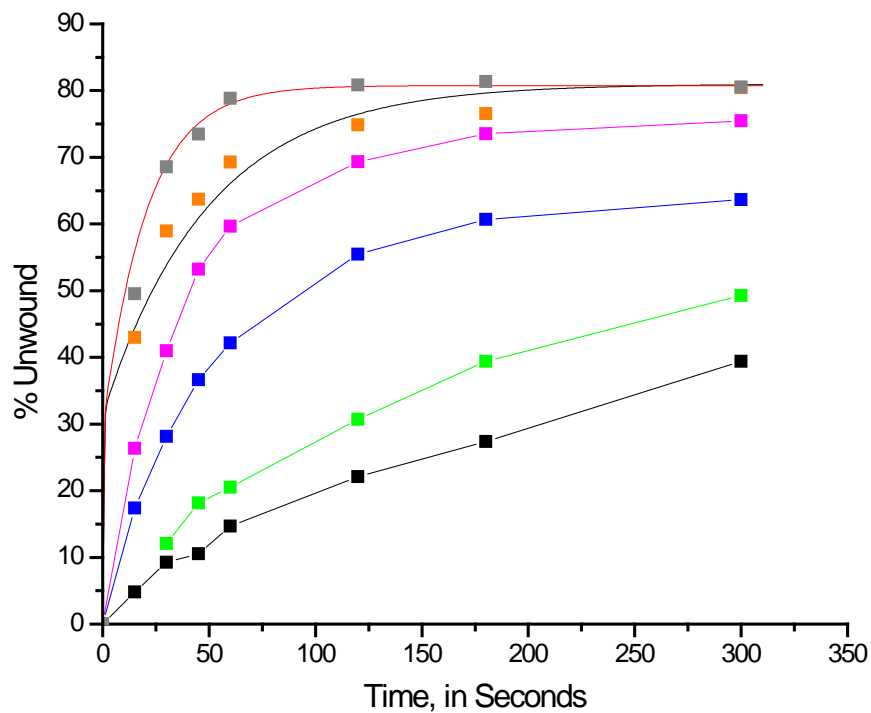
**Figure 2.35: Plot showing unwinding of 1 nM 12nt:20bp by increasing concentrations of RecD2.** Lines connected by data points represent averages of two independent experiments conducted as detailed in Materials and Methods. Black squares- 1 nM; Green squares- 2 nM; Blue Squares- 4 nM; Mauve squares- 10 nM RecD2. Unconnected data points represent averages of three independent experiments; error bars are omitted for clarity. Orange squares- 20 nM; Grey squares- 100 nM RecD2. Simulated curves generated with a four step kinetic mechanism (detailed above) are shown in black (20nM) and red (100nM).

## 2.4 Discussion

Management of DNA in the cell is performed by enzymes acting at a variety of association levels. Some SF1 helicases, such as *E. coli* TraI helicase, are functional as a monomer (88). Unwinding of DNA by *E. coli* UvrD helicase is performed by a dimer of the enzyme (77). For the unwinding of DNA ahead of a replication fork, DnaB helicase requires 6 subunits (a homohexamer) acting as a single complex, unwinding substrate DNA in a cooperative fashion (71-73,89). The helicase RepA also acts as a hexamer (90,91).

We set out to directly address the functional unit size of RecD2, using SEC and glutaraldehyde cross-linking. The size exclusion results showed evidence of only one soluble form eluting from the column. The single population eluted with a calculated molecular mass only slightly smaller than the mass of a monomer, suggesting that a monomer may be a relevant form of the protein. Our experiments were conducted under three different concentrations of RecD2, suggesting that the protein stays in the same form across a range of concentrations.

Cross-linking of RecD2 with glutaraldehyde was performed under a variety of conditions. When RecD2 was cross-linked in the absence of DNA, a large molecular weight species appeared. This species was observed independent of reaction time, and was also present whether or not DNA was present in the reaction system.

Binding of RecD2 with a 12nt 5'-overhang hairpin substrate (HP1- see table 3.1) was carried out as previously reported (15). The $K_d = 2.31$ nM (see section 2.3.3) calculated for RecD2 was tighter than the binding reported for another SF1 helicase UvrD, with $K_d = 17$ nM (92). Binding affinity of RecD2 was similar to the SF1

helicase Pif1 ($K_d$ = 3 nM) (93). On the whole, we found RecD2 displayed tight binding affinity to its preferred substrate relative to other SF1 helicases.

A single turnover reaction system was utilized to efficiently carry out the kinetic characterization of RecD2. With this system, we performed the unwinding of a range of dsDNA substrates by RecD2 under excess enzyme conditions. Unwinding of the 20nt:12bp substrate in the presence of trap ("C" reactions) was simulated with the program KinTekSim. Based on these simulations we found unwinding of dsDNA under single turnover conditions occurred at a rate of approximately 15-20 bp/ sec. An unwinding rate of 2 bp/ sec was previously reported (15) obtained under multiple turnover conditions. Multiple turnover conditions allow for multiple steps of binding and dissociation so should be different than single turnover results, which measure unwinding independent of binding. An unwinding rate of 15-20 bp/ sec is much slower than the translocation rate of 95 s$^{-1}$ reported previously for movement along ssDNA (62), but is reasonable given the extra effort necessary to separate dsDNA.

The unwinding rate found for RecD2 is much slower than other SF1 helicases. The unwinding rate for *E. coli* RecBCD is 790 bp/ sec (94). Characterization of the unwinding rate for *E. coli* RecD was hindered by low solubility (50). Unwinding rates for other SF1 helicases generally vary from 29 bp/ sec for *B. stearothermophilus* PcrA (95), 44 bp/ sec for bacteriophage T$_4$ Dda helicase (67),  to as much as 1120 bp/ sec for *E. coli* TraI (88).

Modeling of unwinding by RecD2 was performed with KinTekSim. We worked with several substrates, to get the best possible modeling of the unwinding of substrate DNA by RecD2. We found good correlation between the curves generated

by the model for each substrate and the unwinding data for that substrate, across a range of RecD2 concentrations. In modeling the unwinding, we found the rate of unwinding at each kinetic step to be independent of the concentration of the substrate. The rate constant for dissociation from partially unwound substrate was also independent of the concentration of the substrate. We found the structure of the substrate changed the rate of binding of RecD2 to substrate, with RecD2 more readily binding to the fork than to the 5'- overhang.  Self-association of RecD2 to itself in the absence of DNA was observed in the glutaraldehyde cross-linking (section 2.3.2), and we found that adding this to the kinetic model made the model fit the observations substantially better. Further examination of the self-association would therefore be warranted to more accurately describe the nature of the species formed. We modeled this species as a dimer to simplify the model, with positive results.

We determined the kinetic step size for dsDNA unwinding by RecD2 to be in the range of 3-4 bp/ step (section 2.3.16). Keeping in mind that the kinetic step is defined as the slowest step in the overall process of unwinding by the enzyme, 3-4 bp/step is in broad agreement with other SF1 helicases. Values ranging from 3.4 bp/ step for RecBCD (96), 4 bp/ step for *B. stearothermophilus* PcrA (97), to 6-8 bp/ step for *E. coli* TraI (88) have been reported. Processivity of RecD2 ($P = 0.74$) is in the range for helicases, which range from $P = 0.27$ for *B. stearothermophilus* PcrA (97), to $P = 0.90$ for *S. cerevisiae* Isw2 (98), and $P = 0.99997$ for *E. coli* RecBCD (99).

The processivity for RecD2 may be significantly increased *in vivo* by interaction with other proteins, as in the case of *E. coli* RecBCD or *B. stearothermophilus* PcrA in interaction with the replication initiator protein RepD

(100). Experiments conducted in the Julin lab by Zheng Cao used an Affi-gel column

(Bio-Rad) charged with RecD2 to search for binding partners in *D. radiodurans*

(101). The most prominent of the proteins bound were three subunits of RNA

polymerase, pointing to a role for RNA polymerase in regulation of RecD2. Future

work may expand on this, to determine if other proteins change the enzymatic

properties of RecD2.

# Chapter 3: Domain Analysis of RecD2

## 3.1 Introduction

Based on sequence analysis, the C-terminal region of RecD2 from *D. radiodurans* has been grouped as a member of the RecD-like helicases (15). RecD-like helicases are a sub-grouping of the SF1 helicases. Superfamily I helicases are defined by the presence of seven conserved helicase motifs. These motifs, numbered I, Ia, and II to VI, all contain residues necessary for ATP binding (motifs I and II are Walker A and B ATP hydrolysis motifs) and translocation along DNA (75).

RecD helicases are grouped into two major divisions (figure 3.1). These are proteins that associate with other enzymes in order to perform their activity, and those for whom no associated enzymes have been identified. RecD-like enzymes that associate with other enzymes to form an active complex are termed RecD1 enzymes. The prototypical member of this group is RecD from *E. coli*, which binds to RecB and RecC to form the RecBCD complex. RecD-like enzymes with no identified binding partner are termed RecD2. The best characterized member of this group is RecD2 from *D. radiodurans*.
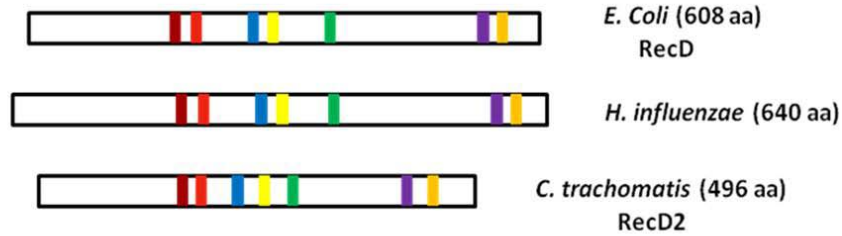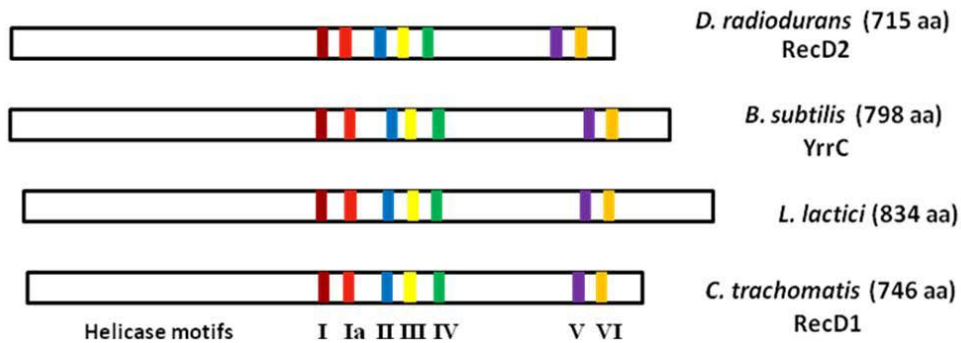
**Figure 3.1: Representative members of the RecD-like helicases.** Shown at the top
are RecD1 proteins that bind to other proteins to form RecBCD complexes. Shown at
the bottom of the figure are RecD2 proteins with no known binding partners.
Organisms with more than one RecD protein are assigned numbers to differentiate
them; thus members of the RecD1 group can be named RecD2, and vice-versa.
Adapted from (15).

A notable difference between enzymes in the RecD1 group and those in the

RecD2 group is the length of the N-terminal region prior to the first helicase motif.

Enzymes of the RecD2 grouping generally have much longer N-terminal regions than

RecD1 enzymes, and the role of this extended sequence is unclear. We conducted

limited proteolysis of RecD2 with subtilisin Carlsberg to identify separable domains.

With characterization of these domains, we hoped to determine the role of this N-

terminal region in DNA unwinding by RecD2 from *D. radiodurans*.

## 3.2 Materials and Methods

### 3.2.1 Limited proteolysis of RecD2 with subtilisin Carlsberg

Structure analysis of RecD2 was performed through the use of subtilisin Carlsberg. Prior to setup of the proteolysis, RecD2 was first dialyzed into a solution containing 150 mM potassium phosphate, pH 7.5, 5 mM DTT, 150 mM NaCl using a mini dialysis cup (Pierce Bio) for a period of two hours. After dialysis, the concentration of RecD2 was determined using absorbance at 280 nm and an extinction coefficient of 52,060 $M^{-1}cm^{-1}$ (ProtParam, ExPasy.org).

To this solution was added a solution of subtilisin Carlsberg (Sigma). The concentration of subtilisin had been calculated using absorbance at 280 nm and an extinction coefficient of 23,740 $M^{-1}cm^{-1}$ (ProtParam, ExPasy.org). Subtilisin and RecD2 were mixed to the ratio of 360 fmol subtilisin for every 200 pmol RecD2. This reaction mixture was placed in a 37 °C water bath for 60 minutes. The reaction was then quenched by addition of 5 mM (final conc.) of PMSF. One part SDS loading buffer was added for every five parts of quenched reaction in a microcentrifuge tube and heated at 96 °C for 1 minute. An aliquot of this was then loaded onto a 12 % SDS-PAGE (29:1 acrylamide: bis-acrylamide) and run for 1 hour at 150 V constant voltage. Upon completion, the gel was electroblotted onto a PVDF membrane (Immobilon-P, Millipore, Inc.) via the western blot protocol using CAPS transfer buffer (10 mM CAPS, 10 % methanol, pH 11.0) (102).

The resulting blot was stained with Coomassie stain for sequencing blots (40 % methanol, 1 % acetic acid, 58.9 % water, and 0.1 % Coomassie blue R-250) and destained with 50 % methanol/water. The blot with a major band identified at 45 kDa

was submitted to the Molecular Structure Facility at UC Davis for peptide sequencing. Sequencing was via Edman degradation on an Applied Biosystems Edman Sequencer.

## 3.2.2 RecD2 truncation constructs

The *D. radiodurans recD2* gene had been previously cloned into the vector pDrRecD.ptz19r by Jianlei Wang of this lab. This plasmid served as a template for production of truncation constructs comprising the N- and C- terminal regions of RecD2. In addition, a catalytically inactive mutant was generated by Steve Polansky of this lab (103), with the lysine at amino acid 366 (numbering based on the parent sequence) replaced by glutamine. Lysine 366 rests in the Walker A motif, which is necessary for ATP hydrolysis by RecD2. This served as the template for production of C- terminal catalytically inactive mutants.

PCR reactions were done in a buffer solution containing 20 mM Tris·HCl, pH 8.8, 10 mM $(NH_4)_2SO_4$, 10 mM KCl, 2 mM $MgSO_4$, 0.1 % Triton X-100, 2 ng/µl substrate DNA, 200 µM each dNTP, 10 % DMSO and 2 units Vent polymerase (New England Biolabs). Reactions were carried out in an Eppendorf thermocycler with the following conditions. Cycle 1 was 10 minutes at 94 °C (initial denaturation), followed by 30 cycles of the following three steps: step 1, 96 °C for 1 minute (denature); step 2, 57 °C for 1 minute (anneal); step 3, 72 °C for 5 minutes (extension). Following this was a final cleanup extension cycle of 72 °C for 10 minutes. Primers used for constructs are listed in table 3.1.

| | | |
|---|---|---|
| **Table 3.1. Oligonucleotides used** | | |
| **Primer Name** | | **Sequence 5'-3'** |
| **1** | (N)shortpDrRecD 875 | ATAGCTCGAGCTAGGCGGCTTCTGCGGC |
| **2** | DrRecD290Stop | CTAGAAGCTTCGTCTTAATGCGCCCTGATTCTTTCCAACAGC |
| **3** | recD1 | CGCGGAATTCATATGTCTGCTGCTGCCCCTGCC |
| **4** | recD2 | AGTGGGATCCCTGACAGAACTCTTAAGGCGTCTTAATG |
| **5** | shortpDrRecD875(C ) | CTAGCTCGAGGGCGGCTTCTGCGGC |
| **6** | SUMOCTerm290Up | GATCGGATCCGCTACCGGCGAGGGCCG |
| **7** | TruncCtermDrRecDdown (end) | CTCGAGATGCGCCCTGATTCTTTCCAACAGC |
| **8** | TruncCtermDrRecDupstream (875) | CATATGGCTACCGGCGAGGGCCG |

DNA sequences amplified by PCR were ligated into the vector *pCRBlunt* (Invitrogen) following the manufacturer's protocol and transformed into Top10 *E. coli* cells. Sequencing of each construct was conducted by the UMBI-CBR DNA sequencing facility, located at the University of Maryland, College Park. Sequences returned were compared to parent sequences by NIH-BLAST. These constructs were digested with the necessary restriction endonucleases to retrieve the appropriate sequence, which was then ligated into the multiple cloning site of the target vector. This strategy allowed more than one expression construct to be made from a particular sequence.

Constructs consisting of the N- terminal region of RecD2 were named DrDNterm, followed by -15 or -21, to indicate the position of the hexahistidine tag. Those built to comprise the C-terminal domain were named DrRecD290, followed by indication of the affinity label according to the tag. Table 3.2 lists the constructs built and *E. coli* expression strains employed.

| | Table 3.2. Expression Constructs Built | | | | | | |
|---|---|---|---|---|---|---|---|
| | **Expression constructs** | **Vector Name** | **Affinity Tag** | **K366Q made?** | **Tag Terminus** | **MW (kDa)** | **Oligos used** |
| **A** | pDrRecD 290-21 | pET21a | His$_6$ | Yes | C | 46 | 7,8 |
| **B** | pDrRecD290 .pSmt3 | pSmt3 | His$_6$ | Yes | N **and** C | 60 | 6,7 |
| **C** | pDrRecD290 Stop.pSmt3 | pSmt3 | His$_6$ | Yes | N | 60 | 2,6 |
| **D** | pDrDNterm21 | pET21a | His$_6$ | N/A | C | 35 | 1,3 |
| **E** | pDrDNterm15 | pET15b | His$_6$ | N/A | N | 35 | 3,5 |
| **F** | pDrRecD 290-15 | pET15b | His$_6$ | No | N | 50 | 1,4 |
| **G** | pDrRecD290 .pMalP2X | pMalP2X | MBP | Yes | N | 91 | 2,6 |
| **H** | pDrRecD290 .pGEX4T1 | pGEX4T1 | GST | Yes | N | 72 | 7,8 |

## 3.2.3 Expression of the N- terminal domain of RecD2

The plasmid for the construct expressing the N-terminal domain of RecD2

(construct pDrDNterm21) was transformed into *E. coli* strain BL21-DE3 [pLysS] by

the chemical transformation protocol. Transformed cells were spread on LB agar

plates containing 34 µg/ml chloramphenicol and 100 µg/ml ampicillin. Overnight

cultures were set up from single colonies in 20 ml liquid LB media and allowed to

grow at 37 °C.

The following day, one of the 20 ml overnight cultures was used to inoculate a

2 L culture for expression. When the culture reached $OD_{600}$ 0.5, IPTG was added to a

final concentration of 1 mM. The flask was moved to a shaker at 30 °C and allowed

to grow a further 2 hours. At this time, cells were harvested by centrifugation at 5,000

x g in a Beckman model J2-21 centrifuge and the cell pellet placed at -80 °C

overnight. The cell pellet was re-suspended in $Ni^{2+}$ ·column buffer (20 mM potassium phosphate, pH 7.5, 0.5 M NaCl, 1 mM DTT) + 20 mM imidazole and sonicated. Sonication was performed on a Branson Sonifier model 450 with a microtip and the settings: duty cycle 50, intensity 5, and duration 10 minutes, on ice. PMSF (5 mM final) was added to the buffer immediately prior to sonication to inhibit serine protease activity. After sonication, the lysate was centrifuged at 10,000 x g for 2 hours at 4 °C and the supernatant filtered through a 0.2 µm filter.

The filtered lysate was then loaded onto a 5 ml $Ni^{2+}$- NTA column (Hi-Trap Chelating HP, GE Life Sciences) and washed with 5 column volumes of wash buffer (*vide supra*). Protein was eluted from the column by a 50 ml gradient of 60-500 mM imidazole in $Ni^{2+}$ column buffer. Samples (24 µl) of each fraction were taken, mixed with 6 µl 6x SDS loading buffer, and placed at 95 °C for 1 minute. These samples were then loaded onto 10 % SDS-PAGE gels (29:1 acrylamide: bis-acrylamide) and run at 150 V (constant) for 1 hour. Gels were then stained with Coomassie brilliant blue gel stain for 30 minutes and destained with fast destain until developed. Fractions containing the highest level of eluted protein were pooled and placed in a dialysis bag (Spectra-Por, MWCO 12-14 kDa, Spectrum Medical) in Mono·Q start buffer (20 mM Tris·HCl, pH 8.0) overnight at 4 °C.

The next day, the dialyzed eluant was filtered through a 0.2 µm filter. The filtrate was loaded on to a 1 ml Mono·Q HR 5/5 column (GE Life Sciences) and washed with 5 column volumes of start buffer + 50 mM NaCl. Elution followed, with a 20 column volume gradient running from 50 mM to 1 M NaCl in 20 mM Tris·HCl, pH 8.0. Fractions were analyzed by 10% SDS-PAGE. Fractions containing the

highest amount of protein were combined into a dialysis bag. This dialysis bag was placed into 2 L of enzyme storage buffer (20 mM potassium phosphate, pH 7.5, 250 mM NaCl, 5 mM DTT, 1 mM EDTA, and 50% glycerol) and dialyzed overnight at 4 °C. The following day, the concentration of the purified DrDNterm was determined by absorbance at 280 nm with a calculated extinction coefficient of 19,940 $M^{-1}cm^{-1}$ (ProtParam, ExPasy.org). Aliquots (50 µl) were numbered and placed in a -80 °C freezer for later use. Best yield from this method was 0.75 mg purified RecD2 from 8 g wet cells.

### 3.2.4 Detection of binding epitope for RecD2 antibody

Purified DrDNterm21 was used to determine the region of the enzyme bound by the RecD2 antibody. Generation and purification of the monoclonal mouse Anti-RecD2 antibody was by Matt Servinsky of this lab (85). This was used as a primary antibody to detect RecD2 in the western blot protocol. Gels were loaded with purified RecD2, cells expressing DrDNterm21, and cells expressing DrRecD290-21.

Samples were run on 10% SDS-PAGE according to the following protocol: For the purified RecD2 lanes, 5 µl of purified RecD2 (23 pmol total) was mixed with 4 µl ddH$_2$O and 1 µl of 6x SDS loading buffer. The mix was then placed at 95 °C for 1 minute before the entire 6 µl was loaded on to the gel. For the cell lysate lanes (DrDNterm-15, DrDNterm-21, and DrRecD290-21), 1 ml of cells were harvested by centrifugation at 13,000 x g for 1 minute. Cells were re-suspended in 100 µl of ddH$_2$O, mixed with 20 µl 6x SDS loading buffer, and placed at 95 °C for 1 minute.

Thirty micro-liters of each prepared cell lysate were then loaded onto a 10% SDS-PAGE gel (29:1 acrylamide: bis-acrylamide) and run at 150 V constant for 1 hour.

This gel was then transferred to a PVDF membrane (Millipore, Inc.) by the western blot protocol (300 mA constant for 30 minutes). After transfer, the blot was shaken in blocking solution (4% powdered milk in tTBS: 1% NaCl, 0.1% Tween 20, and 0.3% Tris, pH 8.3) for one hour, and poured off. Antibody binding followed the protocol: after blocking, the blot was shaken in a solution containing antibody Dr-RecD mAb (1:5,000 in tTBS) for 1 hour. Next, the solution was poured off, and the blot was rinsed with shaking three times for 20 min in tTBS. After this was complete, the rinse was poured off and the blot submerged in secondary antibody. This antibody was AP linked goat derived anti- mouse (Novagen, Inc.) diluted 1:5,000 in tTBS. The blot was allowed to shake for another hour, and the antibody solution was poured off. The blot was rinsed a further three times for 20 minutes in tTBS with shaking. After this set of rinses, the blot was developed with the reagent ECL (GE Life Sciences), according to the manufacturer's protocol. The developed blot was then imaged on a STORM phosphorimager.

### 3.2.5 Expression of C-terminal domain of RecD2

The construct *pDrRecD290-21* was transformed into *E. coli* strain BL21-DE3 by the chemical transformation protocol. Transformed cells were spread on LB agar plates containing 100 µg/ml ampicillin. Overnight cultures were set up from single colonies in 5 ml liquid LB media (1% bacto tryptone, 0.5% yeast extract, 1% NaCl) and allowed to grow at 37 °C. The following day, the overnight culture was used to

inoculate a series of 10 ml cultures for expression testing. When these cultures

reached OD$_{600}$ 0.5, the tubes were then split in two. One set served as a control, so

was left un-induced. In the other set, IPTG was added to a final concentration of 1

mM. Sets of induced and un-induced cultures were placed on shakers at 30 °C or 37

°C. One milliliter aliquots were taken at 1, 2, and 4 hours. These aliquots were

processed as for the cell lysate samples in the previous section. Samples were loaded

on to 10% SDS-PAGE and run at 150 V for one hour. Gels were developed by

Coomassie staining.

## 3.2.6 Use of alternate systems to express RecD2 in *E. coli*

A range of *E. coli* strains were employed with a range of expression protocols

to facilitate production of the above mentioned constructs of the C-terminal domain

of RecD2.  Each of these constructs was transformed into the appropriate strain of *E.*

*coli* by the chemical transformation protocol (*vide supra*) and plated with the

appropriate antibiotic for the construct. Expression of DrRecD290 in the various

constructs was attempted with a range of conditions, mentioned in table 3.3, and

below. Most strains were tried with adjustments to the IPTG protocol. Each protocol

is detailed below.

| Table 3.3. | *E. coli* strains, constructs, and protocols used | |
| :---: | :---: | :---: |
| ***E. coli* strain** | **Constructs used** | **Expression protocols used** |
| **BL21-DE3** | A-H | |
| **BL21-DE3 pLysS** | A-E | |
| **BL21-DE3 BLR** | A | |
| **BL21-DE3 RIL** | A | |
| **BL21-DE3 C41** | A | IPTG, Lac, LBNB, Osmotic Shock |
| **BL21-DE3 C41 pLysS** | A | |
| **BL21-DE3 C43** | A | |
| **BL21-DE3 C43 pLysS** | A | |
| **Origami2-DE3** | A | |
| **Rosetta2-DE3** | A, C-H | |
| **RosettaGami2-DE3** | A,C-E, G, H | |

3.2.7 IPTG

The IPTG expression protocol utilized the reagent Isopropyl β-D-1-thiogalactopyranoside (IPTG). For expression using this reagent, different sized cultures were grown to mid-log phase ($OD_{600}$ 0.5) at 37 °C. At this time, IPTG was added to a final concentration of 0.2 mM. Thereafter, cultures were moved to 30 °C and allowed to continue growth. For time scale growth experiments, 1 ml samples were taken at 1 hour, 2 hours, and 4 hours.

Samples were centrifuged at 16 000 x g for 1 minute. Samples were then re-suspended in a solution containing 20 µl 6x SDS loading buffer and 100 µl $ddH_2O$. Samples were placed at 95 °C for 3 minutes, and then loaded on to a 12% SDS-PAGE gel. Gels were run at 150 V for 1 hour and coomassie stained. Depending on the individual case, IPTG was tested in cultures at levels from 0.2 mM to 1 mM. In addition, some cultures were tried with IPTG at 20 °C (room temperature).

### 3.2.8 Lactose Induction Protocol

This expression protocol is based on the use of lactose to auto-induce expression under control of the T7 promoter (104). An overnight solution of culture is grown in LB media, with appropriate antibiotic, at 37 °C. This overnight culture is diluted 1:20 in auto-induction growth medium ZYP-5052 containing the following: 1% bacto-tryptone, 0.5% yeast extract, 1 mM $MgSO_4$, 25 mM $(NH_4)_2SO_4$, 50 mM $KH_2PO_4$, 50 mM $NaH_2PO_4$, 2.8 mM dextrose, 5.8 mM lactose, and 0.5% glycerol. This culture is transferred to 20 °C, and allowed to shake vigorously for 16 to 18 hours.

After completion, the culture was centrifuged at 5 000 x g for 20 minutes and the supernatant discarded. The cell pellets were stored overnight at -80 °C. The next day, cell pellets were re-suspended in $Ni^{2+}$ ·column buffer (20 mM potassium phosphate, pH 7.5, 0.5 M NaCl, 1 mM DTT) +20 mM imidazole and sonicated. Sonication was performed on a Branson Sonifier model 450 with microtip and the settings: duty cycle 50, intensity 5, duration 10 minutes on ice. After sonication, samples were taken of the soluble (supernatant) and insoluble (cell lysate) fractions. To the soluble fraction was added a 1/5 volume of 6x SDS loading buffer, and the mix was heated at 95 °C for 1 minute. The insoluble fraction was re-suspended in $ddH_2O$ and 6x SDS loading buffer. All samples were loaded on to 12% SDS-PAGE and run at 150 V constant for one hour. Gels were developed with Coomassie stain.

3.2.9 LBNB

This protocol uses modified Lysogeny Broth (LB) (105) media to increase soluble expression of proteins that are otherwise insoluble. The feature of this method is the addition of glucose and betaine to the growth media, along with increasing the NaCl concentration from 170 mM to 500 mM. Glucose acts to suppress basal expression levels for target proteins under control of the T7lac promoter (106). Betaine is believed to act as a cellular osmolyte. Increasing the NaCl concentration increases intracellular stress, causing up-regulation of molecular chaperone proteins (107). To make LBNB media, LB media is supplemented with 500 mM NaCl, 0.2% glucose, and 1 mM betaine and autoclaved. The following method is basically as detailed by Oganesyan, et al (107).

An overnight culture of cells containing the desired plasmid was cultured in a culture tube containing 5 ml of LB media with added 500 mM NaCl and appropriate antibiotic and allowed to grow at 37 °C to saturation. One milliliter of saturated culture was transferred to a 250 ml flask containing 100 ml of autoclaved LBNB media, again with appropriate antibiotic, and placed at 37 °C. After the culture reached $OD_{600}$ 0.5, the culture was induced with IPTG (0.3 mM final) and placed on a shaker at room temperature for overnight.

The next morning, cultures were collected and centrifuged for 20 min at 5000 x g to collect the cell pellet. The cell pellet was re-suspended in Profound lysis buffer (Promega, Corp.) according to the manufacturer's protocol. After treatment, the insoluble and soluble fractions were separated by centrifugation at 16,000 x g for 20 min in a microcentrifuge. Soluble fractions were treated with 6x SDS loading buffer

and boiled for 1 minute. Insoluble fractions were re-suspended in a mixture containing 6x SDS loading buffer and water and boiled for 3 minutes. Samples were run on 10% SDS-PAGE and developed by Coomassie staining.

### 3.2.10 Osmotic Shock

Osmotic shock is recommended as an expression strategy in the pET system manual (106). Expression of constructs in the pMalP2X vector (Novagen) was performed according to the manufacturer's protocol. Samples were collected and analyzed as above by 10% SDS-PAGE and developed by Coomassie staining.

## 3.3 Results

### 3.3.1 Limited proteolysis of RecD2 with subtilisin Carlsberg

A common method of structural characterization of a protein is limited proteolysis (108,109). Proteases used for this purpose ideally cleave a protein in only a small number of places, yielding several fragments that are used to isolate or even identify functions of the overall protein.

Limited proteolysis of RecD2 was carried out with the protease subtilisin Carlsberg (110). Initial experiments were conducted to determine the proper amount of subtilisin necessary to cleave a given amount of RecD2. A series of reactions was set up with a range of concentrations of subtilisin, added to a set amount (~ 200 pmol) of RecD2. The reactions were allowed to proceed at 37 °C for 30 minutes. The results showed formation of a range of products smaller than the 78 kDa of intact RecD2 (Fig. 3.2). Formation of a dominant stable product was observed migrating at 45 kDa.

The proper amount of time for proteolysis of RecD2 by subtilisin was determined next. The results show formation of a single product, at 45 kDa (Fig. 3.3). This product is refractory to further proteolysis by subtilisin, even after 60 minutes.
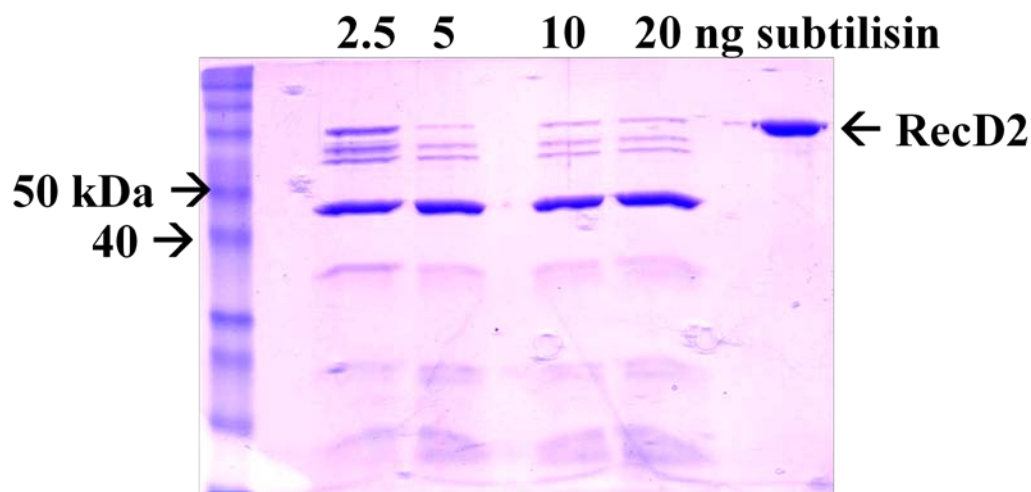
**Figure 3.2: Limited proteolysis of RecD2 with subtilisin Carlsberg.** In each lane, RecD2 (~400 pmol) was subjected to proteolysis by the indicated amount of subtilisin at 37 °C. Reactions were quenched at 30 min by addition of PMSF (5 mM final) and analyzed via 10% SDS-PAGE.

Proteolysis of RecD2 was repeated for the purpose of sequencing the 45 kDa proteolytic product. Reactions were run out on 10% SDS-PAGE and then transferred to a polyvinylidene fluoride (PVDF) membrane by the western blot protocol. The membrane was submitted to the Molecular Structure Facility at UC Davis for peptide sequencing via Edman degradation. The returned sequence (**H₂N- A T G E G R I Y L**) corresponded to cleavage of RecD2 between amino acids 289 and 290 in the complete sequence (shown in figures 3.4 and 3.5).
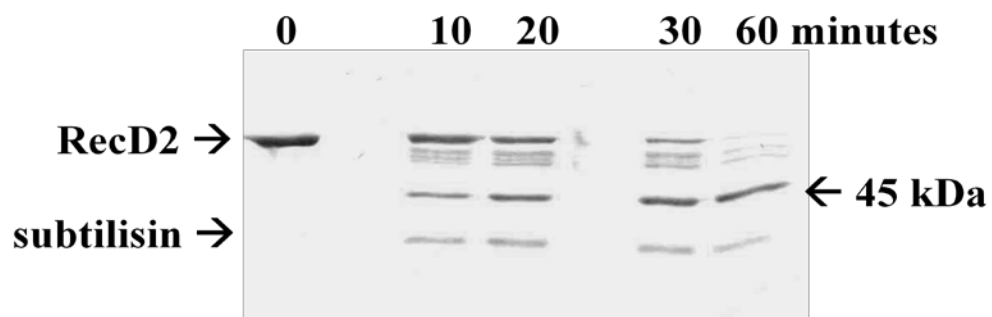
**Figure 3.3: Time course of RecD2 proteolysis by subtilisin.** RecD2 (470 pmol) was reacted with 8 ng subtilisin at 37 °C. Samples were pulled at the indicated times and treated as above.

```
          10         20         30         40         50         60
MSAALPAEPF RVSGGVNKVR FRSDTGFTVM SATLRNEQGE DPDATVIGVM PPLDVGDTFS

          70         80         90        100        110        120
AEVLMEEHRE YGYQYRVVNM VLEAMPADLS EEGVAAYFEA RVGGVGKVLA GRIAKTFGAA

         130        140        150        160        170        180
AFDLLEDDPQ KFLQVPGITE STLHKMVSSW SQQGLERRLL AGLQGLGLTI NQAQRAVKHF

         190      ▼ Wigley      210        220        230        240
GADALDRLEK DLFTLTEVEG IGFLTADKLW QARGGALDDP RRLTAAAVYA LQLAGTQAGH

         250        260        270        280      ▼ subtilisin
SFLPRSRAEK GVVHYTRVTP GQARLAVETA VELGRLSEDD SPLFAAEAAA TGEGRIYLPH

         310        320        330        340        350        360
VLRAEKKLAS LIRTLLATPP ADGAGNDDWA VPKKARKGLS EEQASVLDQL AGHRLVVLTG

Motif I              380        Ia         400        410    Pin    420
GPGTGKSTTT KAVADLAESL GLEVGLCAPT GKAARRLGEV TGRTASTVHR LLGYGPQGFR

         430    II   440        450        460    III   470        480
HNHLEPAPYD LLIVDEVSMM GDALMLSLLA AVPPGARVLL VGDTDQLPPV DAGLPLLALA

         490    IV   500        510        520        530        540
QAAPTIKLTQ VYRQAAKNPI IQAAHGLLHG EAPAWGDKRL NLTEIEPDGG ARRVALMVRE

         550        560        570        SH3        590        600
LGGPGAVQVL TPMRKGPLGM DHLNYHLQAL FNPGEGGVRI AEGEARPGDT VVQTKNDYNN

         610        620        630        SH3   640        V          660
EIFNGTLGMV LKAEGARLTV DFDGNVVELT GAELFNLQLG YALTVHRAQG SEWGTVLGVL

         670        VI         690        700        710        720
HEAHMPMLSR NLVYTALTRA RDRFFSAGSA SAWQIAAARQ REARNTALLE RIRAHLEHHH

HHH
```

**Figure 3.4: Annotated protein sequence of RecD2. ▼ Wigley** denotes the start of the RecD2 structure 3E1S reported by Saikrishnan, et al (61). **▼ subtilisin** shows the cut made by subtilisin on RecD2, with the first 10 residues shown in pink. Highlighted in green are the conserved helicase motifs (75). Highlighted in red is the pin region identified by (62). Highlighted in grey is the SH3 domain (61). Shown in yellow is the N-terminal region prior to the subtilisin Carlsberg cleavage site. Shown in purple is a C-terminal His$_6$ tag used for purification (15,61).
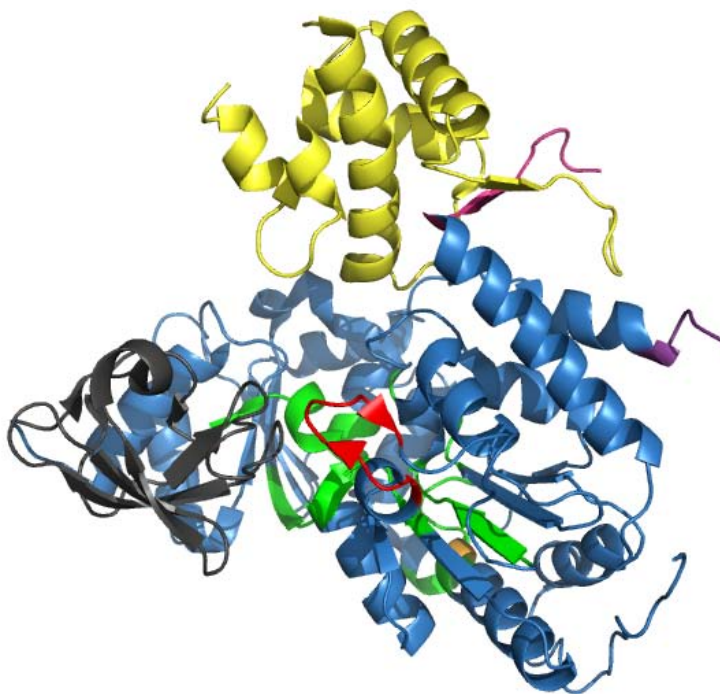
**Figure 3.5: X-Ray crystal structure of ΔNRecD2.** The C-terminal region of RecD2, starting at residue 193, was crystallized by Saikrishnan, et al (61). The primary structure color is blue; Yellow indicates the region from residue 193 to 290. Other colors shown are as detailed in Figure 3.

## 3.3.2 Heterologous expression of RecD2 proteolytic fragments in *E. coli*

Gene constructs for expression of the N- and C- terminal regions identified by subtilisin cleavage were generated. Protein constructs expressing the N- terminal region were named **DrDNterm**, with an expression tag identifier attached to the name. Prrotein constructs expressing the C- terminal region were named **RecD290**, with an expression tag identifier attached to the name. Table 3.2 lists the constructs built for the expression of the regions of RecD2.

### 3.3.3 Detection of binding epitope for the RecD2 antibody

DrDNterm was expressed and purified as detailed in section 3.2. Our N-terminal constructs of RecD2 contain none of the previously identified helicase motifs present in RecD2 (see section 3.1). Use of this protein was limited to use in detection of the binding epitope for the RecD2 antibody. The RecD2 antibody was generated by Matt Servinsky of this lab (85). The antibody (termed Dr-RecD mAb) is a mouse derived monoclonal antibody that targets RecD2.

*E. coli* cells expressing the RecD2 protein constructs DrDNterm-15, DrDNterm-21, and DrRecD290-21 were tested. Samples were treated as detailed in section 3.2 and run out on 10% SDS-PAGE. Gel transfer was performed to the western blot protocol and the resulting blot was developed with the antibody Dr-RecD mAb (primary) and goat anti-mouse alkaline phosphatase linked antibody (secondary). Results from this experiment show that the antibody Dr-RecD mAb only binds to the N-terminal region of RecD2 (Fig. 3.6).
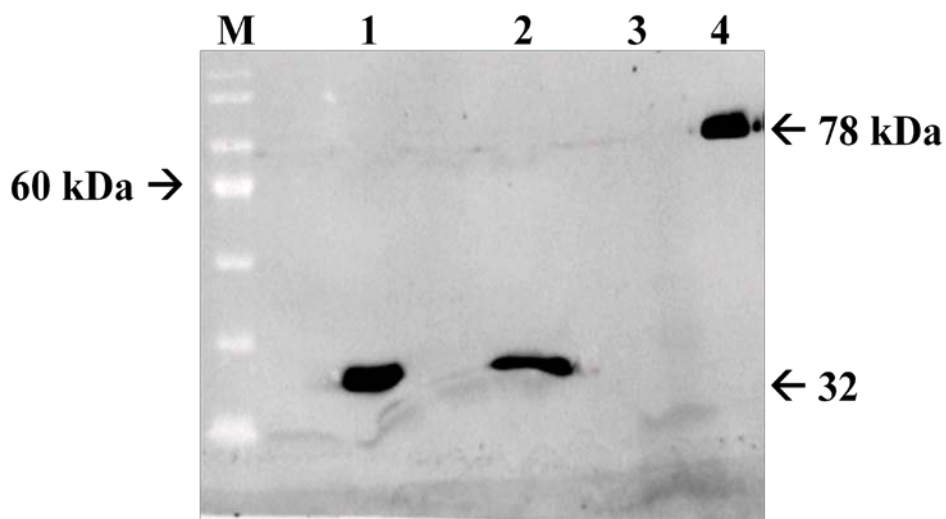
**Figure 3.6: Determination of Dr-RecD mAb binding epitope on RecD2.** Whole cell lysates expressing DrDNterm21 (Lane 1), DrDNterm15 (Lane 2), or DrRecD290-21 (Lane 3), were treated as detailed in **Materials and Methods**. Purified RecD2 (5 ng) was loaded in lane 4 as a positive control.

## 3.3.4 Expression of DrRecD290 in *E. coli*

Expression of protein constructs expressing the C-terminal region of RecD2 was performed. Shown in Fig. 3.7, expression of DrRecD290-21 in BL21-DE3 yielded no visible product, even under a range of conditions (detailed in section 3.2). One explanation for this observation was that expression of DrRecD290 was toxic to the host; this is a known complication with heterologous expression systems (for an example, see (111)). Previous work by Steve Polansky of this lab also suggested that RecD2 was toxic to the *E. coli* host (103), possibly due to its helicase activity. A range of techniques and proprietary products was tried to address this issue.
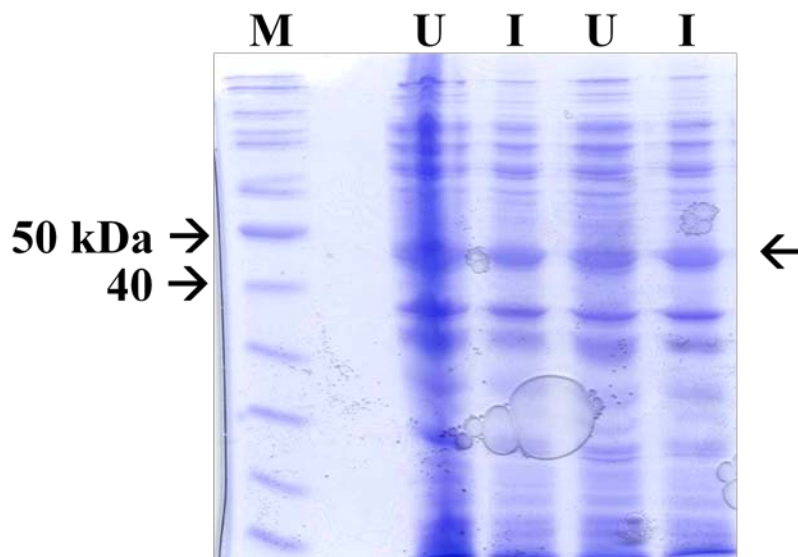
**Figure 3.7: Expression of DrRecD290-21 in *E. coli* BL21-DE3.** Results of two different expression trials are shown above. Induction and sample preparation were carried out as detailed in section 3.2. U: Uninduced whole cell lysates. I: Induced with 1 mM IPTG for 2 hours at 30 °C. The arrow on the right side of the picture shows the migration region for the expected protein product, at 46 kDa.

Our first attempt to address this issue was to include RecD290K366Q constructs in our testing. RecD290K366Q constructs are based on RecDK366Q, made by Steve Polansky of this lab (103). This mutant has lysine replaced by glutamine at residue 366. This is located in the Walker A motif of RecD2 and is based on the consensus that mutation at this residue will cause RecD2 to become catalytically inactive. Expression of DrRecD290K366Q- 21 was attempted in *E. coli* strains C41 and C43 (OverExpress, Inc. - C41 and C43 are *E. coli* BL21-DE3 strains resistant to toxic proteins), without production of an obvious protein product on the SDS gel (data not shown).

Our attempt to solve this dilemma involved use of the construct *pDrRecD290.pMalP2X*, which carries a periplasmic localization sequence for export

of the protein product out of the cytoplasm. Protein products with this tag are transported to the periplasmic space between the inner and outer membranes of *E. coli*. This acts to lower the potential for toxic interactions with host proteins. Again, no product was observed, when expression was attempted in BL21-DE3 (data not shown).

An attempt was made to express DrRecD290 with an N-terminal SUMO tag (112). The hypothesis was that co-expression of this fusion protein could reduce the toxicity of DrRecD290. Western blot analysis (Fig. 3.8) with an anti-His antibody showed production of a smaller protein product (30 kDa, Fig. 3.8) in the lanes, detectable even when the cells were uninduced.
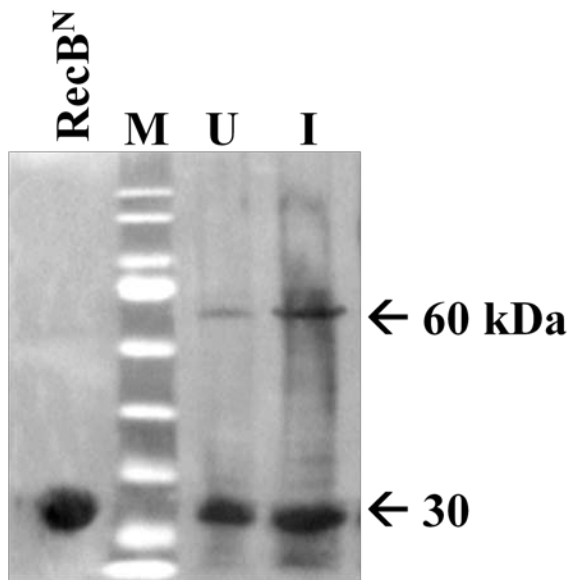


**Figure 3.8: Western blot of expression of DrRecD290.pSmt3 in BL21-DE3.**
Analysis was carried out as detailed in section 3.2, with the Anti- His antibody (Novagen). RecB[N]- Nuclease domain of *E. coli* RecB (53), used as a positive control. M- Fermentas pre-stained protein ladder. U- Uninduced control. I- Induced as detailed in section 3.2.

Expression with the gene construct *pDrRecD290.pGEX4T1* in BL21-DE3 resulted in the production of a large amount of a protein smaller than intended (Fig. 3.9, indicated by an arrow). Observation of the same effect with two different expression systems (not shown) led to the hypothesis that this effect was due to codon bias. Smaller peptides than the full length protein can be made in cases of codon bias. This can occur when the host strain is forming many different truncated products, due to premature termination from ribosomal stalling (113).
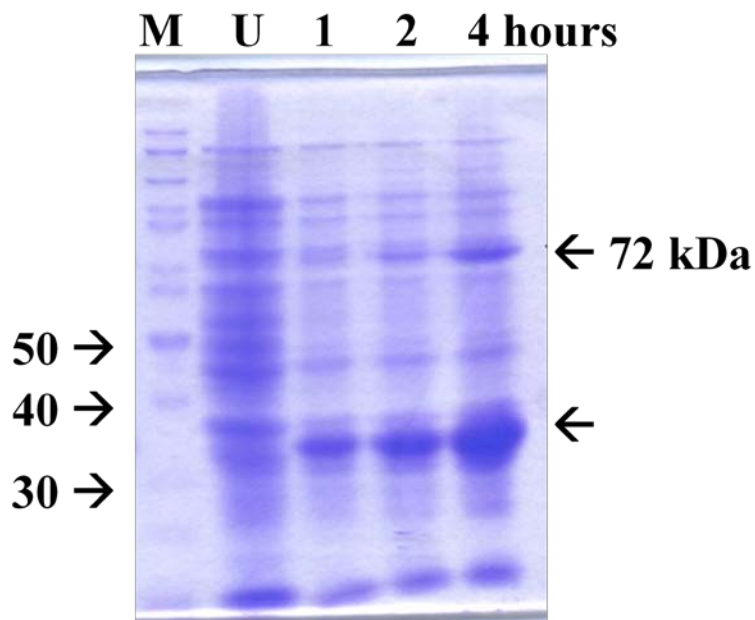


**Figure 3.9: Expression of DrRecD290.pGEX4T1 in BL21-DE3.** Expression was carried out as detailed in **Materials and Methods**. Samples pulled at times indicated. U- Uninduced.

Codon bias occurs as a byproduct of the use of degenerate tRNAs for addition of amino acids to the growing protein chain during translation (113). The primary strategy to deal with this problem relies on co-expression of rare tRNAs via co-

transformation with plasmids such as *pRARE2*. Expression of RecD290 was tried

with the *E. coli* strain Rosetta 2-DE3 (Novagen). The Rosetta 2 strain carries the

*pRARE2* plasmid, which co-expresses the genes for the seven tRNAs that are rarest in

*E. coli*.
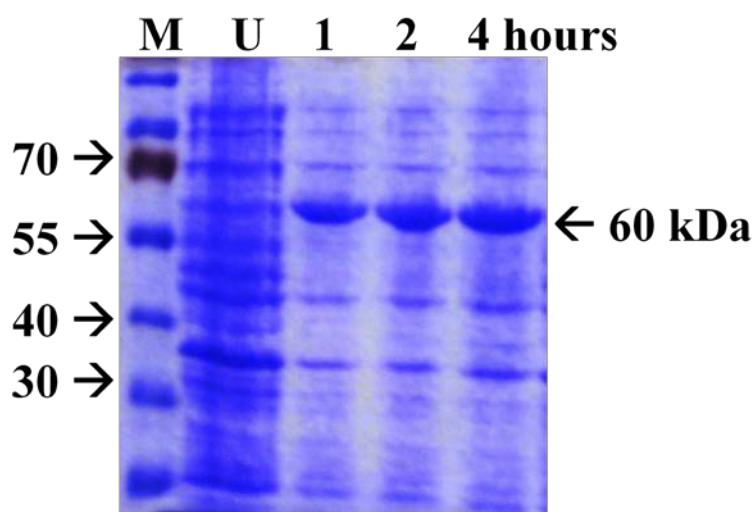


**Figure 3.10: Expression of DrRecD290.pSmt3 in Rosetta2-DE3.** Expression was
carried out as detailed in **Materials and Methods**. Samples were pulled at times
indicated. U- Uninduced.

Use of *E. coli* Rosetta2-DE3 for expression of DrRecD290 constructs allowed

production of large amounts of the desired protein products, regardless of construct

(Fig. 3.10). Cultures were next tested for solubility of the protein product, and all

DrRecD290 constructs were determined to be insoluble under normal (IPTG)

induction conditions. A range of alternate expression conditions (detailed in section

3.2) was tried with a range of constructs and *E. coli* strains. No production of any

soluble protein was observed under any expression conditions tried (example shown

in Fig. 3.11).

114
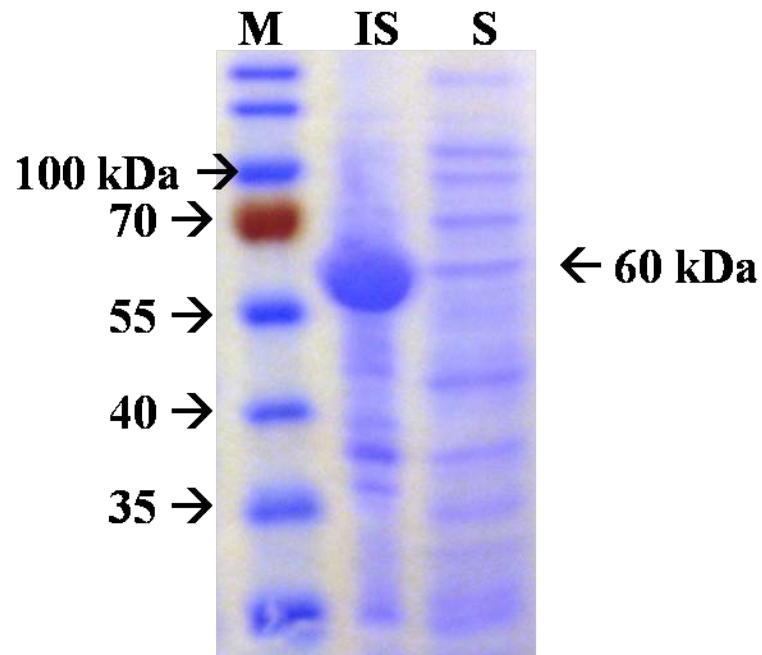
**Figure 3.11: Expression of DrRecD290Stop.pSmt3 in Rosetta2-DE3.** Cultures were induced with 0.2 mM IPTG for 2 hours at 30 °C. Samples were sonicated as detailed in section 3.2. **M:** Fermentas prestained PAGERuler; **IS**: Insoluble; **S**: Soluble.

## 3.4 Discussion

Our characterization of the N- and C- terminal regions of RecD2 required first the ability to separate the protein into two pieces. We set about to identify a region of the enzyme where the structure was sufficiently labile to allow proteolysis. With the products of the proteolysis identified, we hoped to characterize these domains individually, to better understand the role of each in the activity of the overall enzyme.

Our limited proteolysis with subtilisin Carlsberg allowed us to cleave RecD2 at a location immediately prior to the start of the first conserved helicase motif, in between amino acids 289 and 290 (Fig. 3.4). We aimed to produce expression constructs that reflected this cleavage site, to generate sufficient quantities for *in vitro* analysis. Initial attempts to produce the C-terminal domain via heterologous expression met with difficulty, due to codon bias. In response to the identification of this issue, we made use of *E. coli* Rosetta2-DE3, which co-expresses some of the tRNA's rarely utilized by *E. coli*. This allowed us to produce large quantities of the C-terminal region of RecD2, expressed as a fusion construct.

Attempts at purification of the C-terminal region of RecD2 were stymied by the insolubility of the initial C- terminal construct. Expression of the C-terminal region of RecD2 was carried out with a range of fusion partners (table 3.3), in an effort to produce soluble protein. In addition, we tried expression under a range of conditions designed to increase yields of soluble protein, to no avail.

The crystal structure of a C-terminal construct of RecD2 was reported in 2008 (61). This structure relied on truncation of the first 150 residues of RecD2 (out

of 715). The structure showed RecD2 from residue 191 to the end of the sequence.

The authors reported the overall similarity to RecD from *E. coli*, and used it as a basis

for further refinement of the *E. coli* RecBCD structure. This structure (shown in

figure 3.5) was produced in the absence of any DNA or nucleotide cofactor. We

examined this structure, and identified the site of our limited proteolysis. An overlay

of the region identified by us on the reported crystal structure confirmed our

hypothesis that the core domains required for helicase activity were contained in the

region identified by our research.
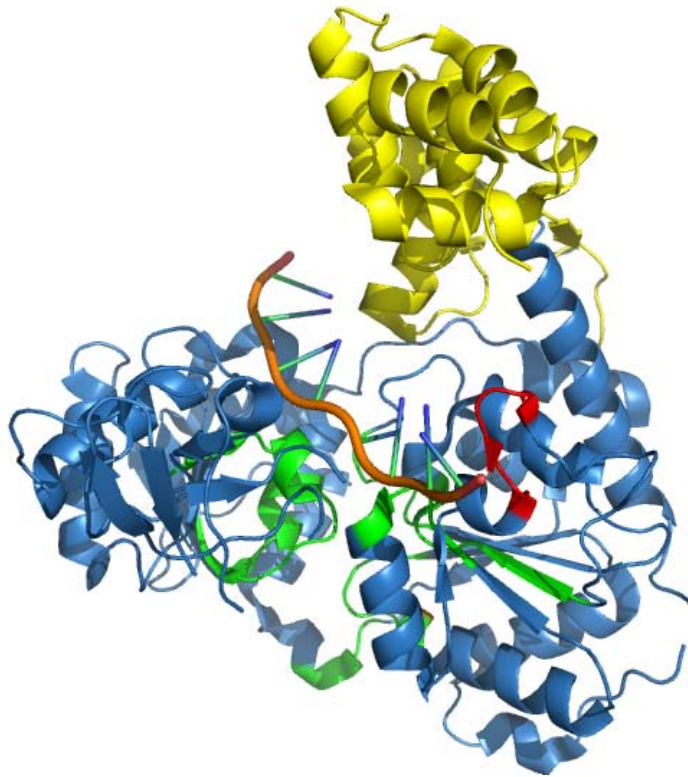


**Figure 3.12: X-Ray crystal structure of the ΔNRecD2 bound to dT₁₅.** The C-terminal region of RecD2, starting at residue 193, was crystallized by Saikrishnan, et al (62). The primary structure color is blue, and the DNA is orange; the region from residues 193 to 290 is shown in yellow. Other colors shown are as detailed in Figure 3.4.

The authors of the first crystal structure of RecD2 subsequently reported crystallization bound to $dT_{15}$ (62). In this structure, 8 of the 15 thymidine residues are visible. This agrees with the previously identified binding requirement of 10nt (15). By binding the nucleotides ADP or ADPNP (a non-hydrolysable analogue of ATP), the authors found conformational changes in RecD2 that were subsequently used to propose a mechanism of translocation along DNA (detailed in figure 1.5 and accompanying text).

Heterologous expression of the N-terminal region identified by our proteolysis was carried out, with low quantities of protein produced. As there has been no suggestion of a function of this region in the overall activity of RecD2, we limited the use of this protein to identification of the binding epitope for the previously generated RecD2 antibody (85). As we had expression of both ends of the protein (even if one region was insoluble), we were able to conduct western blotting with the antibody Dr-RecD mAb to narrow down where the antibody was binding. Our research was able to confirm that Dr-RecD mAb binds in the N-terminal portion of RecD2.

Further research into the functions of the N- and C- terminal regions of RecD2 will allow a more rigorous determination of the *in vitro* behavior of the C- terminal region of RecD2. The C- terminal region crystallized by Saikrishnan, et al (61,62) can be utilized in helicase and ATPase assays, with the results compared to the full length protein. This should allow researchers to deductively suggest a role for the N-terminal region in the overall activity of RecD2. In the future, both regions of RecD2 may also be used in affinity co-purification (pull down assays) to identify any binding partners that may modulate the activity of RecD2 *in vivo*.

## Chapter 4: Conclusion

Our study of RecD2 from *D. radiodurans* has allowed us to understand the biochemistry of this enzyme in greater kinetic detail than previous researchers have reported. Through the use of a single turnover reaction system, we have established the behavior of RecD2 with a variety of substrates. With the information we have gathered, we have proposed a mechanism for the unwinding of DNA by RecD2, and proposed rates for each of the steps involved in the process.

Processivity and rates of unwinding are highly variable across the SF1 helicases. Our results showed that RecD2 was capable of unwinding a 12 bp segment of dsDNA without dissociating, but not a 20 bp segment. This is not unusual in the context of other SF1 helicases. For example, PcrA monomers are unable to unwind an 18 bp dsDNA substrate (95). BLM helicase monomers have even lower processivity and a reported step size of 1.3 base pairs (76).

When associated with binding partners, the processivity of SF1 helicases can be significantly increased. An example is NS3 from Hepatitis C virus, which partners with NS5B polymerase to increase processivity (114). The RecBCD complex is capable of unwinding segments of dsDNA over 30 kilobases without dissociating (99). Future work may identify binding partners that increase the processivity of RecD2 on DNA.

The role of the N-terminal domain of RecD2 is still unsettled, as no separate activity for this region of the enzyme has been determined. A repeat of our kinetic analysis on the truncated enzyme reported by Saikrishnan, et al (61) could deductively shed light on the role of the N-terminal domain in the overall activity of

RecD2. Further biochemical characterization of both forms of RecD2 with new substrates will be necessary to discover the role of this enzyme in DNA management in *D. radiodurans*.

Continued exposure to IR causes the fragmenting of DNA based on direct cleavage of the sugar phosphate backbone and reactions primarily with OH• radical (5,6). Presumably, the size of the DNA products grows smaller as the exposure to IR increases. Research into the role of RecD2 in *D. radiodurans* has found that Δ*recD* mutants are not sensitive to IR until after exposure of cultures to over 4 kGy (59). Previous work in our lab has found RecD2 has a poor ability to unwind dsDNA substrates of 76 bp (15).

Based on this information, and our observation of the poor processivity of RecD2 when unwinding even 20 bp of dsDNA, we suggest RecD2 may have a role in the biology of DNA repair in *D. radiodurans* that may not become important until a certain amount of damage has been sustained by the cell. At this time, the pool of DNA present in the cell may contain a large number of fragments with only very small stretches of dsDNA. In order to restore the genome of *D. radiodurans* according to the ESDSA model (22), it may be necessary to have an enzyme capable of efficiently unwinding very short pieces of dsDNA. These unwound pieces would then either be processed into larger fragments for reconstitution of the genome, or be degraded to supply a ready pool of nucleotides for repair processes.

There also exists the possibility that a binding partner may be necessary for activity of RecD2 *in vivo*. Pull down assays performed by Zheng Cao (101) identified three subunits of RNA polymerase interacting with RecD2. Future work may support

this finding, or even find other proteins modulating the activity of RecD2 in the cell. Precedence exists for binding partners increasing the processivity and unwinding rate of SF1 helicases (114).

The behavior of the RecD helicase outside the context of the RecBCD complex is poorly characterized. Superfamily I helicases perform a variety of functions within the cell. The processing of double strand breaks for HR in *E. coli* is the responsibility of the RecBCD complex (*vide supra*). Unwinding DNA ahead of a replication fork is the task of DnaB (71-73,89). A range of disorders with names like Bloom's syndrome, Werner's syndrome, and Schimke immuno-osseous dysplasia (115) can come about from mutations in the RecQ helicases in humans (116,117). These disorders are characterized by premature aging and a high incidence of cancer.

Helicases are an important component of DNA management in the cell. The ability to unwind double stranded regions is requisite to the efficient copying, transcription, and repair of DNA. Helicases have been targeted as a strategy for treatment of cancer (118,119) and in the treatment of bacterial infections (120). A host of human disorders have been found due to mutations in genes coding for helicases (121).

The study of helicases in model organisms such as *D. radiodurans* offers the opportunity to see the extreme end of the spectrum of DNA repair. At the same time, we can use this knowledge to develop new uses for this organism, based on the established ability of *D. radiodurans* to withstand extreme conditions. Among the uses considered for *D. radiodurans* is use in the bioremediation of radioactively polluted sites, present in every country that utilizes nuclear power (122). Through a

more detailed knowledge of the mechanisms of repair in organisms such as *D. radiodurans* we can learn more about the helicases that are an integral part of the management of our own DNA.

# Appendix

## A.1 Structural characterization of the nuclease domain of RecB from *E. coli*

Previous research conducted in the Julin lab focused on the various activities of subunits of the heterotrimeric RecBCD enzyme complex from *E. coli*. Experiments first recognized ATP-independent nuclease activity of RecBCD in mutants of RecBCD in 1997 (50). Limited proteolysis of RecB followed soon after, leading to the discovery that RecB carried its helicase and nuclease activities in different domains of the enzyme (51). Limited proteolysis of RecB with the protease subtilisin Carlsberg allowed separation of the helicase and nuclease activities into a 100 kDa N-terminal domain and a 30 kDa C-terminal domain. By removal of the C-terminal domain from the overall complex, they were able to completely remove all nuclease activity, while leaving ATPase and helicase activities of RecBCD intact (52).

These results led to the hypothesis that the 30 kDa C-terminal domain of RecB was responsible for the nuclease activity of RecBCD (51). A construct expressing the truncated form of the C-terminal nuclease domain (RecB$^{N}$) showed activity when incubated with substrate M13 ssDNA. Further research found activity of the nuclease domain of RecB to be metal dependent and ATP independent in its cleavage of ssDNA (52,53).

Research into the nature of metal binding in the active site of the nuclease domain of RecB involved testing of a range of divalent metal cations ($Ca^{2+}$, $Co^{2+}$, $Cu^{2+}$, $Mn^{2+}$, $Mg^{2+}$, $Ni^{2+}$, and $Zn^{2+}$, tested at 5 mM ) for their respective effect on

activity of the truncated form of the nuclease domain (RecB$^{\text{N}}$). In addition to an effect found from identity of the metal center, activity of the enzyme was also found to be dependent on concentration of the metal, with high concentrations of Mg$^{2+}$ (100 mM) inhibiting activity of the enzyme (123).

Comparison of domains by amino acid sequence analysis identified a group of residues conserved among RecB and several other proteins (124). This led to construction of single point mutants with changes at residues D1067, D1080, Y1081, K1082, and Y1114 of *recB*. A conserved aspartate at residue D1080 was mutated to alanine, and all activity in the nuclease domain was disabled (52,53). Mutation at residues D1067 and K1082 reduced the nuclease activity, while mutations at residues Y1081 and Y1114 exhibited no effect on nuclease activity of RecBCD (125).

The three residues in RecB, D1067, D1080, and K1082, are similar to a motif commonly found in type II restriction endonucleases and the core domain of λ-exonuclease (126,127). Restriction endonucleases such as *Eco*RI, *Eco*RV, and *Fok*I harbor a common active site motif of **PDx$_{\text{6-30}}$(D/E)xK** (where **x** is any amino acid) necessary for catalysis (for reviews, see (128,129)).

The structure of the RecB nuclease domain was determined as part of the RecBCD crystal structure (41). The structure confirmed a structural relationship between RecB$^{\text{N}}$ and the phage λ exonuclease, and several restriction endonucleases. The RecB residues D1067, D1080, and K1082 are structurally homologous to the **PDx$_{\text{6-30}}$(D/E)xK** grouping. A calcium ion was seen bound to D1067 and D1080, as well as to H956.

To assess the effect of the conserved Asp residues (D1067 and D1080) on the metal binding capacity of the RecB nuclease active site, iron-mediated cleavage of the RecB nuclease domain D1067A and D1080 mutants was performed. Results were compared to wild type. This process uses Fenton chemistry, which involves cycling of Fe ions from the +2 to the +3 oxidation state and back again with the assistance of a reducing agent (such as ascorbate). This causes formation of hydroxyl radicals from a variety of substrates, among them diatomic oxygen or hydrogen peroxide.

Hydroxyl radicals (•OH) then cleave the protein by abstraction of C α-hydrogens from the backbone at specific sites, determined mostly by proximity but also reactivity of the C-α-hydrogen (for applications, see (130,131)). These lower molecular weight products can then be separated by Tricine-SDS-PAGE (132) and imaged by staining with Coomassie Blue R-250, or transferred to PVDF for N-terminal sequencing.

Iron-mediated degradation of RecB$^N$ was conducted by Shamali Roychoudhury of this lab (133). Wild type RecB$^N$ gave a degradation pattern consisting of three bands of lower molecular weight than the intact protein. Products were sequenced by Dr. Brian Martin at the NIH. The band found directly underneath the intact protein (at ~27kDa) returned a sequence of **S P G T F L H S L**. This sequence corresponds to residues # 950–958 of RecB protein, which indicates cleavage in that vicinity. This cleavage site is shown as the lower red mark on the structure shown in Figure 1. The reason for this cleavage may be a result of metal binding at H956.

Sequences obtained for the lower two bands were **G S S H H H** (~17 kDa),

and **I D L V F R H E G R** (~13 kDa). The sequence of the 17 kDa band agrees with

the amino-terminal sequence of His-tagged RecB$^N$ lacking the initial methionine

residue. This is the same sequence identified for the intact protein. The sequence of

the 13 kDa band indicates cleavage at the vicinity of residue F1065, indicating

binding nearby, most probably at D1067. This cleavage site is shown as the upper red

mark on the structure shown in Figure A.1.
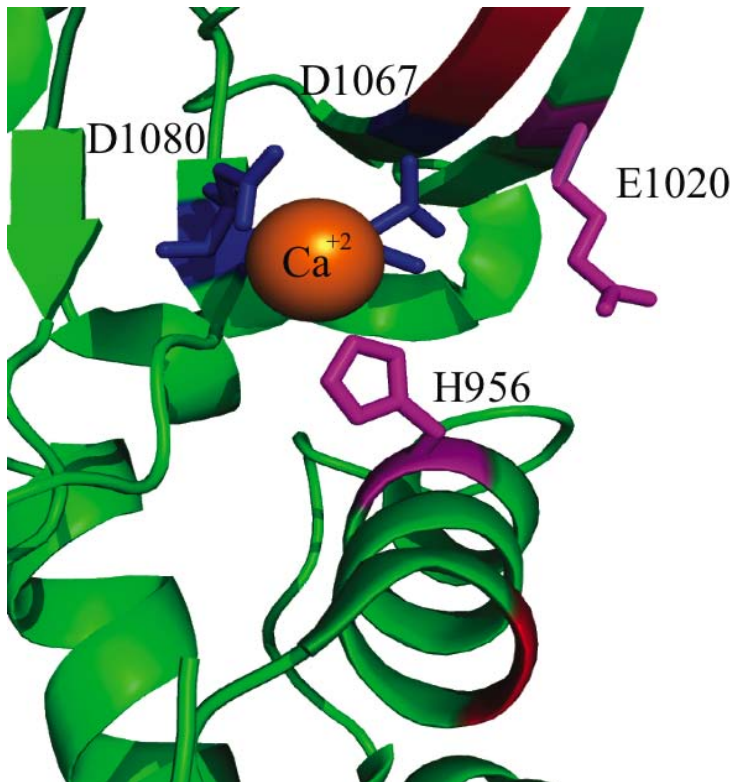


**Figure A.1: Ca$^{2+}$ bound active site of nuclease domain of RecB$^N$, showing important residues H956, E1020, D1067, and D1080.** Cleavage sites are shown in red. Adapted from (41).

In addition to wild type RecB$^{N}$, mutants D1080A and D1067A were subjected to Fe$^{2+}$ cleavage with differing results: D1067A delivered no cleavage products, while D1080A delivered the same pattern as the wild type protein. This would be consistent with D1067A abolishing metal binding at the active site, and D1080A still allowing metal binding (133). A third conserved acidic residue (E1020) was also identified in the amino acid sequence analysis of RecB and other related proteins (124). A third residue (in addition to that in the **PDx$_{6-30}$(D/E)xK** motif) has also been implicated in metal ion binding and catalytic activity of several restriction endonucleases. E1020 is near the bound Ca2+ ion in RecB, but not directly bound to it (Fig. A.1).

To continue analysis of the effect of each residue on activity of the nuclease domain of RecB, new mutants were constructed based on suggestions from the crystal structure of the Ca$^{2+}$-bound form of RecBCD (41). These mutants, termed H956A and E1020A, were based on proximity of residues H956 and E1020 to the bound calcium ion in the crystal structure. Mutants were checked for ssDNA nuclease activity and effect on Fe$^{2+}$-mediated cleavage under the same conditions as the mutants investigated by Shamali Roychoudhury (133).

## A.2 Materials and Methods

### A.2.1 Over-expression and purification of RecB$^N$ wild type and mutants

To an exponentially growing (OD$_{600}$ 0.5, at 37°C) culture of *E. coli* BL21-DE3 transformed with plasmid *pET15b-30* (or mutant form), 1 mM (final concentration) IPTG (Isopropylthio-β-galactoside) was added and allowed to grow an additional 2 hours. Cells were harvested by centrifugation at 5000 x g in a Beckman model J2-21 centrifuge and the cell pellet placed at -80 °C overnight.

The following day, the cell pellet was re-suspended in Ni$^{2+}$·column buffer (20 mM potassium phosphate, pH 7.5, 0.5 M NaCl, 1 mM DTT) +20 mM imidazole and sonicated. Sonication was performed on a Branson Sonifier model 450 with microtip and the settings: duty cycle 50, intensity 5, duration 10 minutes on ice. PMSF (5 mM final) was added to the buffer immediately prior to sonication to inhibit serine protease activity. After sonication, the lysate was centrifuged at 10000 x g for 2 hours at 4 °C and the supernatant filtered through a 0.2 µm filter.

The filtered lysate was loaded onto a 5 ml Ni$^{2+}$-NTA column (Hi-Trap Chelating HP, GE Life Sciences) and washed with 5 column volumes of wash buffer (60 mM potassium phosphate, pH 7.5, 0.5 M NaCl, 20 mM imidazole, and 1 mM DTT). Protein was eluted from the column by a 50 ml gradient of 60-500 mM imidazole in Ni$^{2+}$ column buffer.

Samples (24 µl) of each fraction were taken, mixed with 6 µl 6X SDS loading buffer (350 mM Tris·HCl pH 6.8, 10% SDS, 30% glycerol, 6 mM DTT, 0.01% Bromphenol Blue), and placed at 95 °C for 1 minute. These samples were then loaded

onto 10% Tricine-SDS-PAGE gels (29:1 acrylamide: bis-acrylamide) and run at 150 V constant voltage for 2 1/2 hours.

Gels were then stained with coomassie brilliant blue gel stain for 30 minutes and destained with fast destain until developed. Fractions containing the highest level of eluted protein were pooled and placed in a dialysis bag in Mono·Q start buffer (20 mM Tris·HCl, pH 8.0) overnight at 4 °C.

The next day, the dialyzed eluant was filtered through a 0.2 µm filter. The filtrate was loaded onto a 1 ml Mono·Q HR 5/5 column (GE Life Sciences) and washed with 5 column volumes of start buffer containing 50 mM NaCl. Elution followed, with a 20 column volume gradient running from 50 mM to 1 M NaCl in 20 mM Tris·HCl, pH 8.0. Fractions were analyzed by 10% Tricine-SDS-PAGE. Fractions containing the highest amount of protein were combined into a dialysis bag. This dialysis bag was placed into 2 L of enzyme storage buffer (20 mM potassium phosphate, pH 7.5, 250 mM NaCl, 5 mM DTT, 1 mM $Na_2$·EDTA, and 50 % glycerol) and dialyzed overnight at 4 °C. The following day, concentration of the purified RecB$^N$ was determined by absorbance at 280 nm with a calculated extinction coefficient of 39,400 $M^{-1}cm^{-1}$ (ProtParam, ExPasy.org). Aliquots (50 µl) were numbered and placed in a -80 °C freezer for later use.


A.2.2 Nuclease Assay (53)

In a microcentrifuge tube the following components were mixed (final concentrations): 1.8 µM enzyme, 50 mM Tris-HCl, pH 8.8, 20 mM $MgCl_2$, 25 nM (circles) M13 ssDNA, and 10% PEG 8000. Reactions were mixed by briefly

vortexing due to the viscosity of PEG. An aliquot was pulled to serve as a **0** minute time point and quenched with 1/6 volume nuclease quench (53). A separate tube was set up containing all components except enzyme- this was placed into the bath alongside the reaction tube for the duration of the assay. The reaction mixture and control were placed in a 37 °C bath. Samples were pulled every 30 minutes until 90 minutes. As each time point was quenched, they were placed in a -80 °C freezer until all time points were taken.

When all time points had been collected, each sample was loaded on a 0.8% agarose gel and run at 100 V (constant) until tracking dye from the quench reagent just ran out of the gel. Next, each gel was placed into a water solution containing ethidium bromide and allowed to stain for 1 hour. Afterwards, the gel was transferred to distilled water and rinsed twice. The gel was de-stained by soaking in distilled water 20-30 minutes, with checking on a UV light box every 10 minutes. When de-stained satisfactorily, the gel was imaged with a digital camera equipped with a UV filter.

## A.2.3 $Fe^{2+}$ mediated cleavage (133)

In a micro-centrifuge tube the following components were mixed: 50 μM enzyme (freshly dialyzed in mini dialysis cups into 40 mM Tris-HCl, pH 7.4) and 100 μM $FeSO_4$ (freshly prepared within the hour). The mixes were allowed to sit on ice for 15 minutes, and then 25 mM (final concentration) sodium ascorbate was added. Each tube was then transferred to a bench top (~20 °C) and timing commenced. Aliquots were pulled at 30, 60, and 90 minutes and quenched with 1 mM EDTA plus

1/6 volume 6x SDS loading buffer. These samples were heated at 95 °C for 1 minute, and placed in a -80 °C freezer until the time course was over. As a control, a tube containing only enzyme was carried through the same steps.  All samples were loaded on a 12% Tricine-SDS-PAGE gel and run at 120 V (constant) until the dye front just touched the bottom of the gel. Gels were stained with Coomassie Blue R-250 stain for 30 minutes, followed by de-stain until developed. Gels were imaged using a flat bed scanner.

Alternately, gels were electroblotted onto a PVDF membrane (Immobilon-P, Millipore, Inc.) via the western blot protocol with CAPS transfer buffer (10 mM CAPS, 10% methanol, pH 11.0). The resulting blot was stained with coomassie stain for sequencing blots (40% methanol, 1% acetic acid, 58.9% water, and 0.1% coomassie blue R-250) and destained with 50% methanol in water. Stained blots containing degradation products were sent to Dr. Brian Martin at the NIH for sequencing via Edman degradation.

## A.3 Results

Mutant proteins were first analyzed for nuclease activity compared to the wild type enzyme. Results from nuclease digestion (shown in Figure A.2) show that mutation at residues H956 and E1020 both cause loss of nuclease activity as compared to wild–type protein. Where the wild-type enzyme was able to digest 20 nM (circles) of M13 ssDNA within 30 minutes, neither mutant was able to, even after 90 minutes. This would suggest that residues H956 and E1020 are both involved in activity of the protein.
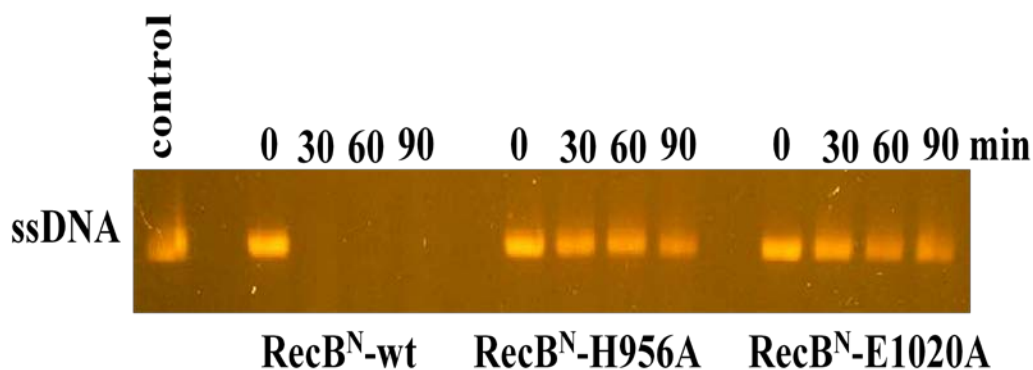


**Figure A.2: Time courses of M13 ssDNA digestion by RecB$^N$, RecB$^N$-H956A, and RecB$^N$-E1020A**. Lane 1, control; lanes 3-6, RecB$^N$, 0, 30, 60,and 90 minutes; lanes 8-11, RecB$^N$-H956A, 0, 30, 60,and 90 minutes; lanes 13-16, RecB$^N$-E1020A, 0, 30, 60,and 90 minutes.

Iron mediated degradation of each mutant was also performed. Results indicate a different cleavage pattern for each of the mutants as compared to the wild type protein (shown in Figure A.3). With mutant H956A, the pattern of degradation indicates favoritism towards the 17 and 13 kDa bands (Fig. A.4).

132

**Figure A.3:  Time course showing iron mediated cleavage of RecB$^N$-wt.** Lane 1, Benchmark protein ladder (Invitrogen); Lane 1, No Fe$^{2+}$ control; Lane 2, 0 minutes; Lane 3, 30 minutes; Lane 4, 60 minutes; Lane 5, 90 minutes.

A shift in cleavage pattern would seem to indicate a shift in the binding of the metal in the active site pocket. Without residue H956 to bind metal, the metal may be shifted upwards, causing more hydroxyl radicals to attack the C α-hydrogen on residue 1066. This would not cause all cleavage at residue 949 to cease, as there would still be a small amount of hydroxyl radical available in that area. This suggests H956 causes tighter binding of site of RecB$^N$, helping keep the metal center set correctly in the active site for proper functioning.

**Figure A.4: Time course showing iron mediated cleavage of RecB$^N$-H956A.** Lane 1, Benchmark protein ladder (Invitrogen); Lane 1, No Fe$^{2+}$ control; Lane 2, 0 minutes; Lane 3, 30 minutes; Lane 4, 60 minutes; Lane 5, 90 minutes.

In the case of E1020A (Fig. A.5), the cleavage pattern and peptide sequencing indicate a shift in the opposite direction, indicating favoritism towards abstraction of the C α-hydrogen at residue 949. At the same time, cleavage at residue 1066 is reduced. Here again, mutation seems to be causing a shift in positioning of the metal in the active site pocket as compared to the wild-type protein. This again, may indicate residue E1020 is involved in metal binding.
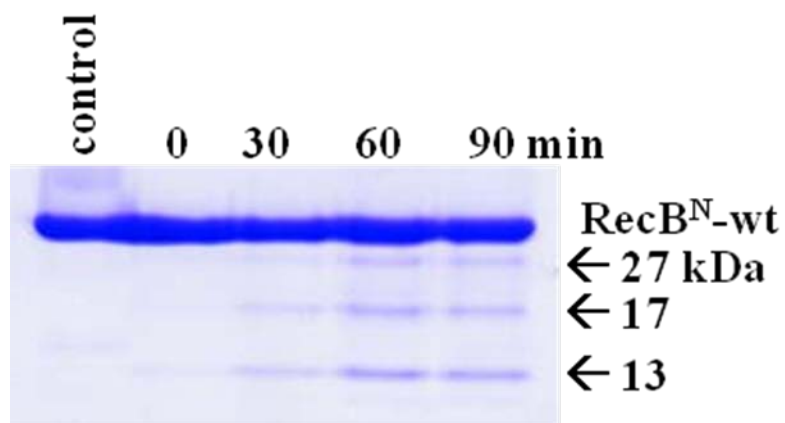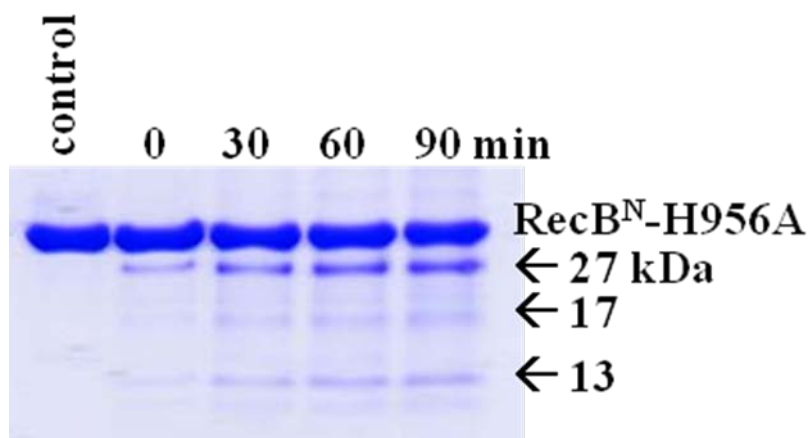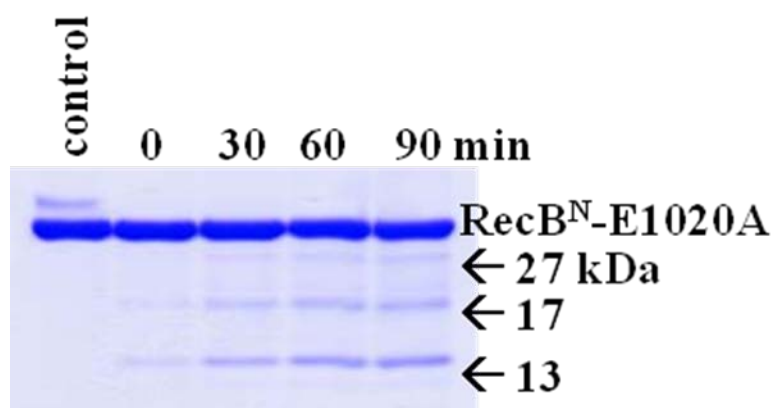
**Figure A.5: Time course showing iron mediated cleavage of RecB$^N$-E1020A.**
Lane 1, Benchmark protein ladder (Invitrogen); Lane 1, No Fe$^{2+}$ control; Lane 2, 0 minutes; Lane 3, 30 minutes; Lane 4, 60 minutes; Lane 5, 90 minutes.

## A.4 Conclusion

Work completed has focused on the nuclease domain of RecB from *E. coli*. Through mutagenesis studies, we have explored the role of various residues in the active site of the nuclease domain of RecB. It is difficult to say conclusively whether the nuclease activity of RecB requires a single metal atom or two at the active site during catalysis. Enzymes bearing the catalytic motif **PDx$_{6\text{-}30}$(D/E)xK** such as *Eco*RV have been characterized with anywhere from one to three metal ions in the active site. This makes it difficult to decide absolutely the role of metal ions in the catalytic mechanism. Enzymes such as *Bgl*II and *Eco*RI are estimated to use a one metal mechanism, while *Pvu*II and *Bgl*I have been characterized as utilizing a two-metal mechanism (reviewed in (128)). Information gathered from mutation at residues in the active site of the nuclease domain of RecB show several amino acids are important to the catalytic activity of the enzyme. From this, we have found metal binding in the active site of the nuclease domain of RecB to be more complex than previously thought. A greater understanding of the nuclease domain of RecB may yet be necessary before conclusions can be drawn about its mechanism of catalytic activity.

Several suggestions can be offered for further work on the nuclease domain of RecB. Among these is examining regulation of the enzyme's activity. RecBCD has been shown to be regulated at several points in its progression along the DNA. During the course of progression of RecBCD along the DNA, the enzyme switches its nuclease activity "off" for one strand of the DNA, and "on" for the other strand (discussed in more detail above). This requires regulation in some form for the

enzyme, and while evidence would suggest that the source of regulation lies elsewhere in the complex, studies can be conducted to analyze the effect of ss- or dsDNA on the nuclease activity of $RecB^N$.

At the same time, Fe-mediated cleavage of $RecB^N$ in the presence of ss- or dsDNA can also examine the effect of DNA on metal binding in the active site. Previous studies on the metal dependence of $RecB^N$ activity have not examined the effect of $Fe^{2+}$ on nuclease activity. While it seems reasonable that a metal that causes cleavage of the protein backbone would not yield an active enzyme, it also seems reasonable to investigate. This can be examined by performing the nuclease assay in the presence of $Fe^{2+}$ as cofactor.

Mutant D1080A of RecB has been found to be deficient in RecA loading *in vivo* (134). This result was not expected based on previous work with RecBCD, which brings up an interesting avenue of research- what are the effects of other mutants on activity of the overall complex? Mutants of RecBCD at residues H956, E1020, D1067, and K1082 of RecB could be constructed with the goal of characterizing the effect of each of these mutants on the response of *E. coli* to DSB events.

Understanding of the mechanism of any enzyme can be greatly enhanced by co-crystallization of enzymes bound to catalytically intermediate structures. In the process of characterization of phosphate transfer enzymes, crystal structures solved with a vanadate analog of the phosphate substrate have served as a powerful tool (for a review, see (135)). This technique is limited by only serving as a potential analog of

associative mechanisms, as the utility of vanadate derives from its penta-coordinate

trigonal bi-pyramidal geometry around the metal center.

# Bibliography

1.    Friedberg, E. C. W., G.C.; Seide, W.; Wood, R.D.; Schultz, R.A.; Ellenberger, T. (2006) *DNA Repair and Mutagenesis, 2/e*, ASM Press, Washington, DC

2.    Kogoma, T. (1997) *Microbiol Mol Biol Rev* **61**(2), 212-238

3.    Hada, M., and Georgakilas, A. G. (2008) *J Radiat Res (Tokyo)* **49**(3), 203-210

4.    Mahaney, B. L., Meek, K., and Lees-Miller, S. P. (2009) *Biochem J* **417**(3), 639-650

5.    Hutchinson, F. (1985) *Prog Nucleic Acid Res Mol Biol* **32**, 115-154

6.    Gates, K. S. (2009) *Chem Res Toxicol* **22**(11), 1747-1760

7.    Shuman, S., and Glickman, M. S. (2007) *Nat Rev Microbiol* **5**(11), 852-861

8.    Hartlerode, A. J., and Scully, R. (2009) *Biochem J* **423**(2), 157-168

9.    Brissett, N. C., and Doherty, A. J. (2009) *Biochem Soc Trans* **37**(Pt 3), 539-545

10.   Mimitou, E. P., and Symington, L. S. (2009) *DNA Repair (Amst)* **8**(9), 983-995

11.   Dillingham, M. S., and Kowalczykowski, S. C. (2008) *Microbiol Mol Biol Rev* **72**(4), 642-671

12.   Battista, J. R., Earl, A. M., and Park, M. J. (1999) *Trends Microbiol* **7**(9), 362-365

13.   Blasius, M., Sommer, S., and Hubscher, U. (2008) *Crit Rev Biochem Mol Biol* **43**(3), 221-238

14.   Makarova, K. S., Aravind, L., Wolf, Y. I., Tatusov, R. L., Minton, K. W., Koonin, E. V., and Daly, M. J. (2001) *Microbiol Mol Biol Rev* **65**(1), 44-79

15.   Wang, J., and Julin, D. A. (2004) *J Biol Chem* **279**(50), 52024-52032

16.   Moseley, B. E., and Evans, D. M. (1983) *J Gen Microbiol* **129**(8), 2437-2445

17.   Hansen, M. T. (1978) *J Bacteriol* **134**(1), 71-75

18.   Battista, J. R. (1997) *Annu Rev Microbiol* **51**, 203-224

19. Cox, M. M., and Battista, J. R. (2005) *Nat Rev Microbiol* **3**(11), 882-892

20. Liu, Y., Zhou, J., Omelchenko, M. V., Beliaev, A. S., Venkateswaran, A., Stair, J., Wu, L., Thompson, D. K., Xu, D., Rogozin, I. B., Gaidamakova, E. K., Zhai, M., Makarova, K. S., Koonin, E. V., and Daly, M. J. (2003) *Proc Natl Acad Sci U S A* **100**(7), 4191-4196

21. Daly, M. J., Ouyang, L., Fuchs, P., and Minton, K. W. (1994) *J Bacteriol* **176**(12), 3508-3517

22. Zahradka, K., Slade, D., Bailone, A., Sommer, S., Averbeck, D., Petranovic, M., Lindner, A. B., and Radman, M. (2006) *Nature* **443**(7111), 569-573

23. Rainey, F. A., Ray, K., Ferreira, M., Gatz, B. Z., Nobre, M. F., Bagaley, D., Rash, B. A., Park, M. J., Earl, A. M., Shank, N. C., Small, A. M., Henk, M. C., Battista, J. R., Kampfer, P., and da Costa, M. S. (2005) *Appl Environ Microbiol* **71**(9), 5225-5235

24. Chanal, A., Chapon, V., Benzerara, K., Barakat, M., Christen, R., Achouak, W., Barras, F., and Heulin, T. (2006) *Environ Microbiol* **8**(3), 514-525

25. Anderson, A. W., Nordan, H.C., Cain, R.F., Parrish, G., and Duggan, D. (1956) *Food Technology* **10**, 575-578

26. Mattimore, V., and Battista, J. R. (1996) *J Bacteriol* **178**(3), 633-637

27. White, O., Eisen, J. A., Heidelberg, J. F., Hickey, E. K., Peterson, J. D., Dodson, R. J., Haft, D. H., Gwinn, M. L., Nelson, W. C., Richardson, D. L., Moffat, K. S., Qin, H., Jiang, L., Pamphile, W., Crosby, M., Shen, M., Vamathevan, J. J., Lam, P., McDonald, L., Utterback, T., Zalewski, C., Makarova, K. S., Aravind, L., Daly, M. J., Minton, K. W., Fleischmann, R. D., Ketchum, K. A., Nelson, K. E., Salzberg, S., Smith, H. O., Venter, J. C., and Fraser, C. M. (1999) *Science* **286**(5444), 1571-1577

28. Levin-Zaidman, S., Englander, J., Shimoni, E., Sharma, A. K., Minton, K. W., and Minsky, A. (2003) *Science* **299**(5604), 254-256

29. Englander, J., Klein, E., Brumfeld, V., Sharma, A. K., Doherty, A. J., and Minsky, A. (2004) *J Bacteriol* **186**(18), 5973-5977

30. Daly, M. J., Gaidamakova, E. K., Matrosova, V. Y., Vasilenko, A., Zhai, M., Venkateswaran, A., Hess, M., Omelchenko, M. V., Kostandarithes, H. M., Makarova, K. S., Wackett, L. P., Fredrickson, J. K., and Ghosal, D. (2004) *Science* **306**(5698), 1025-1028

31. Touati, D. (2000) *Arch Biochem Biophys* **373**(1), 1-6

32. Neyens, E., and Baeyens, J. (2003) *J Hazard Mater* **98**(1-3), 33-50

33. Ziegelhoffer, E. C., and Donohue, T. J. (2009) *Nat Rev Microbiol* **7**(12), 856-863

34. Jakubovics, N. S., and Jenkinson, H. F. (2001) *Microbiology* **147**(Pt 7), 1709-1718

35. Dermic, D., Halupecki, E., Zahradka, D., and Petranovic, M. (2005) *Res Microbiol* **156**(3), 304-311

36. Wong, C. J., Rice, R. L., Baker, N. A., Ju, T., and Lohman, T. M. (2006) *J Mol Biol* **362**(1), 26-43

37. Wong, C. J., Lucius, A. L., and Lohman, T. M. (2005) *J Mol Biol* **352**(4), 765-782

38. Kowalczykowski, S. C., Dixon, D. A., Eggleston, A. K., Lauder, S. D., and Rehrauer, W. M. (1994) *Microbiol Rev* **58**(3), 401-465

39. Rocha, E. P., Cornet, E., and Michel, B. (2005) *PLoS Genet* **1**(2), e15

40. Kuzminov, A. (1999) *Microbiol Mol Biol Rev* **63**(4), 751-813

41. Singleton, M. R., Dillingham, M. S., Gaudier, M., Kowalczykowski, S. C., and Wigley, D. B. (2004) *Nature* **432**(7014), 187-193

42. Arnold, D. A., and Kowalczykowski, S. C. (2000) *J Biol Chem* **275**(16), 12261-12265

43. Spies, M., and Kowalczykowski, S. C. (2006) *Mol Cell* **21**(4), 573-580

44. Fulconis, R., Mine, J., Bancaud, A., Dutreix, M., and Viovy, J. L. (2006) *Embo J* **25**(18), 4293-4304

45. Weaver, R. F. (2005) *Molecular Biology*, *3/e*, McGraw-Hill, New York

46. Roman, L. J., and Kowalczykowski, S. C. (1989) *Biochemistry* **28**(7), 2863-2873

47. Korangy, F., and Julin, D. A. (1994) *Biochemistry* **33**(32), 9552-9560

48. Churchill, J. J., and Kowalczykowski, S. C. (2000) *J Mol Biol* **297**(3), 537-542

49. Masterson, C., Boehmer, P. E., McDonald, F., Chaudhuri, S., Hickson, I. D., and Emmerson, P. T. (1992) *J Biol Chem* **267**(19), 13564-13572

50. Chen, H. W., Ruan, B., Yu, M., Wang, J., and Julin, D. A. (1997) *J Biol Chem* **272**(15), 10072-10079

51. Yu, M., Souaya, J., and Julin, D. A. (1998) *J Mol Biol* **283**(4), 797-808

52. Yu, M., Souaya, J., and Julin, D. A. (1998) *Proc Natl Acad Sci U S A* **95**(3), 981-986

53. Zhang, X. J., and Julin, D. A. (1999) *Nucleic Acids Res* **27**(21), 4200-4207

54. Dillingham, M. S., Webb, M. R., and Kowalczykowski, S. C. (2005) *J Biol Chem* **280**(44), 37069-37077

55. Boehmer, P. E., and Emmerson, P. T. (1992) *J Biol Chem* **267**(7), 4981-4987

56. Michel, B., Boubakri, H., Baharoglu, Z., LeMasson, M., and Lestini, R. (2007) *DNA Repair (Amst)* **6**(7), 967-980

57. Bentchikou, E., Servant, P., Coste, G., and Sommer, S. *PLoS Genet* **6**(1), e1000774

58. Chedin, F., Handa, N., Dillingham, M. S., and Kowalczykowski, S. C. (2006) *J Biol Chem* **281**(27), 18610-18617

59. Servinsky, M. D., and Julin, D. A. (2007) *J Bacteriol* **189**(14), 5101-5107

60. Zhou, Q., Zhang, X., Xu, H., Xu, B., and Hua, Y. (2007) *FEMS Microbiol Lett* **271**(1), 118-125

61. Saikrishnan, K., Griffiths, S. P., Cook, N., Court, R., and Wigley, D. B. (2008) *Embo J* **27**(16), 2222-2229

62. Saikrishnan, K., Powell, B., Cook, N. J., Webb, M. R., and Wigley, D. B. (2009) *Cell* **137**(5), 849-859

63. Boggon, T. J., and Eck, M. J. (2004) *Oncogene* **23**(48), 7918-7927

64. Mackintosh, S. G., and Raney, K. D. (2006) *Nucleic Acids Res* **34**(15), 4154-4159

65. Subramanya, H. S., Bird, L. E., Brannigan, J. A., and Wigley, D. B. (1996) *Nature* **384**(6607), 379-383

66. Bird, L. E., Brannigan, J. A., Subramanya, H. S., and Wigley, D. B. (1998) *Nucleic Acids Res* **26**(11), 2686-2693

67. Nanduri, B., Byrd, A. K., Eoff, R. L., Tackett, A. J., and Raney, K. D. (2002) *Proc Natl Acad Sci U S A* **99**(23), 14722-14727

68. Wong, I., Chao, K. L., Bujalowski, W., and Lohman, T. M. (1992) *J Biol Chem* **267**(11), 7596-7610

69. Brendza, K. M., Cheng, W., Fischer, C. J., Chesnik, M. A., Niedziela-Majka, A., and Lohman, T. M. (2005) *Proc Natl Acad Sci U S A* **102**(29), 10076-10081

70. Bjornson, K. P., Moore, K. J., and Lohman, T. M. (1996) *Biochemistry* **35**(7), 2268-2282

71. Roychowdhury, A., Szymanski, M. R., Jezewska, M. J., and Bujalowski, W. (2009) *Biochemistry* **48**(29), 6712-6729

72. Roychowdhury, A., Szymanski, M. R., Jezewska, M. J., and Bujalowski, W. (2009) *Biochemistry* **48**(29), 6730-6746

73. Roychowdhury, A., Szymanski, M. R., Jezewska, M. J., and Bujalowski, W. (2009) *Biochemistry* **48**(29), 6747-6763

74. Enemark, E. J., and Joshua-Tor, L. (2008) *Curr Opin Struct Biol* **18**(2), 243-257

75. Hall, M. C., and Matson, S. W. (1999) *Mol Microbiol* **34**(5), 867-877

76. Yang, Y., Dou, S. X., Xu, Y. N., Bazeille, N., Wang, P. Y., Rigolet, P., Xu, H. Q., and Xi, X. G. *Biochemistry* **49**(4), 656-668

77. Ali, J. A., and Lohman, T. M. (1997) *Science* **275**(5298), 377-380

78. Montague, M., Barnes, C., Smith, H. O., Chuang, R. Y., and Vashee, S. (2009) *J Mol Evol* **69**(4), 360-371

79. Liberek, K., Osipiuk, J., Zylicz, M., Ang, D., Skorko, J., and Georgopoulos, C. (1990) *J Biol Chem* **265**(6), 3022-3029

80. Azem, A., Shaked, I., Rosenbusch, J. P., and Daniel, E. (1995) *Biochim Biophys Acta* **1243**(2), 151-156

81. Wu, B., Wawrzynow, A., Zylicz, M., and Georgopoulos, C. (1996) *Embo J* **15**(18), 4806-4816

82. Cheung, D. T., and Nimni, M. E. (1982) *Connect Tissue Res* **10**(2), 201-216

83. Yi, F., Doudevski, I., and Regan, L. *Protein Sci* **19**(1), 19-25

84. Philo, J. S. (2009) *Curr Pharm Biotechnol* **10**(4), 359-372

85. Servinsky, M. D. (2008) Biological Characterization of RecD mutants in *Deinococcus radiodurans*. *Chemistry and Biochemistry*, University of Maryland, College Park, MD

86. Byrd, A. K., and Raney, K. D. (2006) *Nucleic Acids Res* **34**(10), 3020-3029

87. Johnson, J. E., Cao, K., Ryvkin, P., Wang, L. S., and Johnson, F. B. (2009) *Nucleic Acids Res*

88. Sikora, B., Eoff, R. L., Matson, S. W., and Raney, K. D. (2006) *J Biol Chem* **281**(47), 36110-36116

89. Galletto, R., Jezewska, M. J., and Bujalowski, W. (2004) *J Mol Biol* **343**(1), 83-99

90. Jezewska, M. J., Lucius, A. L., and Bujalowski, W. (2005) *Biochemistry* **44**(10), 3865-3876

91. Jezewska, M. J., Lucius, A. L., and Bujalowski, W. (2005) *Biochemistry* **44**(10), 3877-3890

92. Hall, M. C., and Matson, S. W. (1997) *J Biol Chem* **272**(30), 18614-18620

93. Gu, Y., Masuda, Y., and Kamiya, K. (2008) *Nucleic Acids Res* **36**(19), 6295-6308

94. Lucius, A. L., Vindigni, A., Gregorian, R., Ali, J. A., Taylor, A. F., Smith, G. R., and Lohman, T. M. (2002) *J Mol Biol* **324**(3), 409-428

95. Niedziela-Majka, A., Chesnik, M. A., Tomko, E. J., and Lohman, T. M. (2007) *J Biol Chem* **282**(37), 27076-27085

96. Lucius, A. L., and Lohman, T. M. (2004) *J Mol Biol* **339**(4), 751-771

97. Yang, Y., Dou, S. X., Ren, H., Wang, P. Y., Zhang, X. D., Qian, M., Pan, B. Y., and Xi, X. G. (2008) *Nucleic Acids Res* **36**(6), 1976-1989

98. Fischer, C. J., Yamada, K., and Fitzgerald, D. J. (2009) *Biochemistry* **48**(13), 2960-2968

99. Roman, L. J., Eggleston, A. K., and Kowalczykowski, S. C. (1992) *J Biol Chem* **267**(6), 4207-4214

100. Soultanas, P., Dillingham, M. S., Papadopoulos, F., Phillips, S. E., Thomas, C. D., and Wigley, D. B. (1999) *Nucleic Acids Res* **27**(6), 1421-1428

101. Cao, Z. (2009) Biochemical and Biological Characterization of Three DNA Repair Enzymes from *Deinococcus radiodurans*. *Chemistry and Biochemistry*, University of Maryland, College Park, MD

102. Hunkapiller, M. W., Lujan, E., Ostrander, F., and Hood, L. E. (1983) *Methods Enzymol* **91**, 227-236

103. Polansky, S. C. (2006) Expressing *Deinococcus radiodurans* RecD in *Escherichia coli*: Phenotypic Effects in RecBCD(-) and RecD(-) cells. *Chemistry and Biochemistry*, University of Maryland, College Park, MD

104. Studier, F. W. (2005) *Protein Expr Purif* **41**(1), 207-234

105. Bertani, G. (1951) *J Bacteriol* **62**(3), 293-300

106. Novagen. (2003) *pET System Manual*, 10 Ed., Novagen, Inc.

107. Oganesyan, N., Ankoudinova, I., Kim, S. H., and Kim, R. (2007) *Protein Expr Purif* **52**(2), 280-285

108. Hijarrubia, M. J., Aparicio, J. F., and Martin, J. F. (2003) *J Biol Chem* **278**(10), 8250-8256

109. Suh, M. J., Pourshahian, S., and Limbach, P. A. (2007) *J Am Soc Mass Spectrom* **18**(7), 1304-1317

110. Jacobsen, H., Klenow, H., and Overgaard-Hansen, K. (1974) *Eur J Biochem* **45**(2), 623-627

111. Chalker, A. F., Ward, J. M., Fosberry, A. P., and Hodgson, J. E. (1994) *Gene* **141**(1), 103-108

112. Mossessova, E., and Lima, C. D. (2000) *Mol Cell* **5**(5), 865-876

113. Sorensen, H. P., and Mortensen, K. K. (2005) *J Biotechnol* **115**(2), 113-128

114. Jennings, T. A., Chen, Y., Sikora, D., Harrison, M. K., Sikora, B., Huang, L., Jankowsky, E., Fairman, M. E., Cameron, C. E., and Raney, K. D. (2008) *Biochemistry* **47**(4), 1126-1135

115. Postow, L., Woo, E. M., Chait, B. T., and Funabiki, H. (2009) *J Biol Chem* **284**(51), 35951-35961

116. Mankouri, H. W., and Hickson, I. D. (2004) *Biochem Soc Trans* **32**(Pt 6), 957-958

117. Singh, D. K., Ahn, B., and Bohr, V. A. (2009) *Biogerontology* **10**(3), 235-252

118. Chino, M., Nishikawa, K., Yamada, A., Ohsono, M., Sawa, T., Hanaoka, F., Ishizuka, M., and Takeuchi, T. (1998) *J Antibiot (Tokyo)* **51**(5), 480-486

119. Cencic, R., Carrier, M., Galicia-Vazquez, G., Bordeleau, M. E., Sukarieh, R., Bourdeau, A., Brem, B., Teodoro, J. G., Greger, H., Tremblay, M. L., Porco, J. A., Jr., and Pelletier, J. (2009) *PLoS One* **4**(4), e5223

120. Aiello, D., Barnes, M. H., Biswas, E. E., Biswas, S. B., Gu, S., Williams, J. D., Bowlin, T. L., and Moir, D. T. (2009) *Bioorg Med Chem* **17**(13), 4466-4476

121. Popuri, V., Bachrati, C. Z., Muzzolini, L., Mosedale, G., Costantini, S., Giacomini, E., Hickson, I. D., and Vindigni, A. (2008) *J Biol Chem* **283**(26), 17766-17776

122. Appukuttan, D., Rao, A. S., and Apte, S. K. (2006) *Appl Environ Microbiol* **72**(12), 7873-7878

123. Sun, J. Z., Julin, D. A., and Hu, J. S. (2006) *Biochemistry* **45**(1), 131-140

124. Aravind, L., Walker, D. R., and Koonin, E. V. (1999) *Nucleic Acids Res* **27**(5), 1223-1242

125. Wang, J., Chen, R., and Julin, D. A. (2000) *J Biol Chem* **275**(1), 507-513

126. Aravind, L., Makarova, K. S., and Koonin, E. V. (2000) *Nucleic Acids Res* **28**(18), 3417-3432

127. Kovall, R. A., and Matthews, B. W. (1998) *Proc Natl Acad Sci U S A* **95**(14), 7893-7897

128. Galburt, E. A., and Stoddard, B. L. (2002) *Biochemistry* **41**(47), 13851-13860

129. Pingoud, A., Fuxreiter, M., Pingoud, V., and Wende, W. (2005) *Cell Mol Life Sci* **62**(6), 685-707

130. Stadtman, E. R., and Berlett, B. S. (1991) *J Biol Chem* **266**(26), 17201-17211

131. Hlavaty, J. J., Benner, J. S., Hornstra, L. J., and Schildkraut, I. (2000) *Biochemistry* **39**(11), 3097-3105

132. Schagger, H., and von Jagow, G. (1987) *Anal Biochem* **166**(2), 368-379

133. Roychoudhury, S. (2006) Mapping of Metal Ion Binding Sites in the RecBCD Enzyme and the Role of Magnesium in the Subunit Interactions of RecBCD. *Chemistry and Biochemistry*, University of Maryland, College Park, MD

134. Anderson, D. G., Churchill, J. J., and Kowalczykowski, S. C. (1999) *J Biol Chem* **274**(38), 27139-27144

135. Davies, D. R., and Hol, W. G. (2004) *FEBS Lett* **577**(3), 315-321